Locating invisible cultural heritage sites in agricultural fields

Evaluation of methods for satellite monitoring of cultural heritage sites – results 2003.

Ole Grøn, NIKU
Lars Aurdal, NR
Finn Christensen, GeoKem
Hans Tømmervik, NINA
Anke Loska, RA

ISBN: 82-7574-033-9
Oslo, March 2004

Front page illustration: Extract from figure 21, page 23.

Proof reading: Peter Crabb
Graphic design and layout: Elisabeth Mølbach, NIKU
Number printed: 170
Print: Digital Copy Studio AS, Oslo

1. Abstract

The increasingly intensive use and modification of the landscape as a result of modern demands for efficient infrastructure and land use (agricultural production, mining, energy sources, leisure/tourism facilities) exerts growing pressure on areas and sites associated with our cultural heritage. The use of modern support technologies is imperative, if such rapid changes are to be balanced against the sustainable management of this resource.

At present, cultural heritage legislation and management is based on expensive and technologically conservative methods of field survey which underpin regional and national registers of cultural heritage sites. These registers are flawed and contain not only a biased sample of sites in respect to period and region, but also include only a tiny fraction of the total population of all sites which should be included in management strategies. This lack of reliable data not only hampers realistic forecasting, but also causes costly delays and introduces unnecessary conflicts.

This project directly addresses these issues by initiating the development of a basis for a sustainable, up-to-date and cost-efficient decision-support methodology which relies upon satellite remote-sensing, mapping and monitoring of cultural heritage sites. A central methodological element is the development of high-resolution empirical ground data, which facilitate fast and cost-efficient identification of potential cultural heritage anomalies identified in the multispectral data.

Results obtained in the 2001-2002 pilot project indicated the existence of a correlation between cultural heritage sites and variation in the chemical elements in the soil. One central focus of the 2003-project module was to test the possibilities for establishing a concrete correspondence between the observed anomalies interpreted as possible cultural heritage sites and high-resolution field data to support a distinction between the anomalies that represent cultural heritage sites and those that represent geological phenomena, modern disturbances, etc. The results demonstrate that high-resolution geo-chemical sampling appears to be a promising field for the development of cultural heritage indicators.

The strategy suggested for further development involves two main elements: 1) the development of methods for distinction of anomalies in satellite images that can represent cultural heritage sites and 2) the development of ground methods such as soil chemistry to verify or reject the character of such anomalies as cultural heritage sites. These two elements should develop in a feed-back relation with each other to facilitate a precise targeting and mapping of cultural heritage sites that can serve as a basis for a considerably improved monitoring of the cultural heritage and accordingly as an important support technology for the cultural heritage administration.

2. Introduction

2.a. The problem in focus

It is generally recognised that the increasingly intensive use and modification of the landscape resulting from modern demands for efficient infrastructure and land use (agricultural production, mining, energy sources, leisure/tourism facilities) exerts growing pressure on cultural heritage in the landscape.

In order to match the political intentions of updated and sustainable cultural heritage management, a necessary first step is to create a representative picture of the resource that has to be managed. In Norway, where extensive white areas are still to be found on cultural heritage maps; where the registered cultural heritage sites display an unrepresentative concentration in areas with high human activity; and where the registered positions of the sites can easily be 30-40 metres from their true location, it is obvious that something has to be done in order to achieve even this basic goal.

In recognition that a) it will never be realistic to obtain funding for thorough survey and monitoring of the enormous tracts in question using traditional field-survey methods, and b) there is a demand for access to representative and comprehensive cultural heritage data to create a basis for the development of a flexible and up-to-date cultural heritage management, the Norwegian Space Centre (NRS) and the Norwegian Directorate for Cultural Heritage (RA) decided on the basis of a pilot project (2001-2002) to prepare the ground for the development of survey and monitoring methodology involving multispectral satellite data (Grøn and Loska 2002).

The project's aim is to develop a cost-effective method for locating/mapping and monitoring cultural heritage sites. The costs of systematically surveying areas of the scale involved here by means of conventional fieldwork provide the incentive for the development of alternatives. Depending on which field methods are employed, and the type of landscape surveyed, costs for conventional fieldwork will normally be around 250,000 Norwegian Crowns (NOK) per square kilometre. In comparison, high-resolution satellite data cost less than NOK 1,000 per square kilometre, a fraction of conventional fieldwork costs.

Even though the costs connected with the processing of the satellite data will not be insignificant, and fieldwork can probably never be entirely replaced by high-technological methods, it seems plausible that an essentially cheaper, and possibly even qualitatively better, method for the surveying and monitoring of cultural heritage sites can be developed by using multispectral satellite data to target the fieldwork to a degree not possible today.

One central focus of the 2003-project module has been to test the possibilities for establishing a correspondence between the observed anomalies interpreted as cultural heritage sites and high-resolution field data to support a distinction between the anomalies that represent cultural heritage sites and those that represent geological phenomena, modern disturbances, etc. The results demonstrate that high-resolution chemical sampling appears to be a promising field for development of cultural heritage indicators.

A second aim has been to assess the possibilities for application of pattern recognition to the interpretation of satellite data. Also, this field seems promising as a technique that can be built into a management system for cultural heritage.

The most urgent problem in today's cultural heritage management is the 'invisible' cultural heritage sites with no directly visible physical features preserved that are located in the agricultural fields. This group seems to contain a surprisingly large fraction of the prehistoric settlements, but also of the earth-built burial mounds, roads, graves, etc. (Grøn and Loska 2002), that are more vulnerable than, for instance, mounds with a base consisting of bedrock and mounds built of large stones. In spite of their lacking visibility, such cultural heritage sites can have significant features preserved underground and therefore represent an important heritage potential. Also, as corrections to the misleading picture of the prehistoric cultural landscape, the visible cultural heritage provides us with a mapping of the invisible sites which is indispensable.

A second urgent problem is to gather information about the speed and character of the degradation of the different types of cultural heritage sites in relation to their topographical situation, the sediment types they are located on, the types of agricultural activities they are exposed to, etc. Apart from being a qualified candidate for representative mapping of cultural heritage sites,

satellite technologies should also be well suited for the development of methods for long-term monitoring of the preservation status of the cultural heritage sites.

As a cost-efficient support technology for the cultural heritage administration that can provide reliable information about the representative distribution of the different types of cultural heritage sites down to the small-scale level, the method under development should facilitate a significantly more efficient and flexible as well as cheaper planning process in relation to, for example development projects than is possible today. An additional development of methods for monitoring of the preservation status of the cultural heritage sites will add a further important facet to the administrative facilities.

2.b. Aims

The aims of the 2003 pilot project were:

- To look for relationships between anomalies visible in multispectral satellite data and ground features that can be distinguished by soil chemistry, metal-detectors, and vegetation analysis.
- To evaluate the practical potential pattern recognition for locating cultural heritage sites.
- To obtain and interpret a new high-resolution satellite image (Quickbird) from the study area.
- To suggest a strategy for further national initiatives in this field.

an additional point is:

- Collaborate with and communicate the results to the local population, administration, and relevant cultural heritage societies and institutions in the study area.

2.c. Project organisation and funding

The 2003-project was funded by The Norwegian Space Centre (NRS) http://www.spacecentre.no/, and the Norwegian Directorate for Cultural Heritage (RA) http://www.riksantikvaren.no/, with additional project funding from the Norwegian Institute for Cultural Heritage (NIKU) http://www.ninaniku.no/ and the Norwegian Computing Center (NR).

Project leader is Ole Grøn, NIKU. The Steering Committee consists of Guro Dahle-Strøm (NRS) and Anna Lena Eriksson (RA). The project leader acts as counsellor for the steering committee.

The project participants are Ole Grøn, NIKU, Anke Loska, RA, Hans Tømmervik, NINA (Norwegian Institute for Nature Research), Lars Aurdal, NR (Norwegian Computing Centre), and Finn Christensen, GK (GeoKem).

Apart from the officially defined project elements, an important factor in the fieldwork has been the collaboration and helpfulness of the local landowners, Rygge municipal administration, as well as the Cultural Heritage department in Østfold County Council.

2.d. The study area

The study area is an 11 by 11 km large square in Rygge Municipality, Østfold Fylke. In WGS-84 UTM co-ordinates this is 592626-603618 E, 6575139-6586131 N (system 32). It is a typical, intensively exploited, agricultural production area with a quite moderate topography in Norwegian terms. With the exception of a few protruding ridges and rocks, the landscape is flat and hilly. Areas not occupied by fields and not covered by forests form an extremely limited proportion of the area.

2.e. Methodological choices and limitations

Whereas the application of radar images and hyperspectral data are discussed as potentially useful methods in the project, its immediate focus is on multispectral images, because they have already proved their usefulness in relation to cultural heritage site localisation and monitoring (Grøn et al. 1999; Holm-Olsen et al. 1999; Shennan and Donoghue 1991).

With regard to landscape types, the focus is on agricultural field because 1) the cultural heritage sites here are more exposed to damage than in the other landscape types and 2) the possibilities for observation are better than in other landscape types. It appears that the density of registered cultural heritage sites in agricultural fields is less than 2% of what it could have been (Grøn and Loska 2002).

Fig. 1 The study area is approximately 11 by 11 km in size and covers a part of Rygge Municipality, Østfold County. The locations of the sites analysed is shown in the satellite image (IKONOS - copyright: Space Imaging and the Satellite Data Archive of the Norwegian Mapping Authority).

3. Verification of observed anomalies as cultural heritage sites.

Essential for the use of satellite data for detecting and mapping cultural heritage sites is the availability of a cost-effective field method that can confirm or reject the character of the anomalies distinguished in the satellite images as potential cultural heritage sites. The 2003-project has demonstrated that soil chemistry is a candidate with a significant potential. The information about the chemical signatures of different types of cultural heritage sites is important as feed-back data for the interpretation methods during their development, and after the development phase a catalogue of chemical signatures will open for new possibilities for fast and cheap verification of potential cultural heritage sites.

3.a. Soil chemistry

The 2003 project took its starting-point in the basic assumption that a high level of human presence within a restricted area (settlement, burial mound being constructed, etc.) will have a long-term impact on the chemical composition of the soil (Grøn and Loska 2002). Even though the physical features of cultural heritage sites are no longer observable on the surface, they will often be preserved as distinguishable chemical anomalies. The accumulation of waste (bones, vegetable elements, etc.) will cause the formation of significant concentrations of phosphates (P), iron (Fe), etc. In houses the clearing out of waste from the inside will often create an inner zone with only small concentrations of 'garbage-related' chemical components, whereas these can appear in high concentrations outside. The construction of burial mounds, clay-plastered house walls, etc. is also likely to involve the introduction of 'foreign' chemical components or local chemical components in unusual concentrations, so that it should actually be possible to distinguish these physical features on the basis of their chemical signatures. In 2001-2002 a promising correlation between supposed cultural heritage sites and

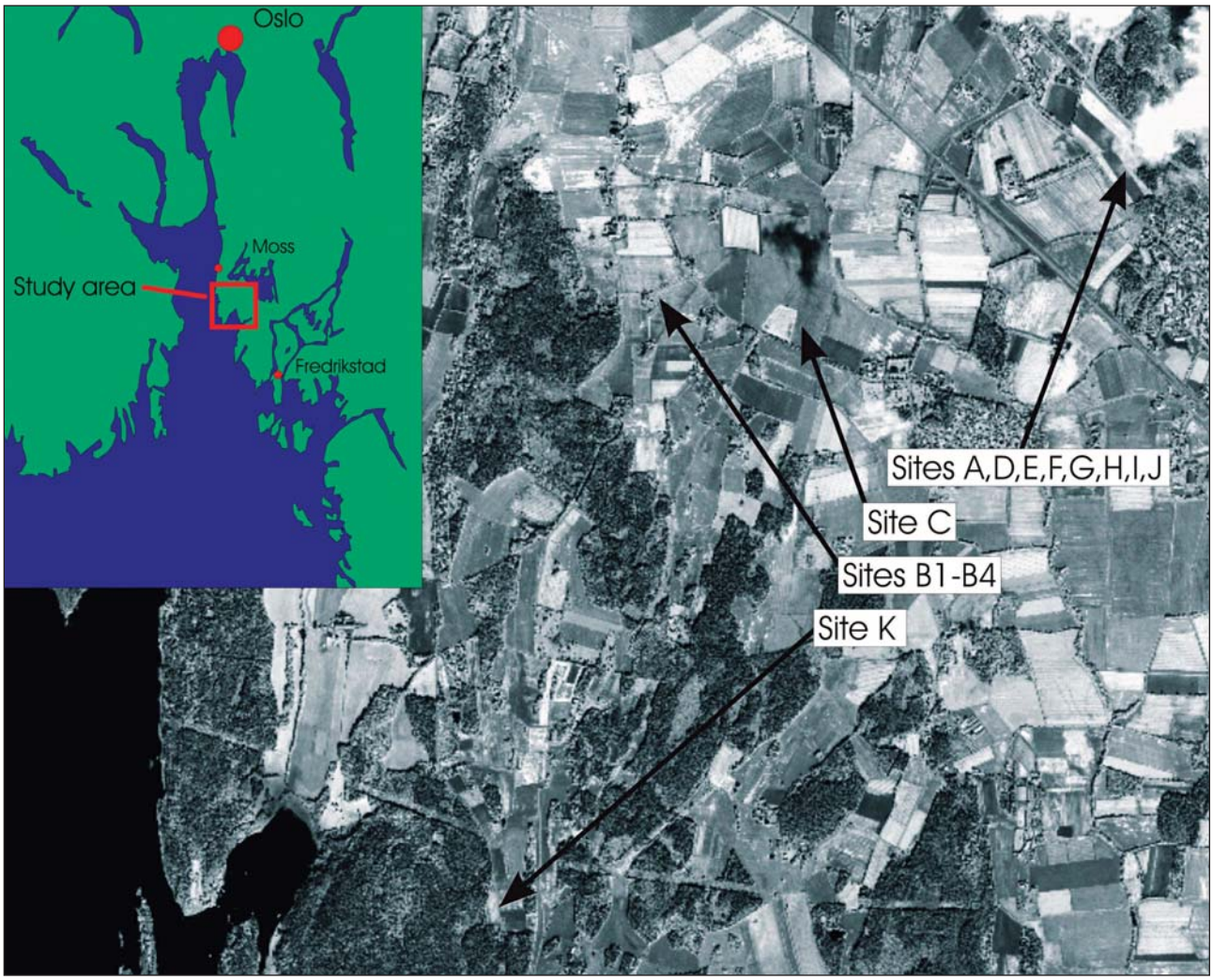

local variations in the iron and phosphate content of the plough-soil and the sediment immediately below it could be observed.

To improve the quality of the soil-chemistry data, the resolution was reduced to 1-2 m and it was decided to cut all smaller anomalies with two profiles instead of only one to improve the spatial quality of the information. It was furthermore in some cases decided to cover anomalies assumed to represent well-defined units with grids with 2 m between the points. Samples were always taken both from the top of the plough-soil (30-40 cm thick) and from the sediment 5 cm below the plough horizon to get some idea of the effect of minerals artificially added to the soil and the horizontal displacement-effect due to ploughing. If the sediment below the plough soil was humic or looked as if it might be coloured by cultural activity a third sample was taken 40 cm below the bottom of the plough-soil.

Altogether, 1570 samples were taken for analysis. Attempts will be made to speed up the process of sample taking. Each sample was analysed for: phosphates (P), iron (Fe), zinc (Zn), copper (Cu), lead (Pb), manganese (Mn), nickel (Ni), chrome (Cr), cadmium (Cd), and aluminium (Al). Only P, Fe, Zn, Cu, and Mn were found in measurable quantities. Variations in particle size and organic content have furthermore been analysed on an experimental basis. The sample size was so large that further analysis can be carried out, if that should be of interest.

The anomalies sampled were mainly chosen in one field of Gipsund Farm where an extremely high concentration of well-defined anomalies can be observed, but also in a couple of other fields in the vicinity. NIKU was responsible for the sampling and the field observations, whereas GeoKem, Denmark, carried out the analysis of the samples.

3.a.1. Site A, Gipsund Farm: The anomaly, site A, which was interpreted as a house, was covered by a 2 by 2 m grid measuring 30 by 14 m and containing 128 points.

The phosphates (P) below and in the plough-soil show a north-south orientated, approximately 22-25 m long, and 5-6 m broad feature with a significantly low concentration of phosphates (P) compared to the surroundings – especially to its east (fig. 3 B-P and T-P). This fits well with what one should expect for the inner part of a house. The orientation of the feature deviates approximately 20˚ from what was expected. Below and in the plough-soil, iron (Fe), zinc (Zn), copper (Cu), and manganese (Mn) show the same low concentration inside the southern end of the feature – some of them with a small concentration

Fig. 2 Site A, Gipsund Farm. Samples were taken in a grid with 2 m between the points in an area covering feature A, which was interpreted as a prehistoric house. The plan to the left shows equidistant contour lines for the phosphates below the plough-soil, with a focus in the colour signature on the interval from 300-550 ppm. Co-ordinates in metres in UTM system 32. The picture to the right shows the position of the site (IKONOS - copyright: Space Imaging and the Satellite Data Archive of the Norwegian Mapping Authority).

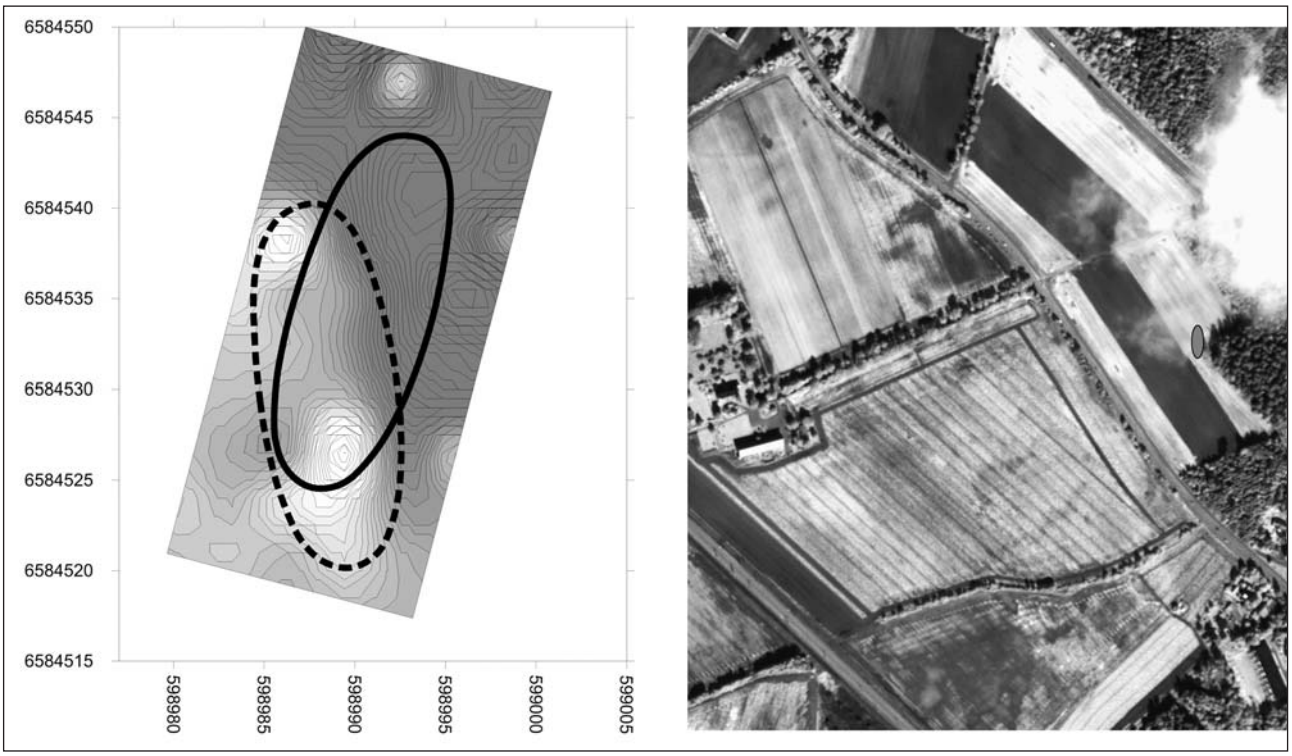

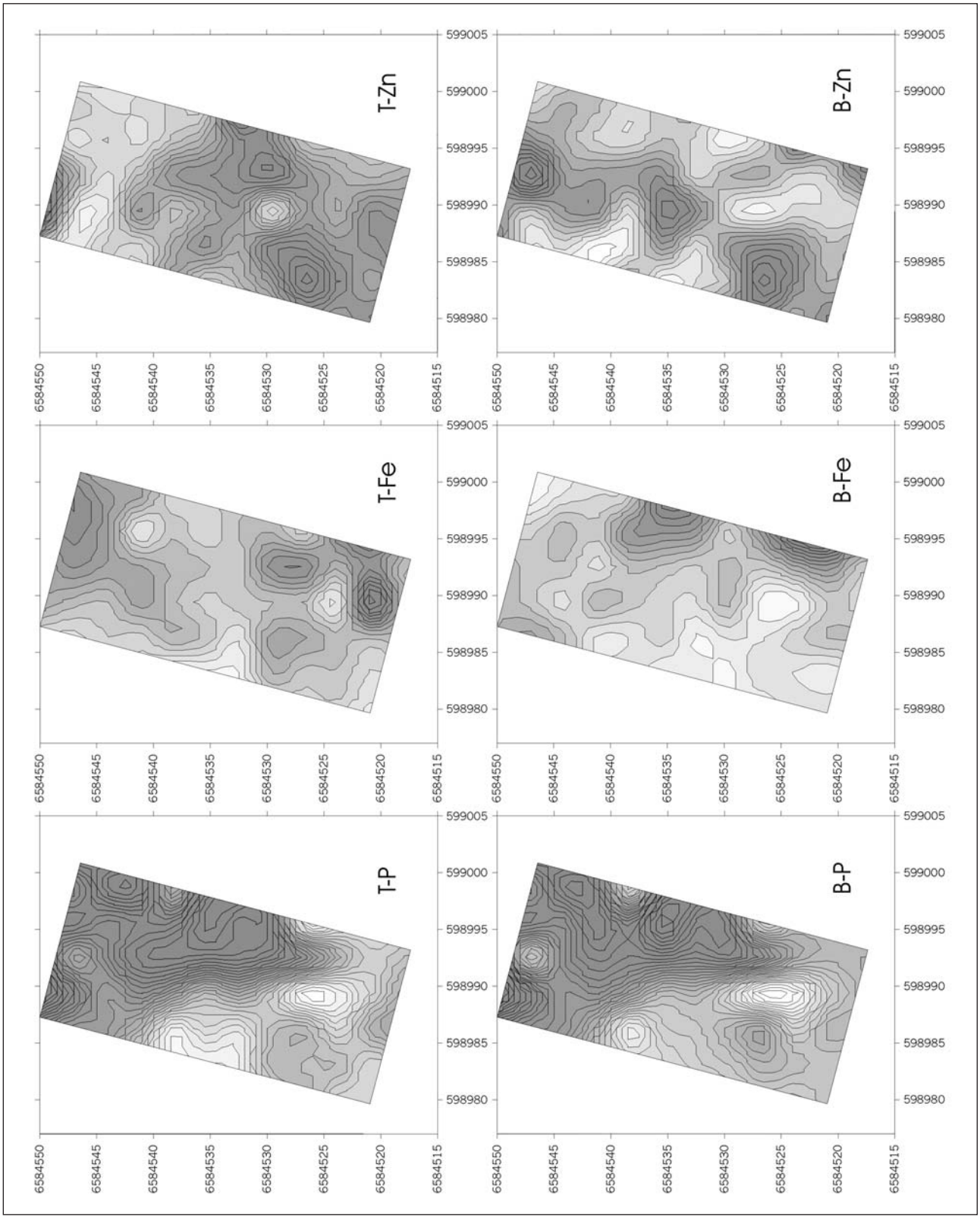

Fig. 3 Site A, Gipsund Farm. The variation in the central chemical components analysed for. The first letters 'T' and 'B' indicate that the data are from the 'top layer' = the plough-soil, or the 'bottom layer' = the sediments immediately below the plough-soil. P = phosphates, Fe = iron, Zn = zinc. The black lines represent the profiles. The interpolation shows equidistant contour lines. It becomes increasingly unreliable the more distant it is from the profiles. The higher the concentration, the darker the colour. The exact values measured for all of the central chemical elements are given in Appendix 1. Co-ordinates in metres in UTM system 32.

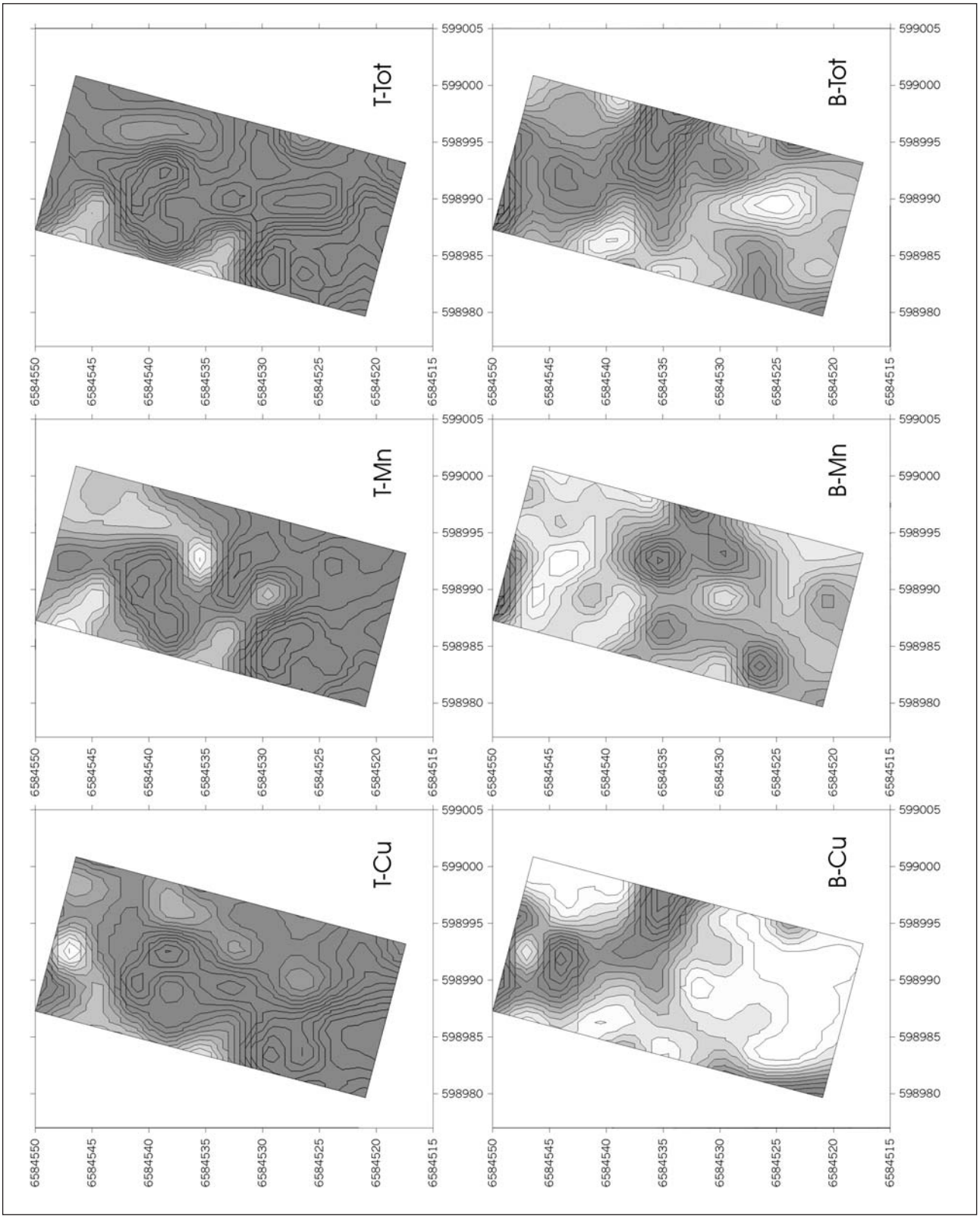

Fig. 4 Site A, Gipsund Farm. The variation in the central chemical components analysed for. The first letters 'T' and 'B' indicate that the data are from the 'top layer' = the plough-soil, or the 'bottom layer' = the sediments immediately below the plough-soil. P = phosphates, Fe = iron, Zn = zinc. The black lines represent the profiles. The interpolation shows equidistant contour lines. It becomes increasingly unreliable the more distant it is from the profiles. The higher the concentration, the darker the colour. The exact values measured for all of the central chemical elements are given in Appendix 1. Co-ordinates in metres in UTM system 32.

inside the feature's northern end. Some of the variation patterns seem to indicate the position of a wall line around the feature – for instance the long N-S orientated high concentration that can be observed immediately to the east of the suggested house feature in the phosphates (P) and the smaller linear high concentrations following the suggested wall line in iron (Fe) and zinc (Zn) below the plough-soil (figs. 2, 3 and 4).

The total variation (Tot) expresses the general spatial variation in the five central chemical components analysed for. The maximum value of each of the five is set to 100%, so that their maxima are equal. After this equalising operation their values are added. The total variation in this case shows the same tendency as the single elements already discussed (fig. 4).

3.a.2. Site B, Tøstad Øvre Farm: A 100 m long profile with a sample taken for each metre was made as a zigzag line from centre to centre through four anomalies assumed to be the remains of mounds. Transverse profiles were made through each of these anomalies as well, with samples for each metre. The present owner of the farm, Svein G. Lyby, remembers the former owner speaking about the removal of several mounds on this piece of land in the 1920s-1930s.

Just around the farm buildings there are a few mounds preserved in relation to the garden. It would not be surprising if all the features observed originally made up a regular cemetery consisting of a larger number of mounds.

The phosphates (P) in and below the plough-soil conjoin roughly with the four features interpreted as the remains of mounds (the three northernmost ones shown in the IKONOS image fig. 5)(fig. 6 B-P and T-P). The concentrations of phosphates (P) below the plough-soil are on the western periphery of the northernmost of the suggested mounds and on the northern periphery of the third from the north. The concentration related to the southernmost of the suggested mounds is less significant than that of the others, but still appears as a distinguishable feature. There seems to be an extra concentration of phosphates to the west of the second presumptive mound from the north that may indicate the earlier existence of two mounds here. No further concentrations of phosphates (P) can be observed in the data from this site. One should allow for some error of positioning in the geo-corrected satellite images. A check has shown that the co-ordinates within the IKONOS image are

Fig. 5 Site B, Tøstad Øvre Farm. A concentration of registered mounds, shown with a red line. A linear feature created by field-cultivation methods is shown as a broken black line. Three anomalies reflecting significant local changes in the soil and interpreted as the remains of mounds with no structural remains preserved above the surface are marked with green circles in the image to the left (IKONOS - copyright: Space Imaging and the Satellite Data Archive of the Norwegian Mapping Authority). To the right is a plan of the profile samples with co-ordinates in metres in UTM system 32. One square is 10 m.

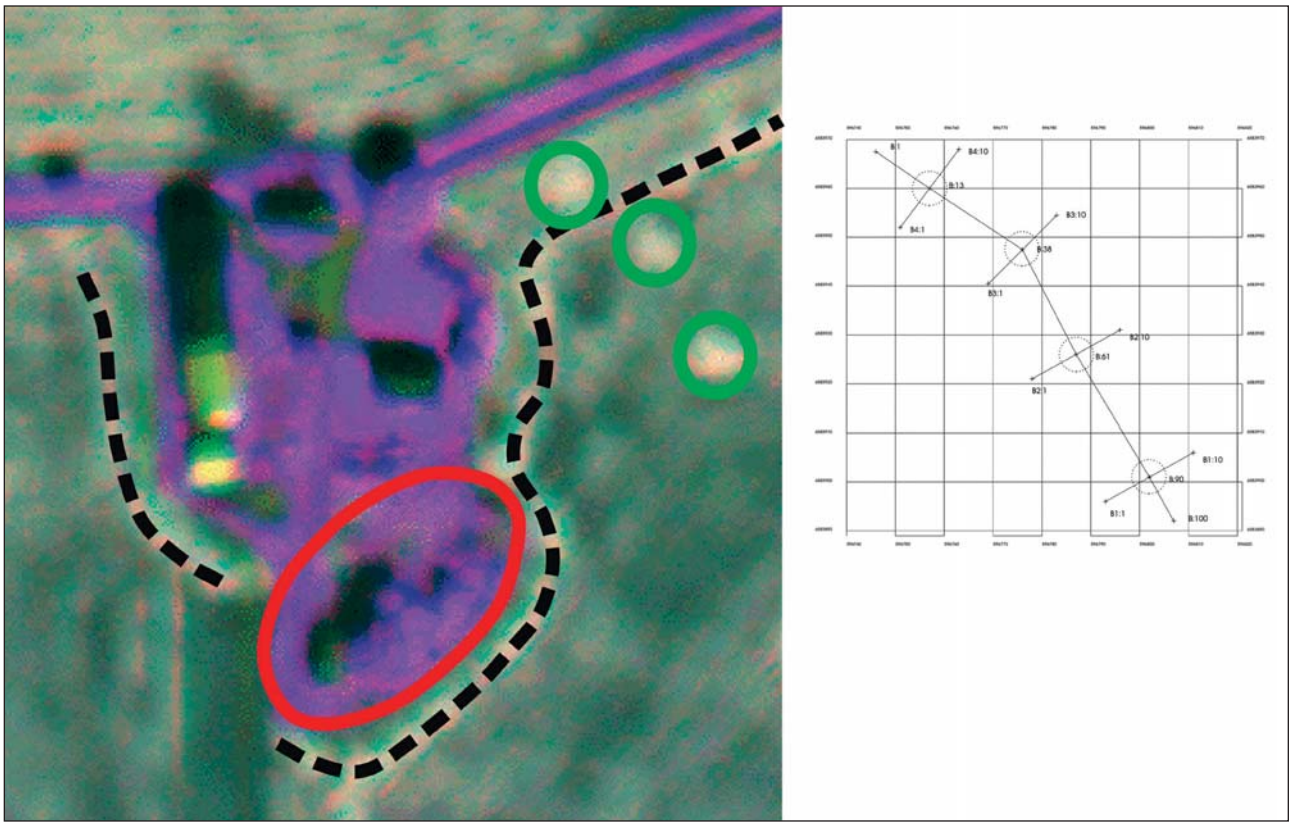

exact within ±2 m. This can explain some – but not all - of the displacement in relation to the observed anomalies.

The significant deviations in the concentration of iron (Fe) below the plough-soil appear generally peripheral to the concentrations of phosphates in the three northernmost features interpreted as mounds – and possibly the southernmost as well (fig. 6 B-Fe). This indicates that something may have happened involving iron on the periphery or a few metres from the mounds. If this proves to be a general pattern, it is very interesting.

Zinc (Zn) below the plough-soil displays general concentrations centrally related to each of the three northernmost putative mounds, each with two significant peaks. The southernmost suggested mound may also display a non-significant version of this pattern. The significant concentration to the west of the second presumptive mound from the north may be related to the pattern that can be observed in the phosphates. Because the basis of the interpolation is two crossing profiles for each of the suggested mounds, and not a grid, these bipartite patterns should not be given too much attention at the present stage of investigation (fig. 6 B-Zn).

Copper (Cu) below the plough-soil shows a general spatial relation to the suggested features without displaying a specific repeated pattern (fig. 7 B-Cu).

Manganese (Mn) below the plough-soil relates spatially to the two central of the suggested mounds, but with two different patterns (fig.7 B-Mn).

The total variation (Tot) shows a general co-variation between significant concentrations of the different chemical elements and the suggested mounds apart from the southernmost one – that is also the one that appears least obvious in the IKONOS image (fig. 7 B-Tot and T-Tot). This indicates that there may be a close correlation between cultural heritage sites and concentrations of some chemical elements. If the different chemical elements furthermore can be shown to display a repeated spatial organisation that can also be observed in preserved monuments, this may prove very useful.

3.a.3. Site C, Navestad Farm: 232 m of profile with samples taken for each metre, was cut through a 90 by 90 m large rhombic feature observed in the IKONOS image in 2001 and interpreted as the possible traces of an Early Medieval church in Rygge 500 m W-NW of the still existing Rygge Church, which is dated to about 1150 AD (fig. 8) (Grøn and Loska 2002).

Close to the southern border of the rhombic feature charcoal was observed in the samples below the plough-soil (C:61-62).

Coinciding with the southern border of the rhombic feature a dark grey sandy layer was observed in the samples C:67-69 below the plough-soil. A similar observation was made immediately to the north of it at the point C1:26. According to Jan Brendalsmo, NIKU, this is the type of deposit found to represent Medieval church dykes in a couple of other situations in Southern Norway (Brendalsmo and Hommedal 2001). In his opinion the existence of a 'church-builder myth' connected to this hill ('they were building a church on this hill but a troll tore it down during the night . . .'), in combination with the grey sand layers, strongly advocates the earlier existence of a second Rygge Church in this position.

During ploughing, the farmer at the top of the hill – probably within the southern part of the rhombic feature - found a loom weight (fig. 9) indicating activities dated to the Viking Age or the Early Medieval Period.

The variation in phosphates (P) below the plough-soil shows local minima that coincide with the rhombic feature and massive maxima immediately outside it (figs.10 and 11 B-P). The same minima can be observed in iron (Fe) and manganese (Mn) below the plough-soil and in phosphates (P) and manganese (Mn) in the plough-soil. Zinc (Zn) below the plough-soil displays maxima where the profiles cut the rhombic structure's northern and eastern sides, whereas it shows a maximum where its southern side is cut. Copper (Cu) below the plough-soil and copper (Cu) and zinc (Zn) in the plough-soil display no patterns that seem related to the rhombic feature. In general, the variations in the concentrations of the chemical elements indicate that this feature formerly had a regular physical character (figs. 11 and 12).

Below and in the plough-soil copper (Cu) displays a few significant concentrations of restricted size that have no obvious relation to the rhombic feature. They may reflect high and local concentrations of copper from single objects that may have dissolved. One of the blotches that could be observed in the vegetation (C:150-156) (fig. 8, 12 T-Cu) coincides with an extremely high copper value in the plough soil. The blotches may represent pits – possibly former pits that have been destroyed by ploughing.

A significant concentration of phosphates (P), iron (Fe), zinc (Zn), and manganese (Mn) indicates that an area to the south inside the rhombic feature was a place of some

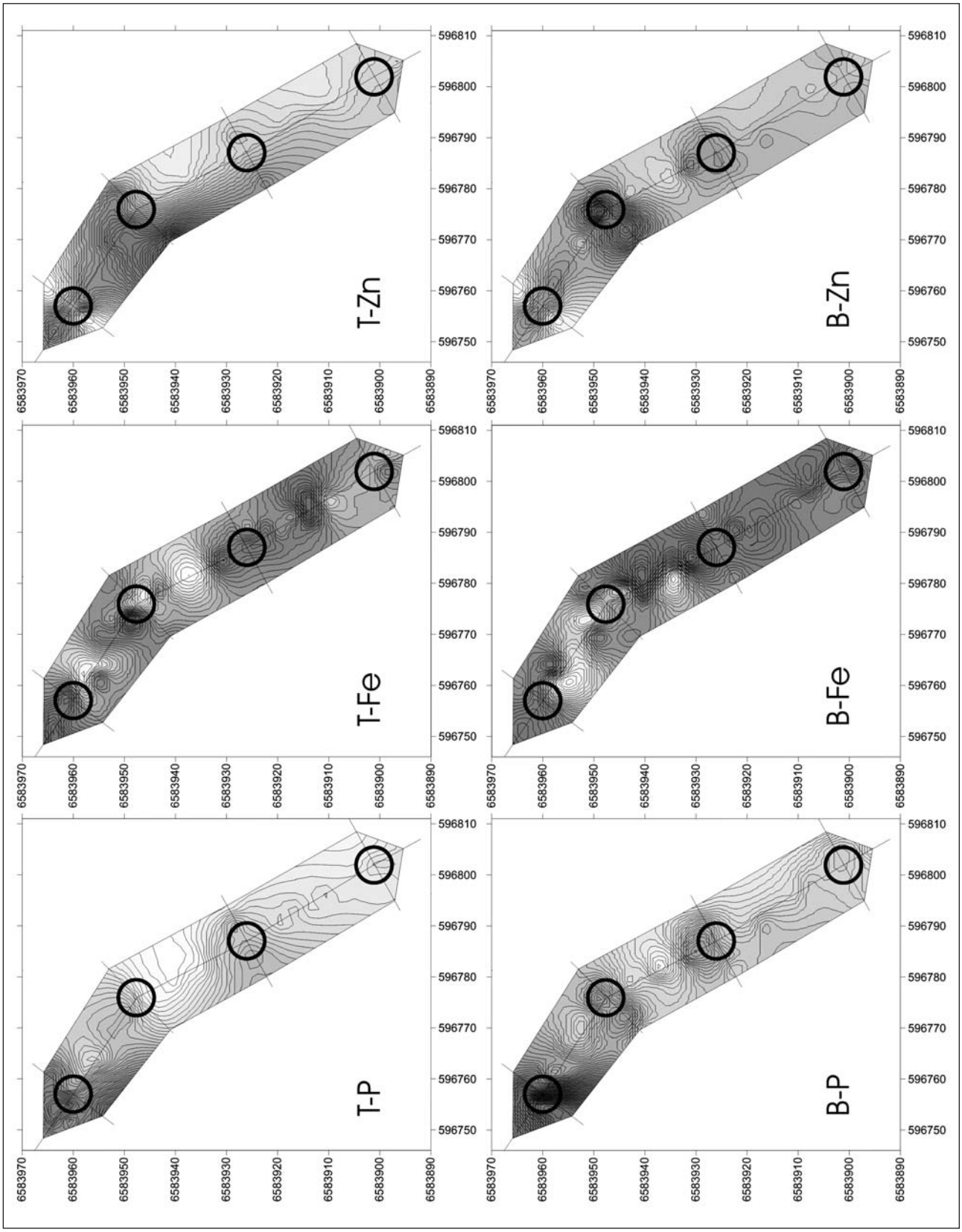

Fig. 6 Site B, Tøstad Øvre Farm. The variation in the central chemical components analysed for. The first letters 'T' and 'B' indicate that the data are from the 'top layer' = the plough-soil, or the 'bottom layer' = the sediments immediately below the plough-soil. P = phosphates, Fe = iron, Zn = zinc. The black straight lines represent the profiles. The interpolation shows equidistant contour lines. The higher the concentration, the darker the colour. It becomes increasingly unreliable the more distant it is from the profiles. The exact values measured for all of the central chemical elements are given in Appendix 1. Co-ordinates in metres in UTM system 32.

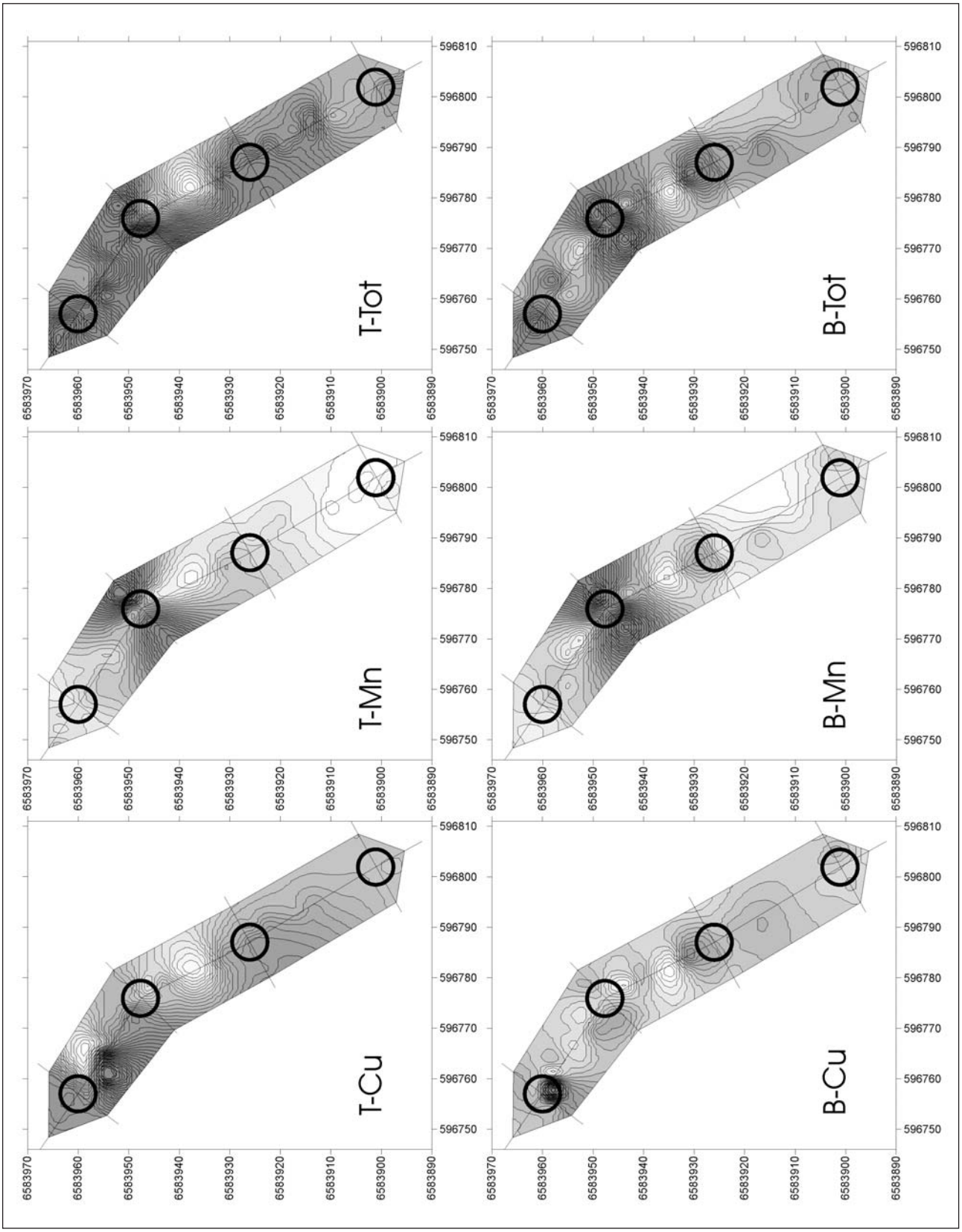

Fig. 7 Site B, Tøstad Øvre Farm. The variation in the central chemical components analysed for. The first letters 'T' and 'B' indicate that the data are from the 'top layer' = the plough-soil, or the 'bottom layer' = the sediments immediately below the plough-soil. Cu = copper, Mn = manganese, Tot = the total variation: the maximum value of each of the five central chemical elements analysed for is set to 100% so that their maxima are equal. Then the values are added. The black straight lines represent the profiles. The interpolation shows equidistant contour lines. The higher the concentration, the darker the colour. It becomes increasingly unreliable the more distant it is from the profiles. The exact values measured for all of the central chemical elements are given in Appendix 1. Co-ordinates in metres in UTM system 32.

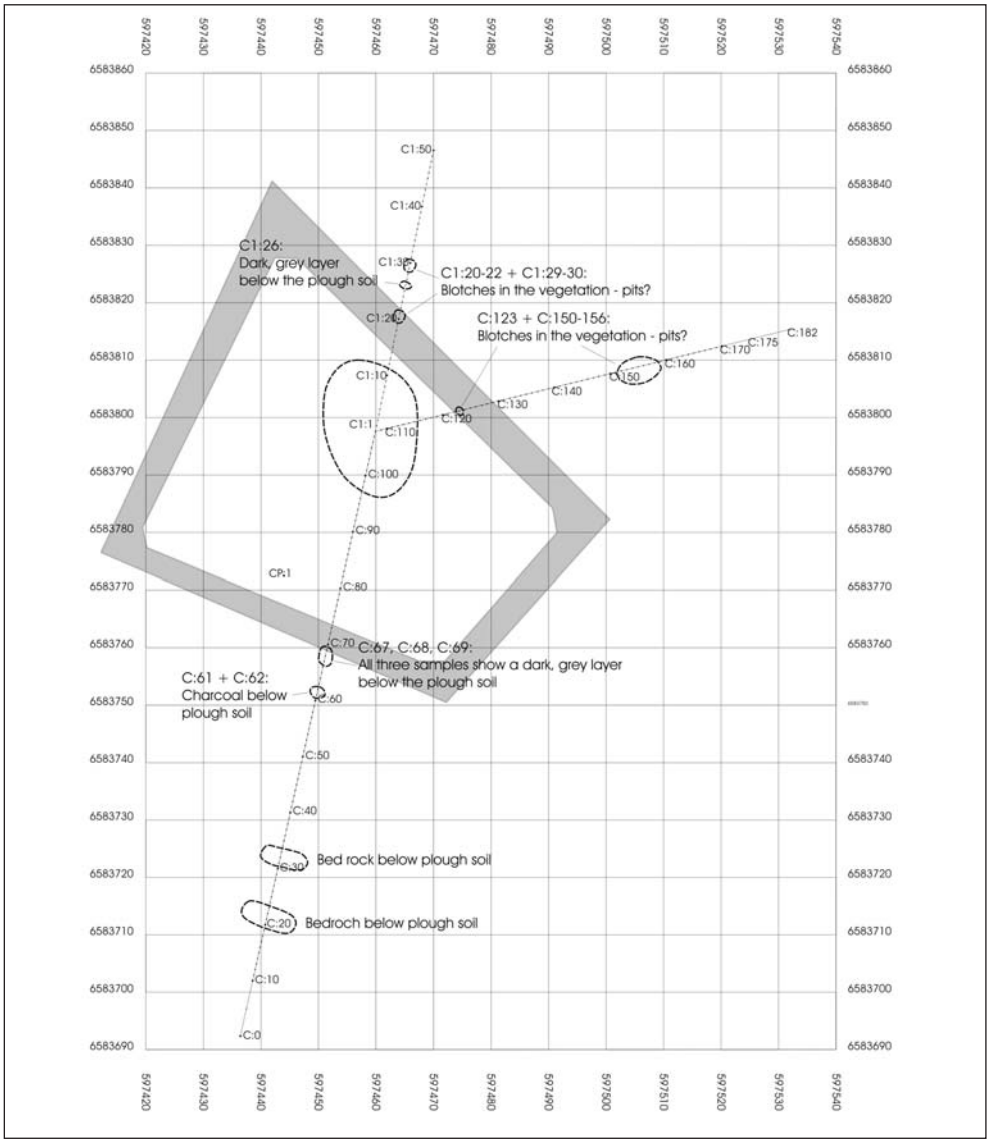

Fig. 8 Site C, Navestad Farm. Profiles through the rhombic feature that may represent a second Early Medieval church in Rygge, a couple of anomalies (C:20-35) that reflect the presence of bedrock immediately below the plough horizon, and a couple of blotches in the vegetation (C1:20 and C1:50), which may represent pits. Co-ordinates in metres in UTM system 32.

Fig. 10 Site C, Navestad Farm. The variation in phosphates (P) below the plough-soil shows local minima that coincide with the rhombic feature and massive maxima immediately outside it, indicating that it physically has influenced the activities. Co-ordinates in metres in UTM system 32.

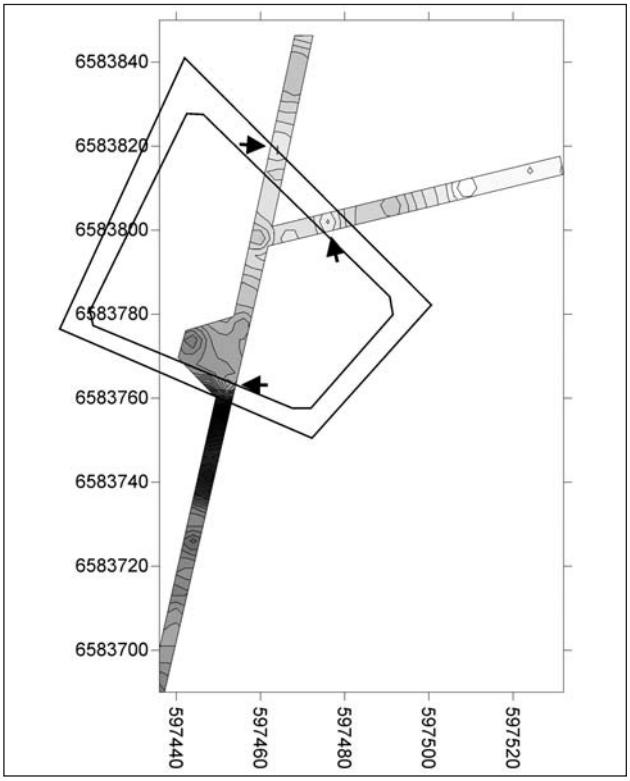

Fig. 9 Loom weight found on top of the hill with the rhombic feature at Navestad Farm – site C. Viking Age or the Early Medieval Period.

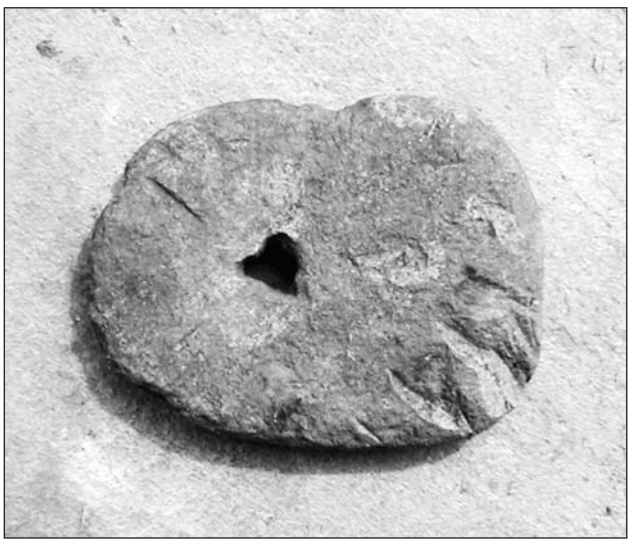

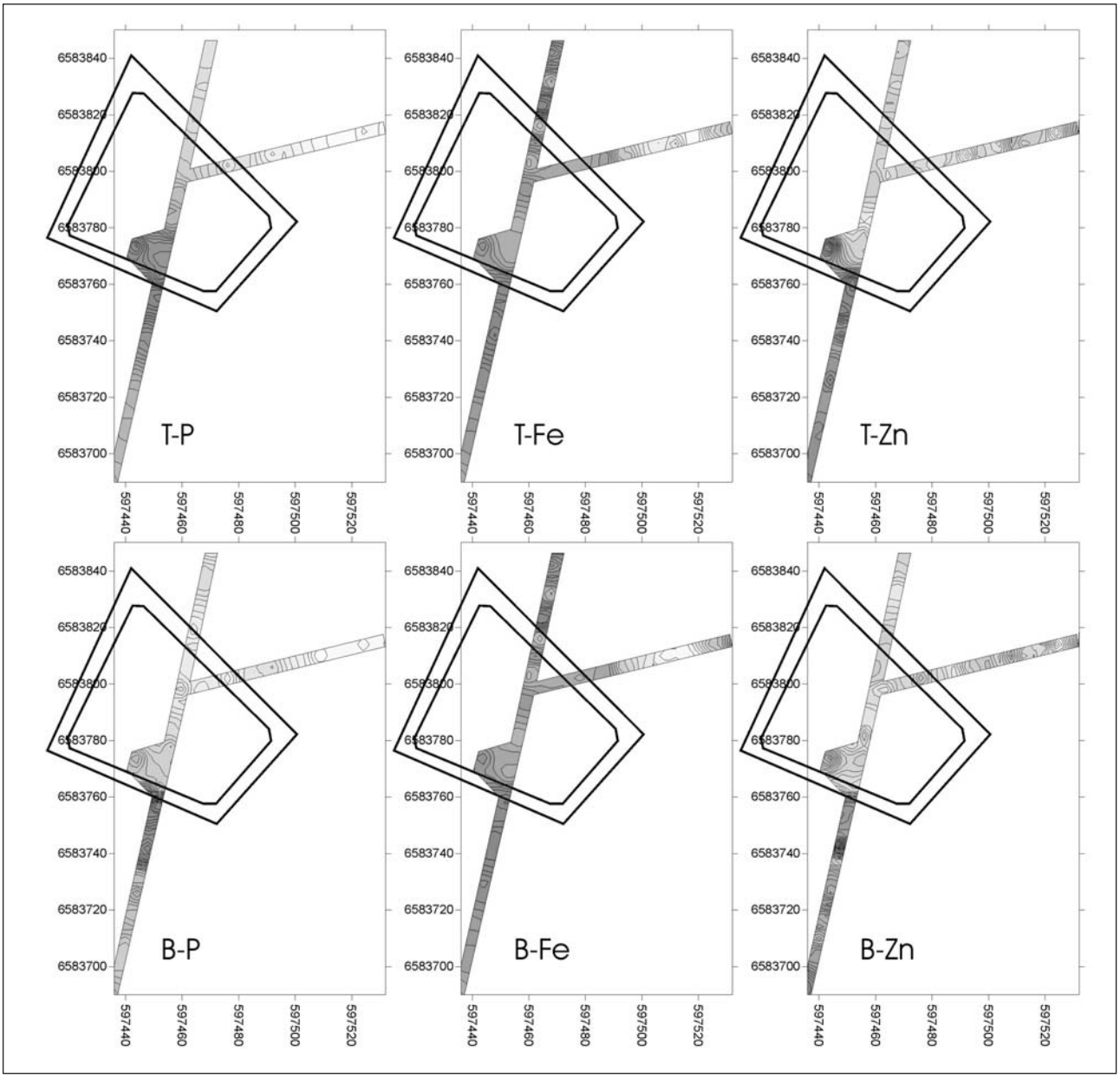

Fig. 11 Site C, Navestad Farm. The variation in the central chemical components analysed for. The first letters 'T' and 'B' indicate that the data are from the 'top layer' = the plough-soil, or the 'bottom layer' = the sediments immediately below the plough-soil. P = phosphates, Fe = iron, Zn = zinc. The interpolation shows equidistant contour lines. The higher the concentration, the darker the colour. The exact values measured for all of the central chemical elements are given in Appendix 1. Co-ordinates in metres in UTM system 32.

Fig. 12 (Top, right) Site C, Navestad Farm. The variation in the central chemical components analysed for. The first letters 'T' and 'B' indicate that the data are from the 'top layer' = the plough-soil, or the 'bottom layer' = the sediments immediately below the plough-soil. Cu = copper, Mn = manganese, Tot = the total variation: the maximum value of each of the five central chemical elements analysed for is set to 100% so that their maxima are equal. Then the values are added. The interpolation shows equidistant contour lines. The higher the concentration, the darker the colour. The exact values measured for all of the central chemical elements are given in Appendix 1. Co-ordinates in metres in UTM system 32.

significance (figs. 11 and 12). Because it matches the position of the existing Rygge Church inside its dyke, one could guess that this concentration reflects the location of a church building – even though a better coverage with chemical samples is necessary to support such an idea in a more concrete way. A logical next step would be to remove the plough-soil in a couple of ditches to see wheter the remains of a church can be observed.

Fig. 13 (Right) The sites D and G, Gipsund Farm. To the left: Plan of the profiles through two features interpreted as the remains of mounds. Co-ordinates in metres in UTM system 32. To the right the location of the site (IKONOS - copyright: Space Imaging and the Satellite Data Archive of the Norwegian Mapping Authority).

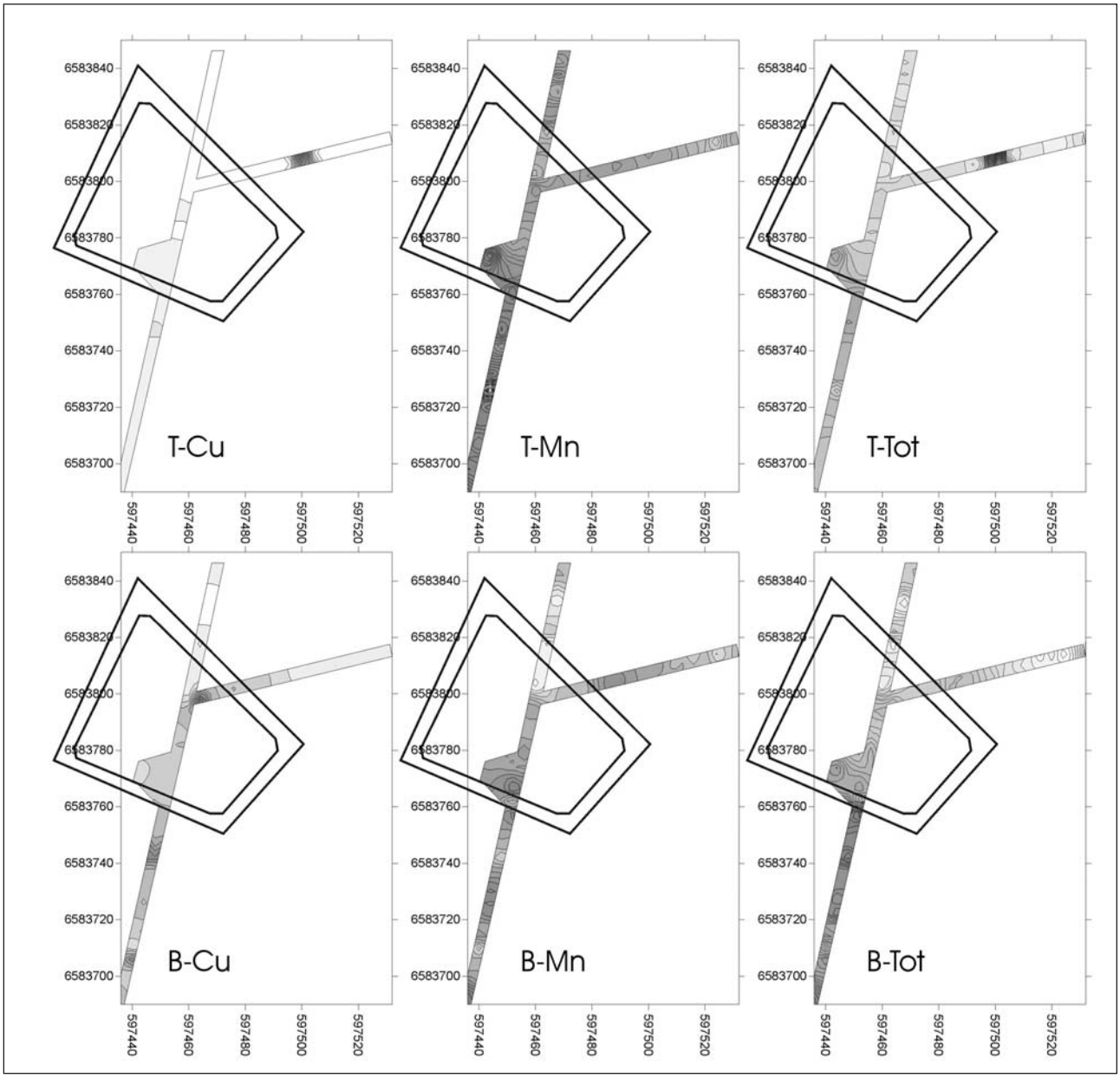
T-Cu
T-Mn
T-Tot
B-Cu
B-Mn
B-Tot
6583840
6583820
6583800
6583780
6583760
6583740
6583720
6583700
597440
597460
597480
597500
597520

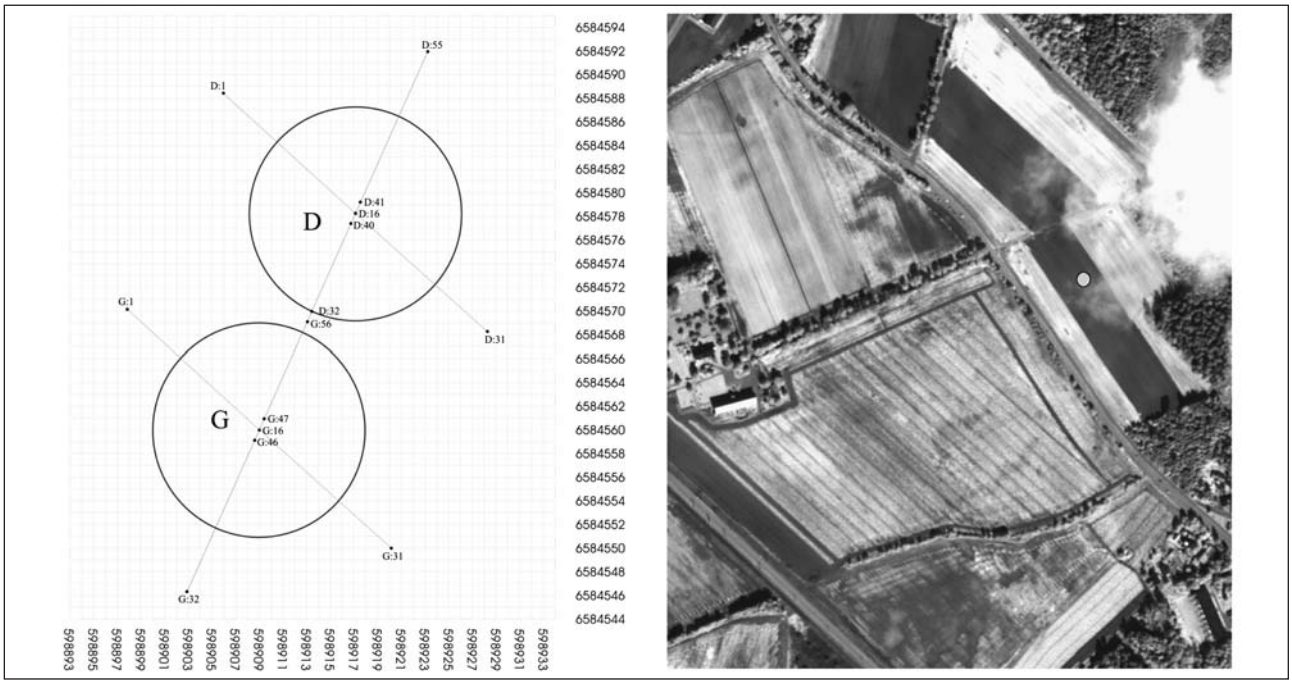
D:55
D:1
D:41
D:16
D:40
D
D:32
G:56
D:31
G:1
G:47
G:16
G:46
G
G:31
G:32
6584594
6584592
6584590
6584588
6584586
6584584
6584582
6584580
6584578
6584576
6584574
6584572
6584570
6584568
6584566
6584564
6584562
6584560
6584558
6584556
6584554
6584552
6584550
6584548
6584546
6584544
598893
598895
598897
598899
598901
598903
598905
598907
598909
598911
598913
598915
598917
598919
598921
598923
598925
598927
598929
598931
598933

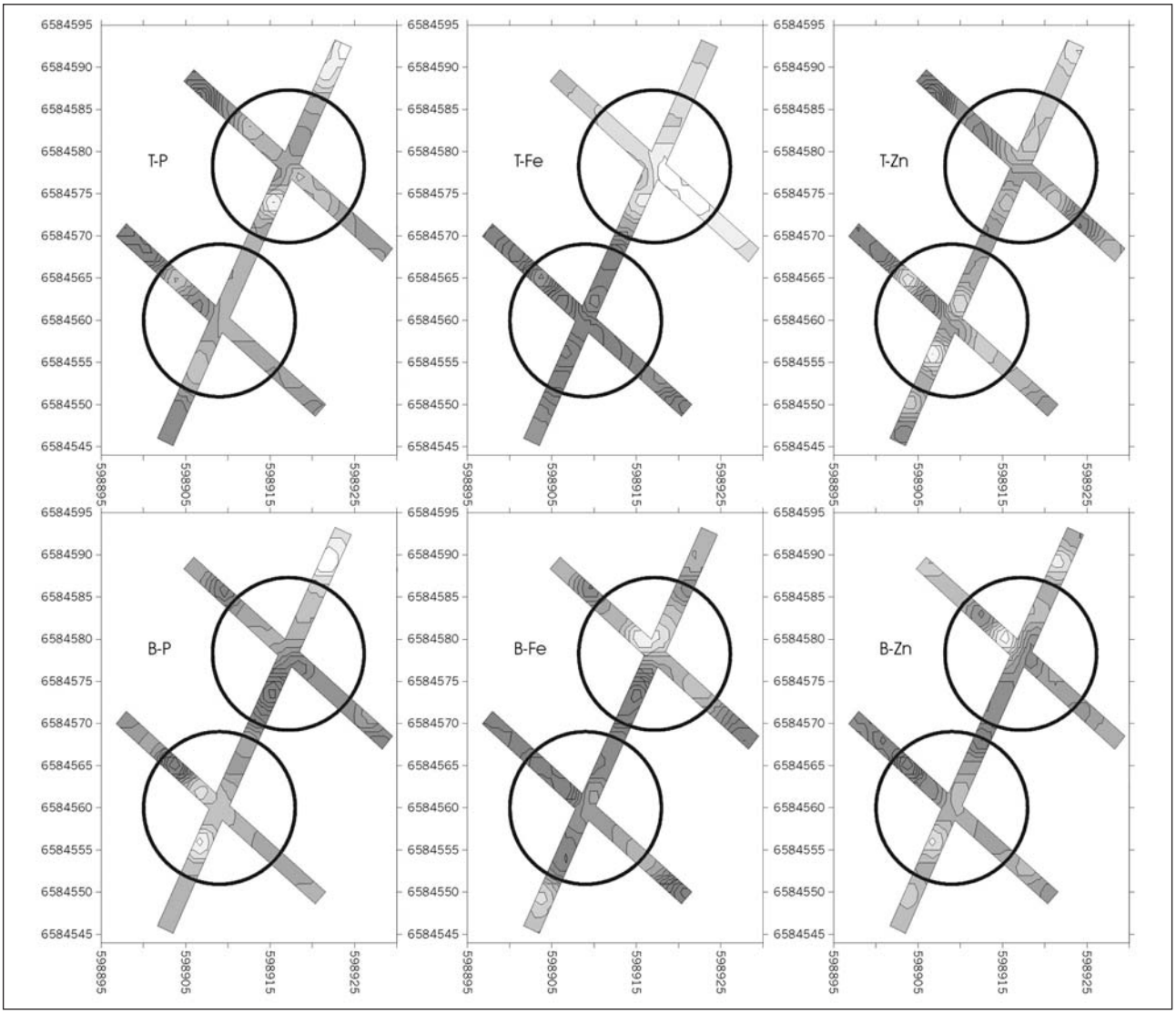

Fig. 14 The sites D and G, Gipsund Farm. The variation in the central chemical components analysed. The first letters 'T' and 'B' indicate that the data are from the 'top layer' = the plough-soil, or the 'bottom layer' = the sediments immediately below the plough-soil. P = phosphates, Fe = iron, Zn = zinc. The interpolation shows equidistant contour lines. The higher the concentration, the darker the colour. The exact values measured for all of the central chemical elements are given in Appendix 1. Co-ordinates in metres in UTM system 32.

Fig. 15 (Top, right) The sites D and G, Gipsund Farm. The variation in the central chemical components analysed. The first letters 'T' and 'B' indicate that the data are from the 'top layer' = the plough-soil, or the 'bottom layer' = the sediments immediately below the plough-soil. Cu = copper, Mn = manganese, Tot = the total variation: the maximum value of each of the five central chemical elements analysed for is set to 100% so that their maxima are equal. Then the values are added. The interpolation shows equidistant contour lines. The higher the concentration, the darker the colour. The exact values measured for all of the central chemical elements are given in Appendix 1. Co-ordinates in metres in UTM system 32.

A couple of anomalies observed in the IKONOS image on the southern slope up to the rhombic feature (C:20-35) appeared to be reflections of bedrock that in this place runs immediately below the plough-soil and thus prevents its draining. Water-deposited sand observed below the plough-soil on the lower part of this side of the hill must reflect phases when it formed part of the seashore.

3.a.4. The sites D and G, Gipsund Farm: The supposed two mounds D and G on Gipsund Farm were each cut by two profiles with samples for each metre.

Fig. 16 (Right) Site E, Gipsund Farm. To the left: Plan of the profiles through the feature interpreted as the remains of a mound. Co-ordinates in metres in UTM system 32. To the right the location of the site (IKONOS - copyright: Space Imaging and the Satellite Data Archive of the Norwegian Mapping Authority).

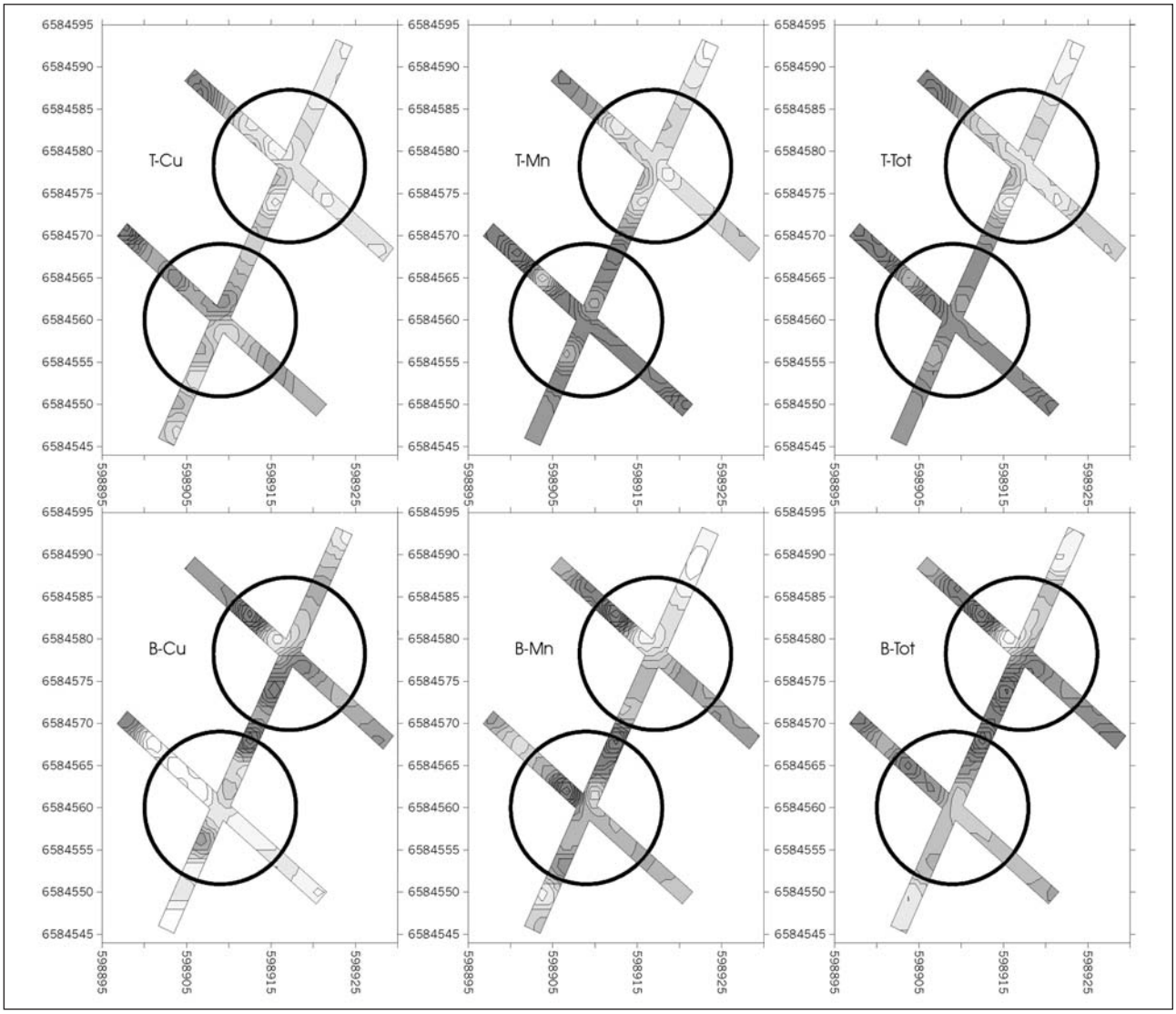
T-Cu
T-Mn
T-Tot
B-Cu
B-Mn
B-Tot
6584595
6584590
6584585
6584580
6584575
6584570
6584565
6584560
6584555
6584550
6584545
598895
598905
598915
598925

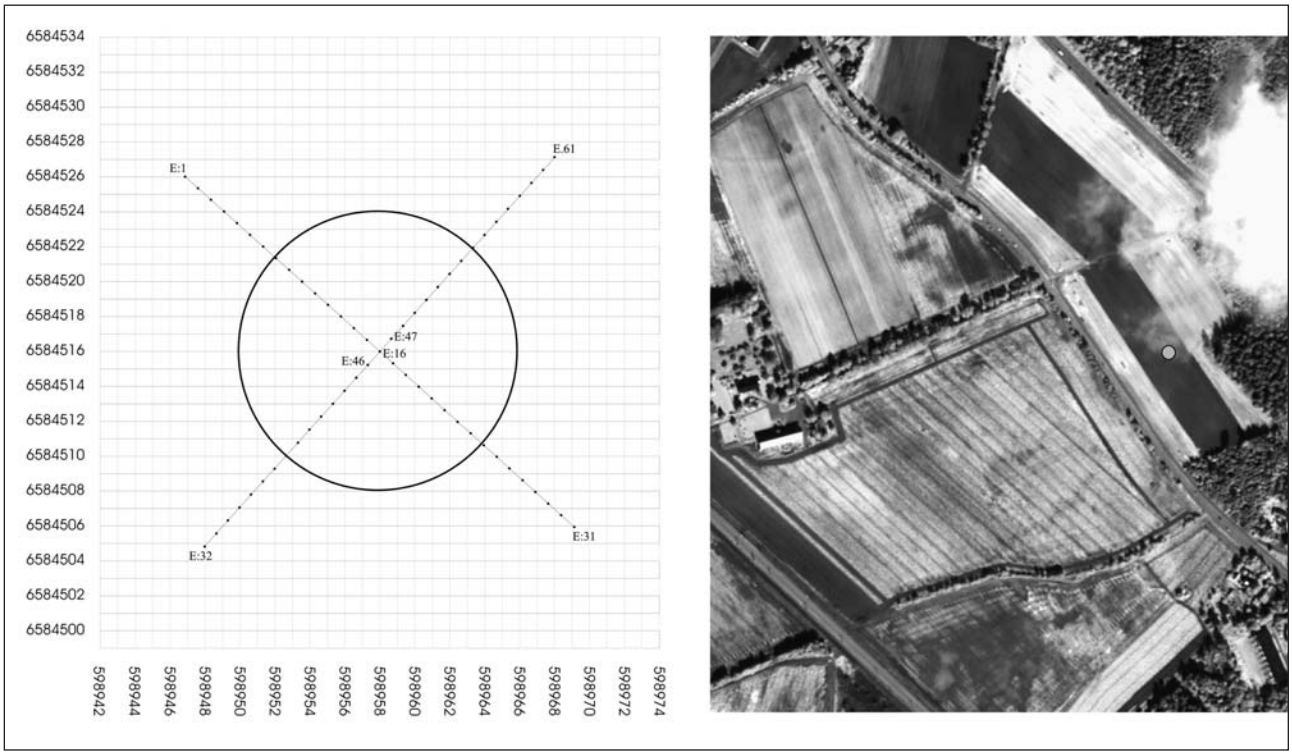
E:1
E.61
E:47
E:16
E:46
E:31
E:32
6584534
6584532
6584530
6584528
6584526
6584524
6584522
6584520
6584518
6584516
6584514
6584512
6584510
6584508
6584506
6584504
6584502
6584500
598942
598944
598946
598948
598950
598952
598954
598956
598958
598960
598962
598964
598966
598968
598970
598972
598974

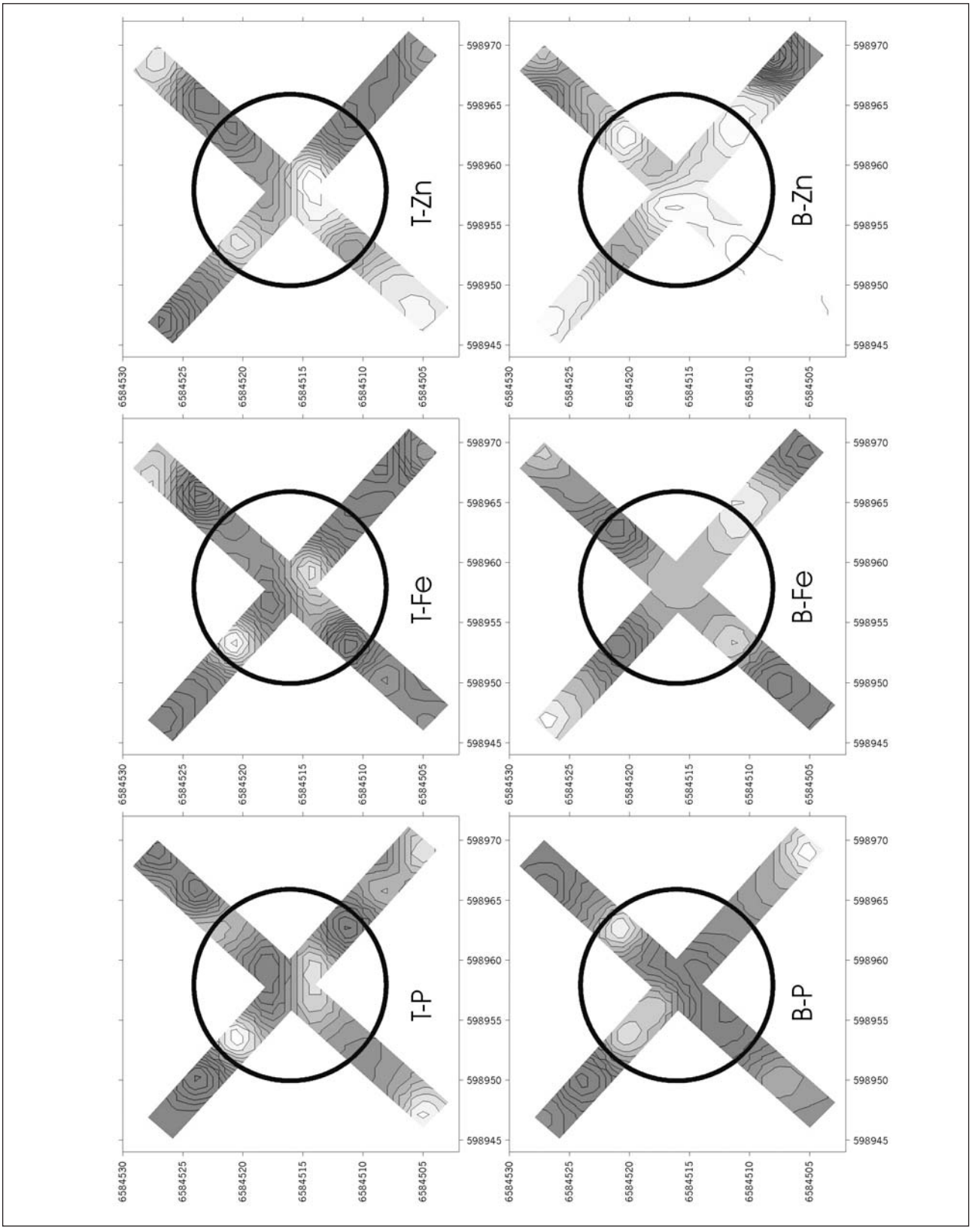

Fig. 17 Site E, Gipsund Farm. The variation in the central chemical components analysed. The first letters 'T' and 'B' indicate that the data are from the 'top layer' = the plough-soil, or the 'bottom layer' = the sediments immediately below the plough-soil. P = phosphates, Fe = iron, Zn = zinc. The interpolation shows equidistant contour lines. The higher the concentration, the darker the colour. The exact values measured for all of the central chemical elements are given in Appendix 1. Co-ordinates in metres in UTM system 32.

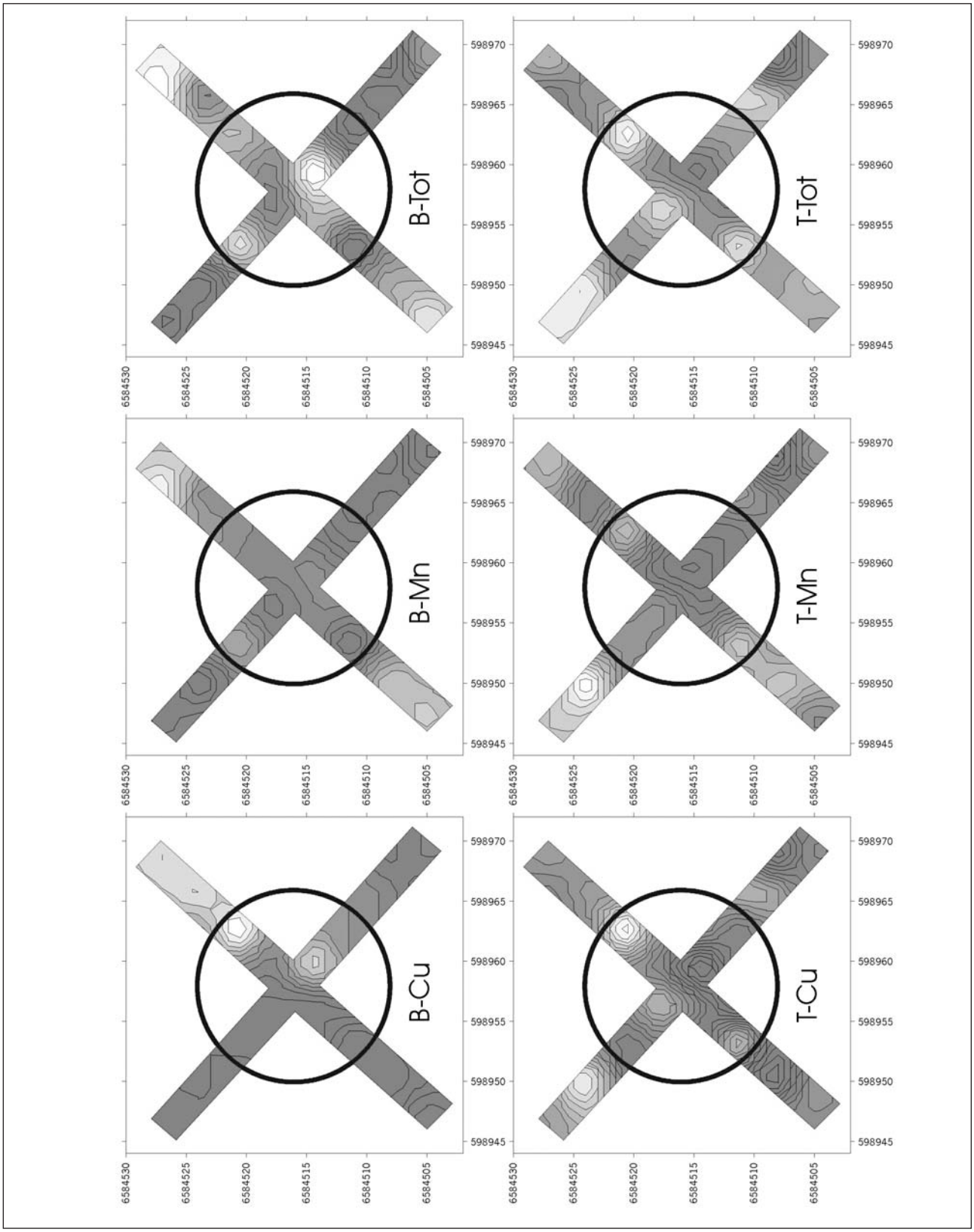

Fig. 18 Site E, Gipsund Farm. The variation in the central chemical components analysed. The first letters 'T' and 'B' indicate that the data are from the 'top layer' = the plough-soil, or the 'bottom layer' = the sediments immediately below the plough-soil. Cu = copper, Mn = manganese, Tot = the total variation: the maximum value of each of the five central chemical elements analysed for is set to 100% so that their maximums are equal. Then the values are added. The interpolation shows equidistant contour lines. The higher the concentration, the darker the colour. The exact values measured for all of the central chemical elements are given in Appendix 1. Co-ordinates in metres in UTM system 32.

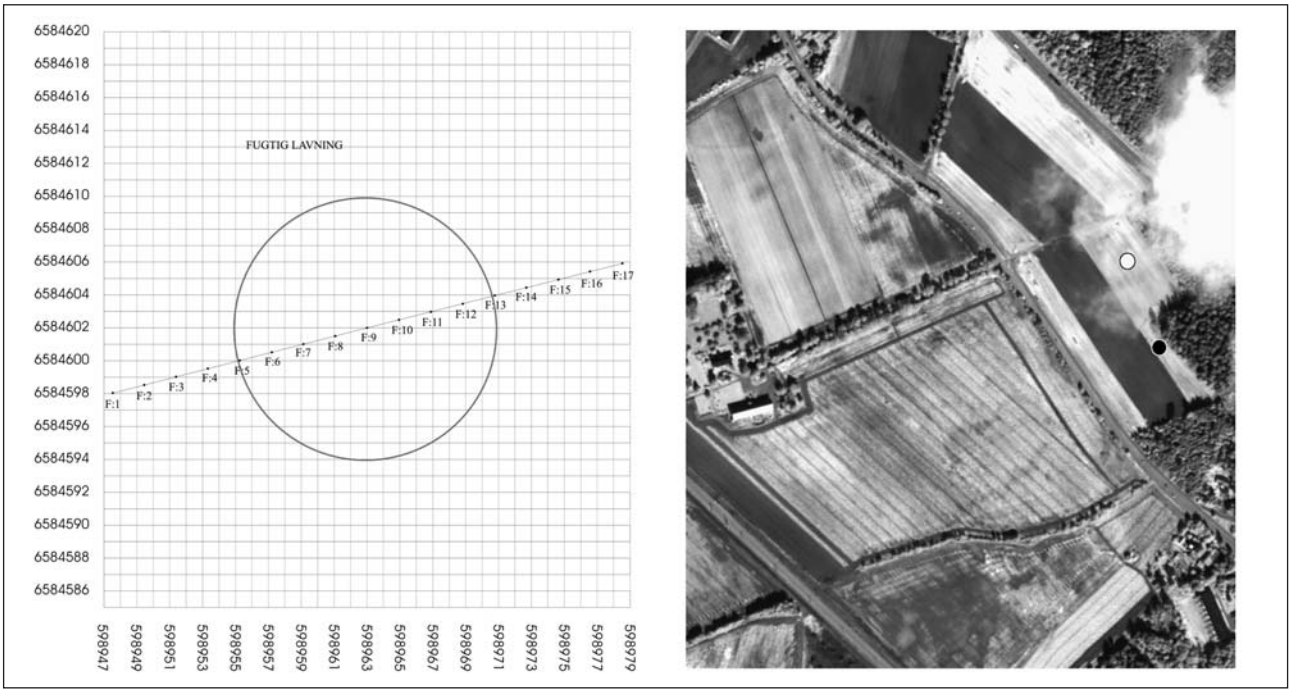

Fig. 19 Site F, Gipsund Farm. To the left: Plan of the profiles through site F - a moist low part of the field that in the satellite images looked like the remains of a mound. Co-ordinates in metres in UTM system 32. To the right the location of site F (white dot) and site H (black dot), (IKONOS - copyright: Space Imaging and the Satellite Data Archive of the Norwegian Mapping Authority).

Fig. 20 (Below) Site F, Gipsund Farm. The variation in the concentration of the four central chemical elements that could be registered at levels above the measuring uncertainty. The first letters 'T' and 'B' indicate that the data are from the 'top layer' = the plough-soil, or the 'bottom layer' = the sediments immediately below the plough-soil. P = phosphates, Fe = iron, Zn = zinc, Mn = manganese. The exact values for all of the central chemical elements are given in Appendix 1.

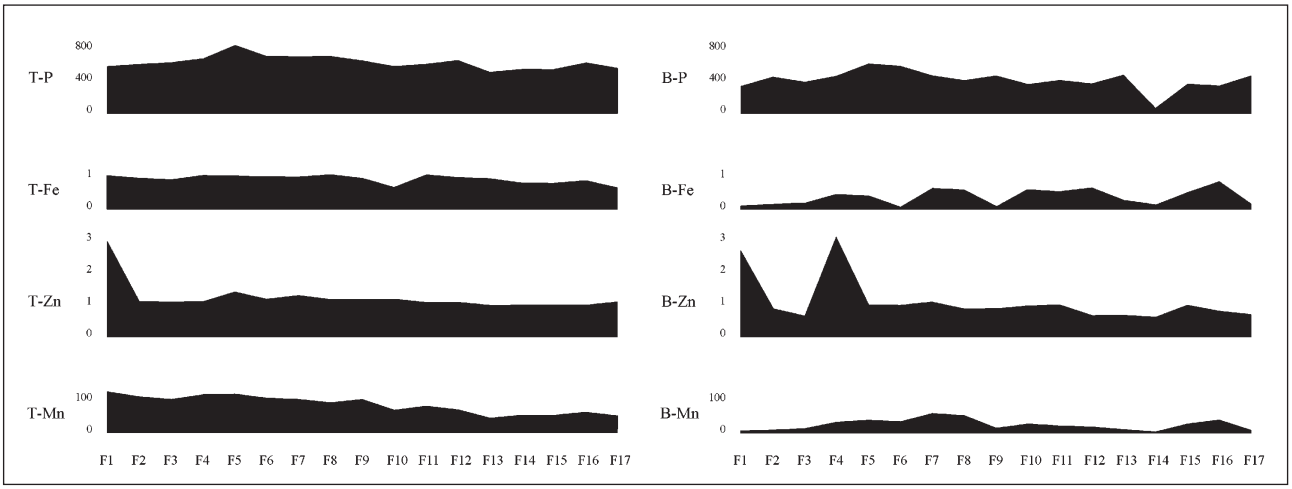

The iron (Fe) below the plough-soil appears in peripheral concentrations in relation to the two suggested mounds. The position of these concentrations indicating that the profiles do not cut each other exactly in the centres of the two features. Between them is a relatively large and significant concentration that may well reflect overlapping peripheral features (B-Fe in fig. 14). Phosphates (P), copper (Cu), and manganese (Mn) under the plough-soil follow the same pattern, with peripheral and no central concentrations – and the two latter display with a smaller 'diameter' than iron (Fe) and manganese (Mn). Zinc (Zn) below the plough-soil also displays a peripheral pattern, but with a tendency to a concentration centrally in the northern feature as well (figs.14 and 15).

3.a.5. Site E, Gipsund Farm: The supposed mound E on Gipsund Farm was cut by two profiles with samples for each metre.

The iron (Fe) below the plough-soil seems concentrated in a circular structure a bit larger and with its centre a few metres to the south of the suggested mound. The phosphates (P) below the plough-soil display a large and significant concentration centrally in the feature, as well as out-

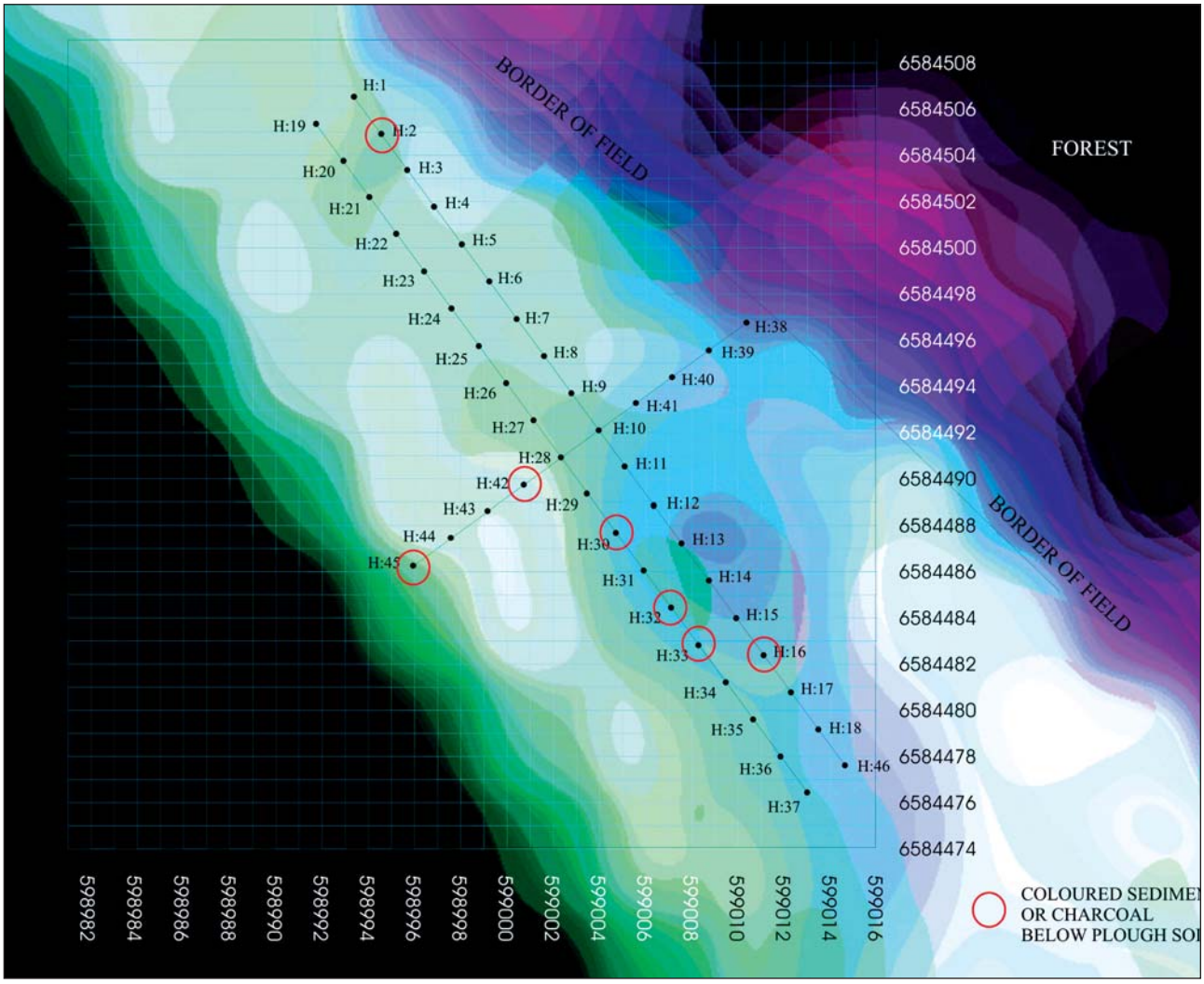

Fig. 21 Site H, Gipsund Farm. Profiles through a feature interpreted as a settlement – most likely from the Stone Age. The measuring grid has been superimposed on a multispectral IKONOS image. The different layers of the image have been weighted to optimise the information immediately around the site. As a consequence, the different crop to the right in the picture appears as a dark area. The dark zone in the upper left corner is forest. The dark blotch around the points H:13-16 coincides with the maximum concentration of the central chemical elements registered in the profiles (fig. 24). Co-ordinates in metres in UTM system 32 (IKONOS - copyright: Space Imaging and the Satellite Data Archive of the Norwegian Mapping Authority).

side the concentrations of iron (Fe) to the north. Interestingly, the concentrations of iron and phosphates appear as spatially well-organised features that exclude each other. Zinc (Zn), copper (Cu), and manganese (Mn) below the plough-soil display a peripheral pattern, the two latter with a central concentration in addition (figs. 17 and 18).

3.a.6. Site F, Gipsund Farm: A single profile with samples for each 2 metre was cut through the anomaly representing a moist low part of the field, because of its immediate similarity with a mound. It is regarded as important to collect data that can elucidate the difference between cultural heritage sites and natural phenomena of similar appearance.

The variation in the concentration of the different chemical elements analysed for is in this case considerably less than at the supposed cultural heritage sites. The concentration of copper was too low to be measured.

3.a.7. Site H, Gipsund Farm: An observed anomaly coinciding with a concentration of worked flints in the field.

The small concentration of worked flints, site H, has for many years been known by Mrs. Ragnhild Sørenssen from Gipsund Farm, who has collected worked flints on the site (fig.19). The material yields no exact typological dating for the feature, and it cannot be ruled out that the site is as late as the Early Bronze Age. However a Stone Age dating seems more likely.

In some of the samples taken under the plough-soil charcoal was observed and in the sampling points H:30-33 a

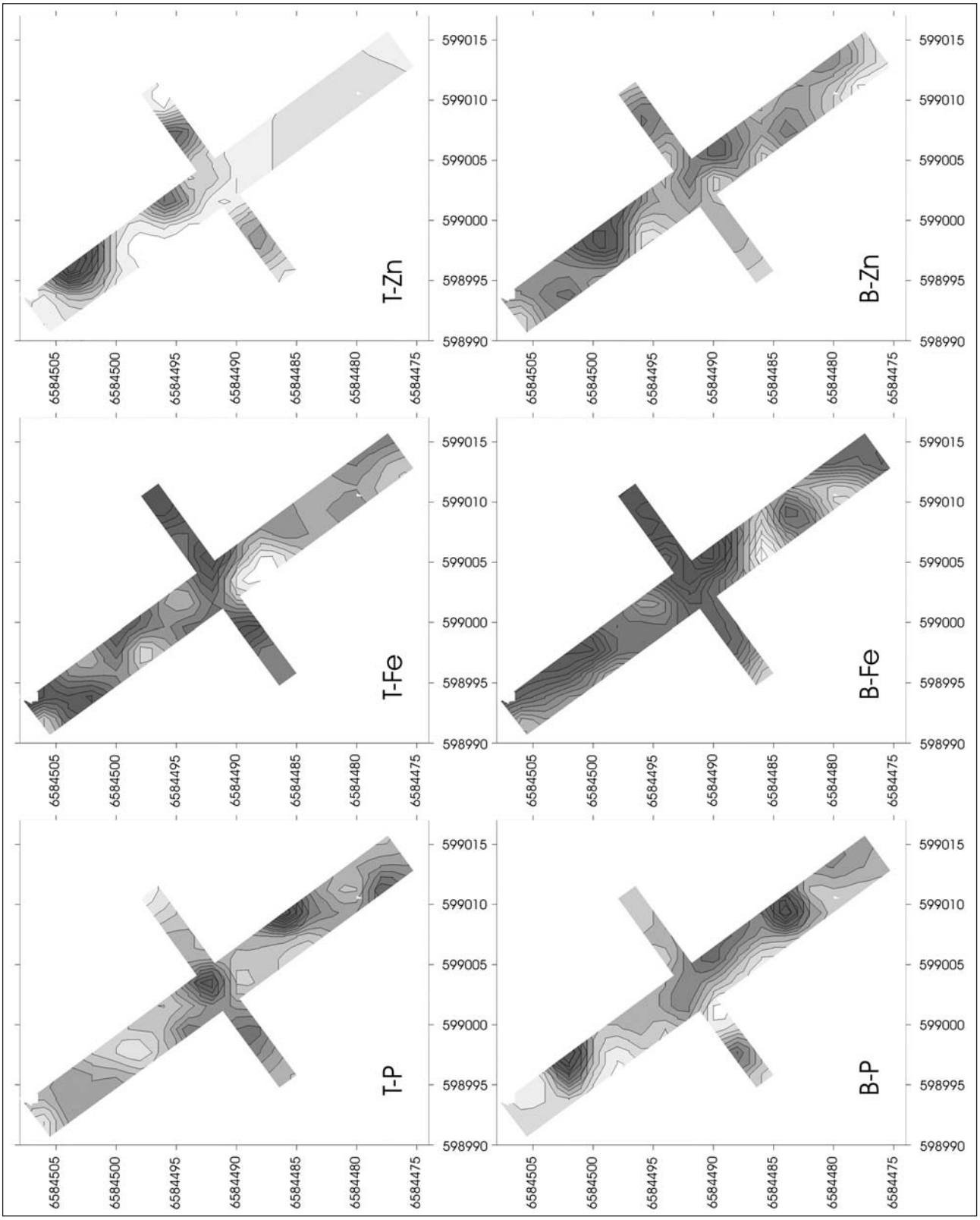

Fig. 22 Site H, Gipsund Farm. The variation in the central chemical components analysed. The first letters 'T' and 'B' indicate that the data are from the 'top layer' = the plough-soil, or the 'bottom layer' = the sediments immediately below the plough-soil. P = phosphates, Fe = iron, Zn = zinc. The interpolation shows equidistant contour lines. The higher the concentration, the darker the colour. The exact values measured for all of the central chemical elements are given in Appendix 1. Co-ordinates in metres in UTM system 32.

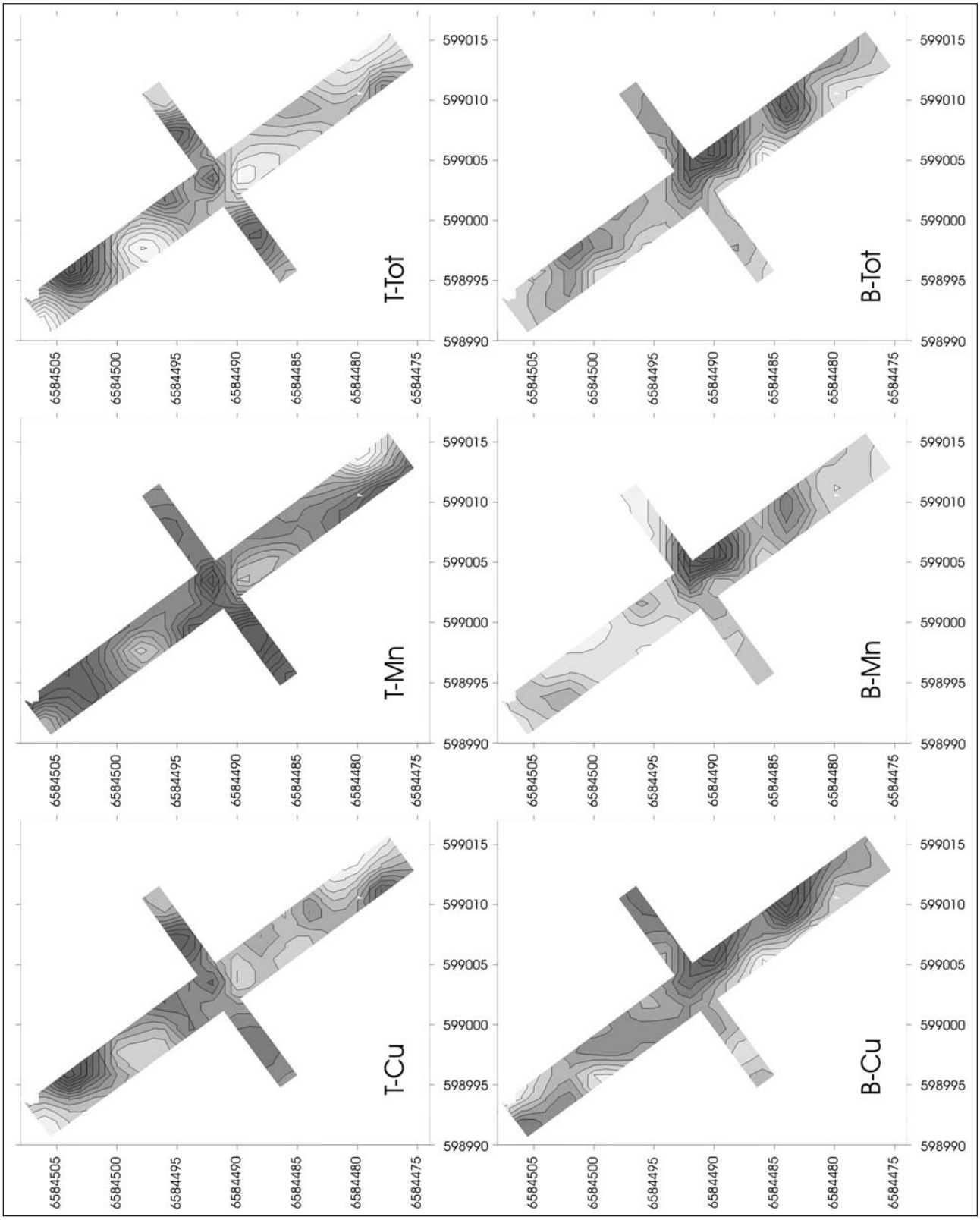

Fig. 23 Site H, Gipsund Farm. The variation in the central chemical components analysed. The first letters 'T' and 'B' indicate that the data are from the 'top layer' = the plough-soil, or the 'bottom layer' = the sediments immediately below the plough-soil. Cu = copper, Mn = manganese, Tot = the total variation: the maximum value of each of the five central chemical elements analysed for is set to 100%, so that their maxima are equal. The interpolation shows equidistant contour lines. The higher the concentration, the darker the colour. The exact values measured for all of the central chemical elements are given in Appendix 1. Co-ordinates in metres in UTM system 32.

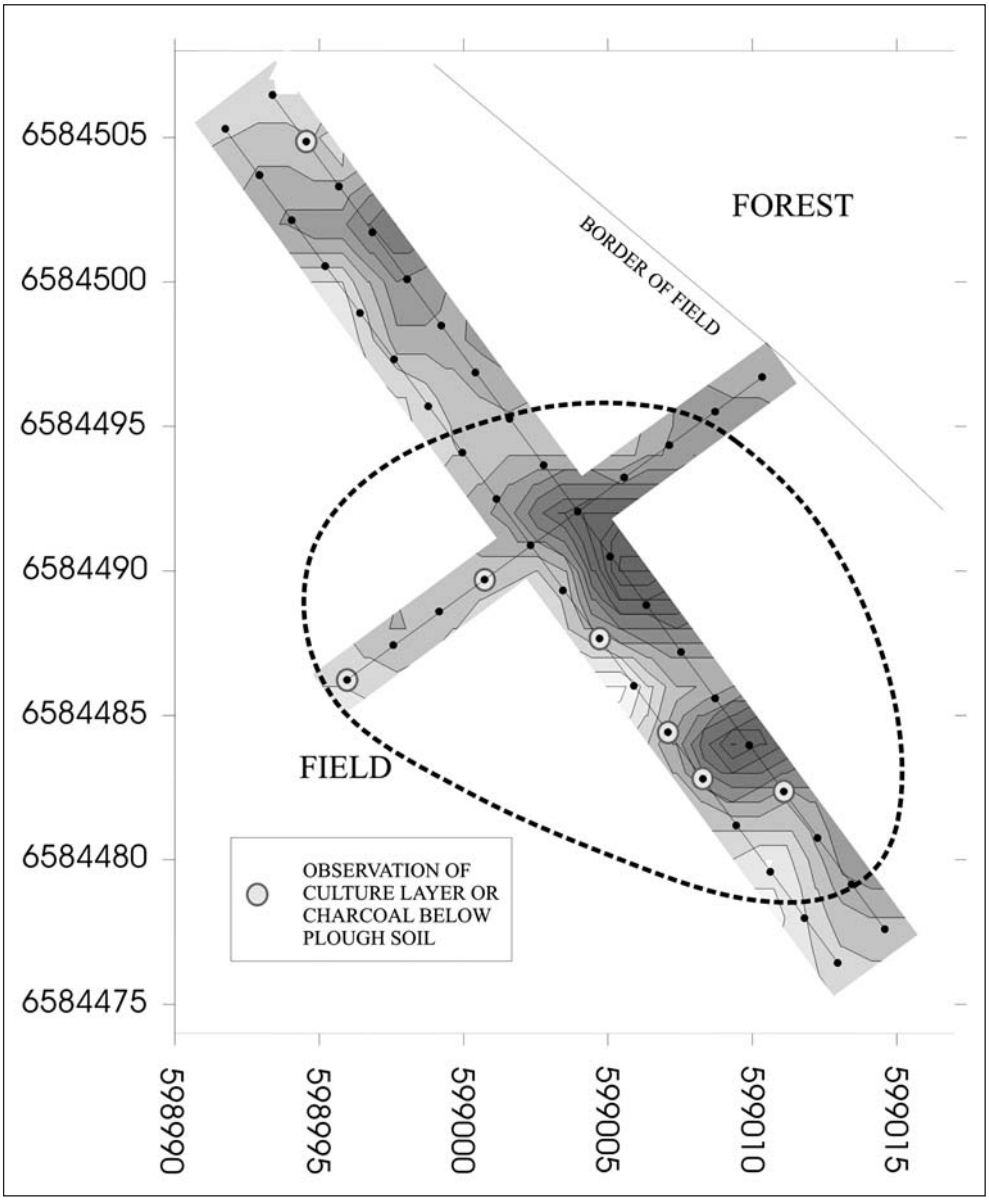

Fig. 24 Site H, Gipsund Farm. The total variation (Tot) of the central chemical elements analysed for is shown. It appears to be related to the sampling points where charcoal or culture layer was observed below the plough-soil as well as the blotch that can be observed in the multispectral data (fig. 21). The broken line shows the area where high values for the chemical elements coincide with the observed cultural features, as should be expected in a central settlement area. Co-ordinates in metres in UTM system 32.

dark layer was observed that may well represent the preserved remains of a shallow dugout dwelling (fig. 21).

Down the slope to the south-west, from some metres below the level of the site, are below the plough-soil more or less well-preserved remains of a layer of water-deposited clay (observed in profile J – site J). This most likely reflects that the site was formerly located close to a quite protected shore with sedimentation of fine-grained material.

Whereas the central chemical components analysed for below the plough-soil are concentrated in the southeastern part of the area – and thus coincide with the blotch that can be observed in the IKONOS image – the chemical components in the plough-soil itself concentrate in its northern part (figs. 21-24). It should be noted that the satellite image in this case seems to reflect the situation below the plough-soil.

3.a.8. Site I, Gipsund Farm: A 2 by 2 m grid was laid out to get an idea of the character of the feature I interpreted as a house. The strategy was to elucidate the relation between the inner part of the structure and the area around in its central part (fig. 25).

Below the plough-soil the central chemical components analysed for all concentrate within two oblong NE-SW orientated features about 5 m from each other and displaced about 3 m to the east in relation to the expected wall lines of the house. Apart from iron (Fe), which also displays a small concentration to the west of the more westerly of these two features, the concentrations are low between and outside them (figs. 26-28).

The same two features can be distinguished in the plough-soil, but here with an additional concentration in the western part of the sampled area (figs. 26-28).

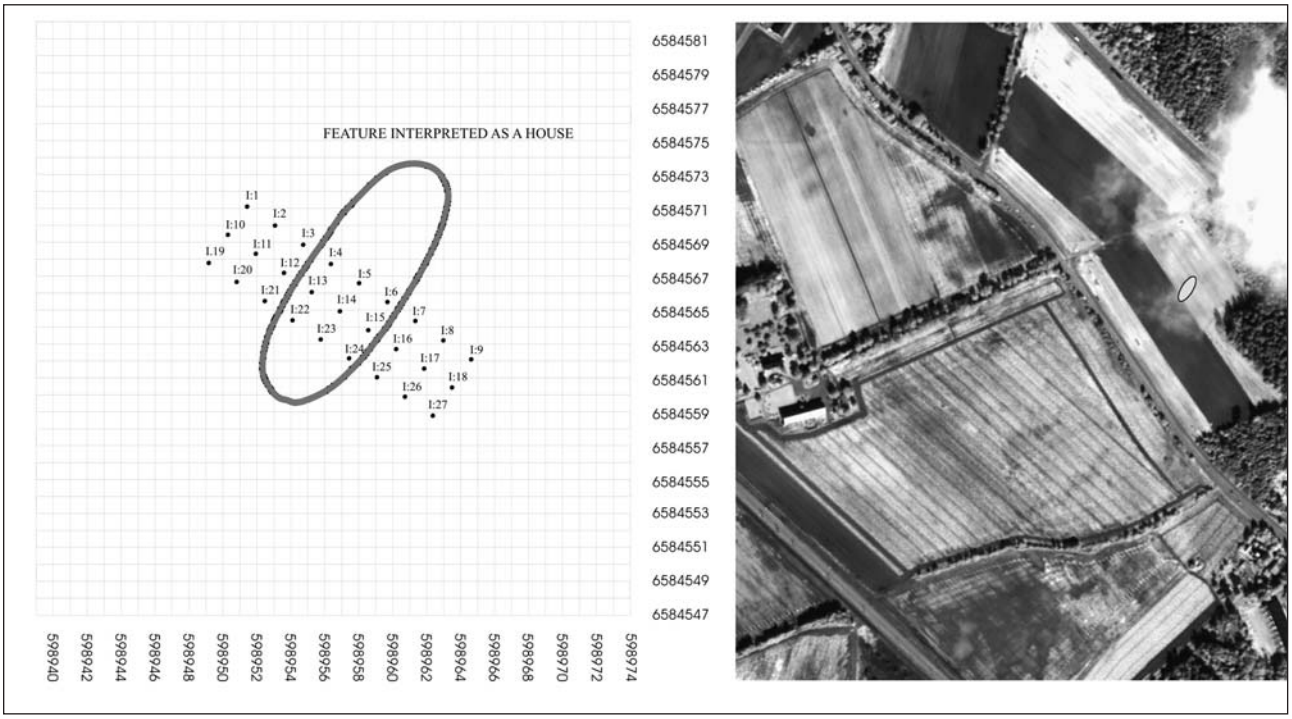

Fig. 25 Site I, Gipsund Farm. To the left: Plan of the profiles through a feature interpreted as a house. The sampling points are shown. Co-ordinates in metres in UTM system 32. To the right the location of the site (IKONOS - copyright: Space Imaging and the Satellite Data Archive of the Norwegian Mapping Authority).

It seems likely that the bipartite pattern with two oblong features can represent the chemical signatures of the wall lines of a prehistoric house – either 'foreign' material from the walls (clay brought in from another location, for instance) or waste deposited immediately outside them. The error of position can well be due to the uncertainties concerning the positions mentioned earlier (fig. 28).

3.a.9. Site J, Gipsund Farm: A profile with 1-2 m between the samples was made to get further information about the supposed continuation of a preserved piece of an old hollow road in the forest immediately to the SE (fig. 29). Samples taken in 2002 suggest that there are several parallel tracks connected to the road (Grøn and Loska 2002).

It is interesting but not surprising that the concentrations of the central chemical elements analysed for vary significantly more just within a zone 3-4 m from the old road than anywhere else in the profile. Normally old roads show a tendency to meander. Therefore it is far from unreasonable if the road is reflected in such a broad zone. It is suggested that a couple of extra profiles cutting the proposed road be made here. A linear feature coinciding with the expected road can be observed in the IKONOS image.

3.a.10. Site K, Børsebakke Farm: Sample points laid out to elucidate the differences between anomalies interpreted as possible pits, a couple of possible houses, and their immediate surroundings. Large amounts of lithic artefacts (flint, stone axes, etc.) from the Late Neolithic/Early Bronze Age have been found in the fields at this site.

Samples were taken in the plough-soil, immediately below it, and to the east of the road, furthermore 30-40 cm below its bottom, because the sediment here was coloured in a way indicating that it could be a cultural deposit. The results of the chemical analysis, however, indicate that there is no significant difference between the supposed pits and the areas outside them. The dark blotches interpreted as pits may represent tree-falls or other natural phenomena that have brought natural colouring of the subsoil up into the plough soil (fig. 30).

The only sample that differs significantly from the average values is K:7 from the westernmost anomaly interpreted as a house (figs. 30, 31). It is suggested that a more detailed investigation be carried out of this anomaly.

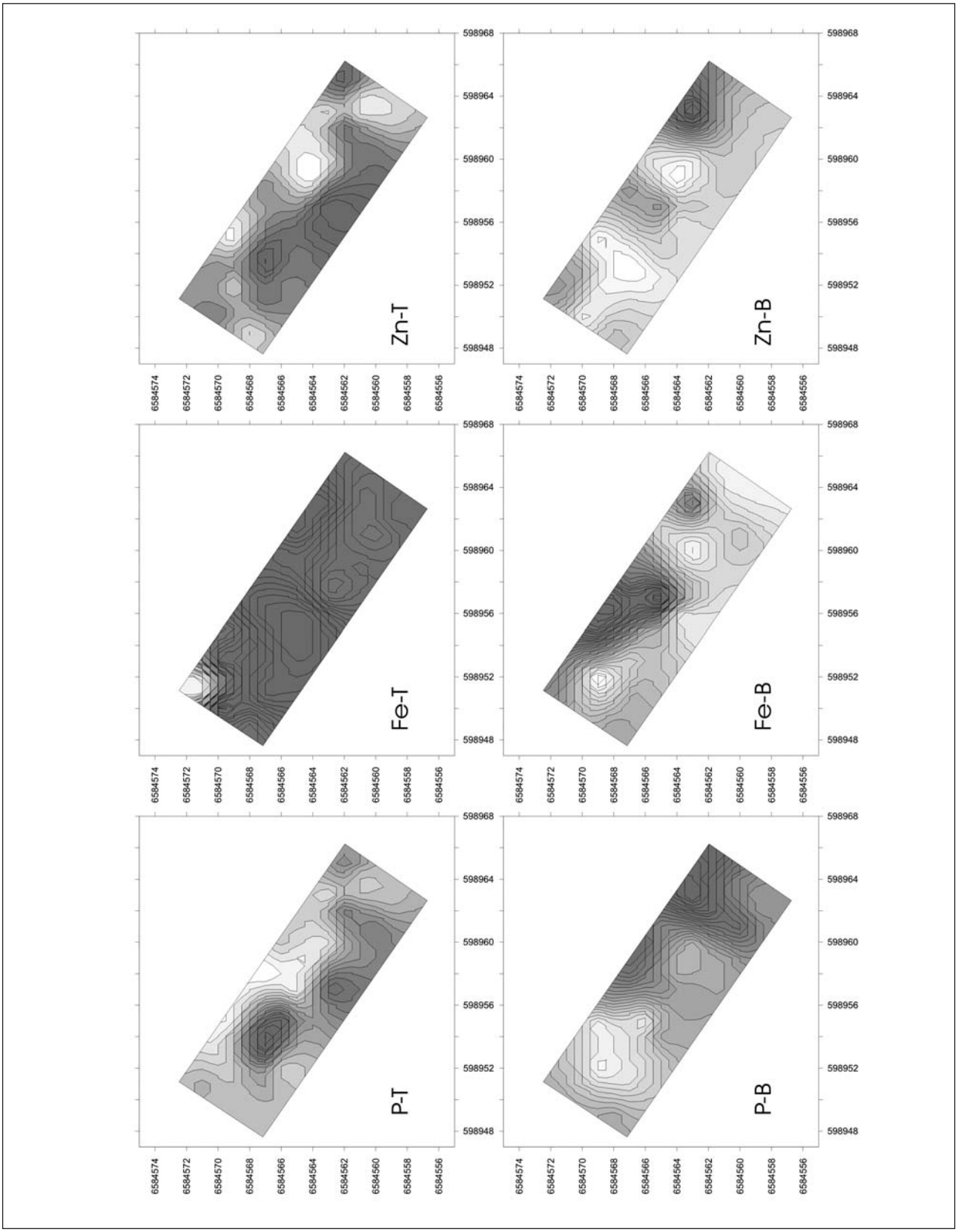

Fig. 26 Site I, Gipsund Farm. A site interpreted as a house. The variation in the central chemical components analysed. The first letters 'T' and 'B' indicate that the data are from the 'top layer' = the plough-soil, or the 'bottom layer' = the sediments immediately below the plough-soil. P = phosphates, Fe = iron, Zn = zinc. The interpolation shows equidistant contour lines. The higher the concentration, the darker the colour. The exact values measured for all of the central chemical elements are given in Appendix 1. Co-ordinates in metres in UTM system 32.

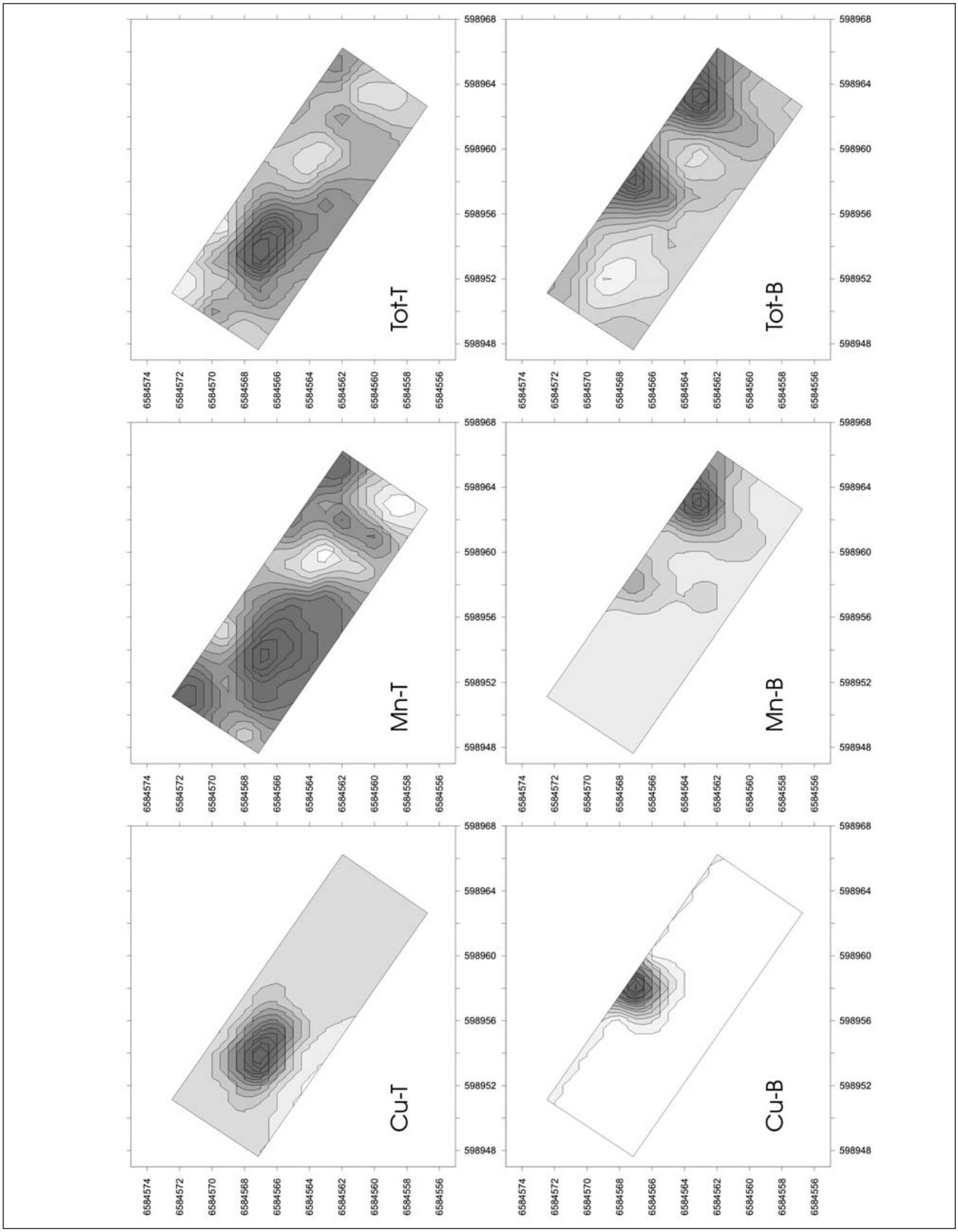

Fig. 27 Site I, Gipsund Farm. A site interpreted as a house. The variation in the central chemical components analysed. The first letters 'T' and 'B' indicate that the data are from the 'top layer' = the plough-soil, or the 'bottom layer' = the sediments immediately below the plough-soil. Cu = copper, Mn = manganese, Tot = the total variation: the maximum value of each of the five central chemical elements analysed for is set to 100% so that their maxima are equal. The interpolation shows equidistant contour lines. The higher the concentration, the darker the colour. The exact values measured for all of the central chemical elements are given in Appendix 1. Co-ordinates in metres in UTM system 32.

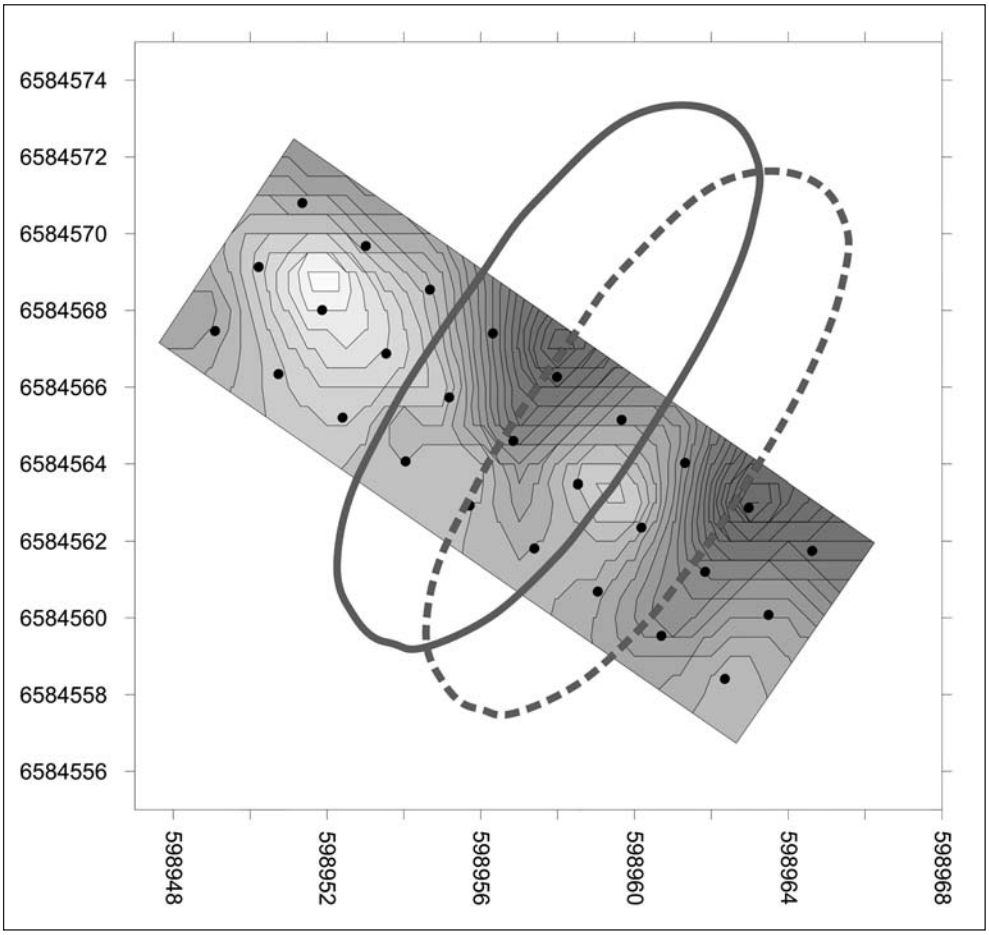

Fig. 28 Site I, Gipsund Farm. The total variation (Tot) of the central chemical elements analysed for is shown. It appears to be related to the sampling points where charcoal or culture layer was observed below the plough-soil as well as the blotch that can be observed in the multispectral data (fig. 21). The broken line shows an area where high values for the chemical elements coincide with the observed cultural features, as it should in a central settlement area. Co-ordinates in metres in UTM system 32.

Fig. 29 Site J, Gipsund Farm. To the left: Plan of the profile cutting the course of an old hollow road a few meters from this feature's NW end. The sampling points are shown. The variation in the concentrations of the zinc (Zn), phosphates (P), iron (Fe), and manganese (Mn) below the plough-soil are shown. Copper (Cu) was below the measuring uncertainty. Co-ordinates in metres in UTM system 32. To the right the location of the site (IKONOS - copyright: Space Imaging and the Satellite Data Archive of the Norwegian Mapping Authority).

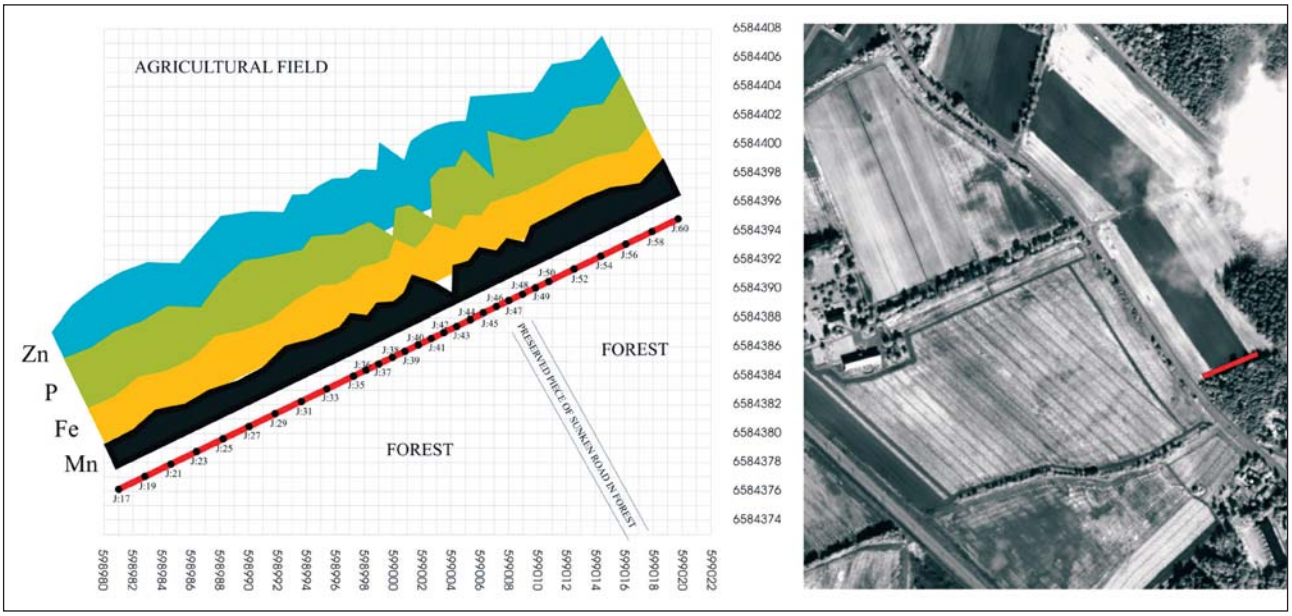

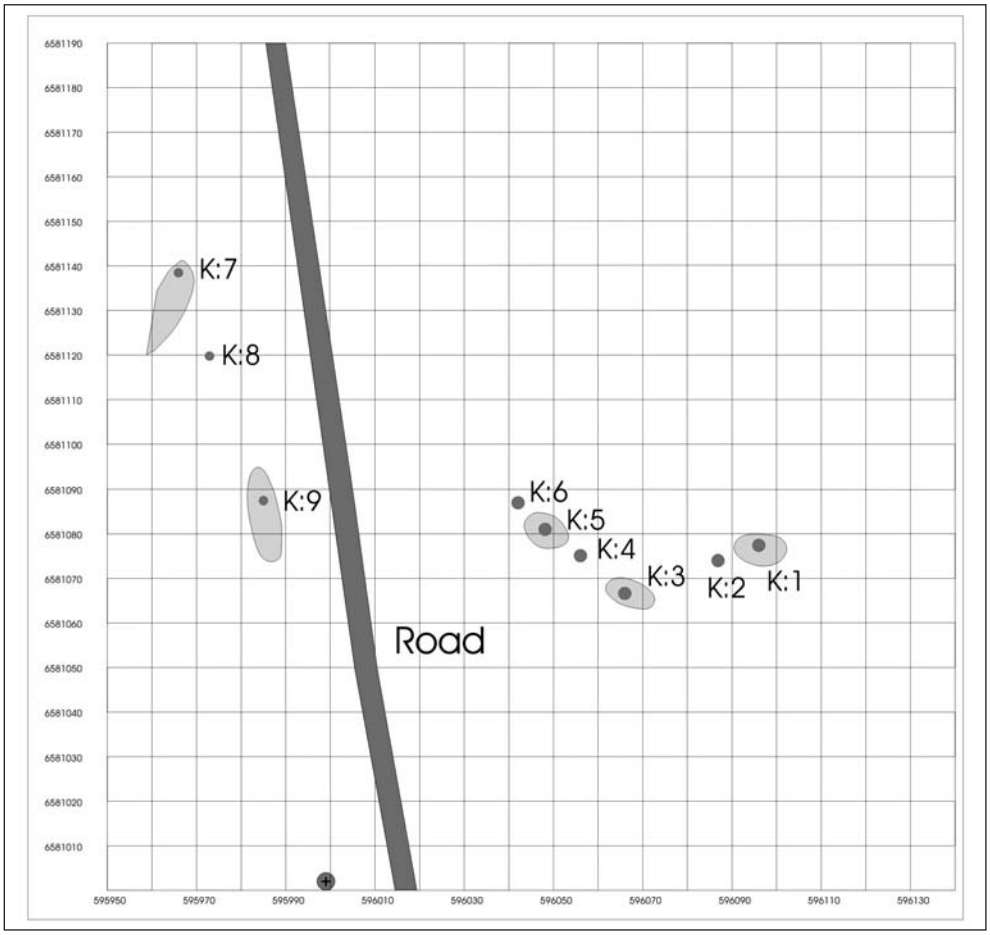

Fig. 30 Site K, Børsebakke Farm. Sampling points in - and outside features interpreted as possible houses to the right of the road and pits to the left of the road. Co-ordinates in metres in UTM system 32. The position of the site is shown in fig. 1.

Fig. 31 Børsebakke Farm – site K. The variation in the concentrations of phosphates (P), iron (Fe), zinc (Zn) and manganese (Mn) are shown. Copper (Cu) was below the measuring uncertainty. See fig. 30.

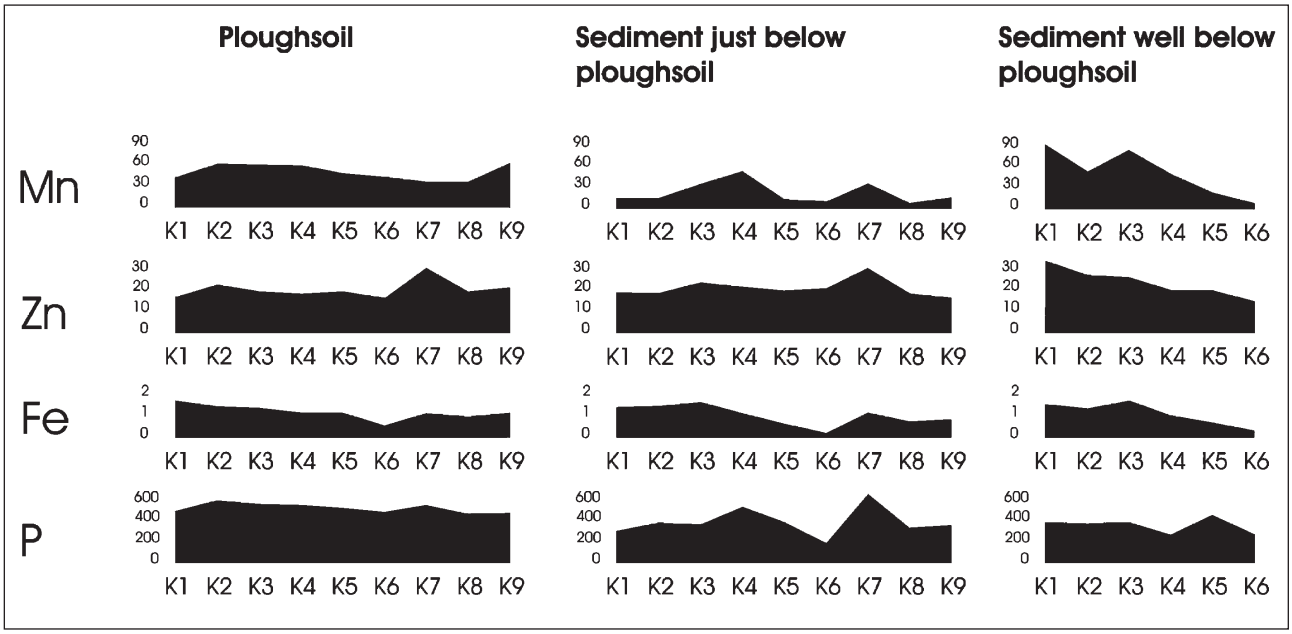

3.b. Metal-detectors

The use of metal-detectors is an obvious way of verifying the character of anomalies that are suspected of being cultural heritage sites. Once it is possible to focus the survey on restricted anomalies, this method has quite a potential for cultural heritage sites from most of the prehistoric periods. Åge Olsen has kindly provided co-ordinates of the finds he has made in the field near site F.

3.c. Ground-based vegetation analysis

Ground-based analysis of the variation in the vegetation composition of the observed anomalies as a means of better understanding their character has been discussed in the project. In the Rygge area, where forest or agricultural monocultures make up the majority of the landscape, it has, however, proved difficult to apply this method.

3.d Verification of observed anomalies - conclusion

Soil chemistry has demonstrated an unexpected potential as a basis for the development of indicators that can be used to verify or otherwise the character of the observed anomalies as cultural herittage sites. It would be obvious to continue the investigation of the chemical signatures of different cultural heritage sites as well as of modern anomalies that can be mistaken for such. The use of metal-detectors – even though it will not be useful in relation to sites from all periods – seems promising as a supplement to other methods.

Because multispectral satellite images seem to produce the best results with regard to distinction of cultural heritage sites when the vegetation is at a minimum, vegetation analysis will not be given priority in the present study.

Fig. 32 Large anomaly (site L) in field north of Gipsund Farm interpreted as a settlement area and shown with a broken blue line. Detector-finds (yellow dots) probably indicating bronze-casting show some relation to this anomaly and may indicate that the settlement area is larger than anticipated. The whole field was surveyed, but finds were made only in its eastern corner (IKONOS - copyright: Space Imaging and the Satellite Data Archive of the Norwegian Mapping Authority).

4. Detection of archeological features by automatic classification of multispectral satellite images

Parallel to and interacting with the development of a ground-methodology for verification of cultural heritage sites observed as anomalies, runs the development of methods for distinction of cultural heritage sites in the multispectral satellite images. An experiment was carried out with automatic classification of the multispectral satellite images by Hans Tømmervik, NINA, Tromsø.

4.a. Method

All satellite data were registered to a common UTM format (WGS-84, zone 32) with a spatial resolution of 25 m. The satellite images were divided into areas with the same colour, using a clustering algorithm (ISODATA) applied on all 6 optical bands. A similar method has been employed in a vegetation-monitoring project in the area of Nikel (Russia) with satisfactory results (Tømmervik et al. 1998). Means were computed to be along the first principal component (PCA) vector and were evenly distributed within the scaling range for the first principal component. The initial number of spectral classes was selected to 255 in order to detect and differentiate different vegetation types important for the reindeer. By using so many initial classes, the algorithm is comparable with hyper-clustering (Myers et al. 1999). The "hyper-clustering" procedure exploits the spatial structure of landscapes through image compression by hyper-clustering to detect patterns of vegetation cover types or environmental change (Myers and Shelton 1998, Myers 1999).

All 255 classes from the unsupervised classification phase were interpreted using colour-composites, spectral signatures, field data, and other sources of information. Based on
this information, it was attempted to link this classification product to archeological features.

4.b. Vegetation monitoring by vegetation indices

Vegetation indices are techniques of multispectral transformation of satellite image data. They use the phenomenon that different types of biomass reflect different amounts of energy in different bands. The reflectance from vegetation measured by any remote-sensing device is governed by the presence of absorbing pigments (i.e. chlorophyll) in the visible part of the spectrum and by multiple internal reflection in the leaves of the plants in the near infrared part of the spectrum. In healthy vegetation, the latter produces typical high reflectance in the near infrared band (Rees 1990).
The reflectance characteristics in the red and the infrared bands have been used to monitor vegetation with remote sensing, and a range of different vegetation indices have been proposed in order to estimate the amount, productivity and health condition of vegetation. Various mathematical combinations of spectral channels have been applied as sensitive indicators of the presence and condition of green vegetation (Tucker and Sellers 1986; Justice et. al. 1985). The simplest of the vegetation indices is the vegetation index (VI) defined as the ratio between the near-infrared channel and the red channel. The Normalised Difference Vegetation Index (NDVI) was found (Sellers 1986; Tucker and Sellers 1986; Prince 1991) to be a representative of plant assimilation condition and of its photosynthetic efficiency.

$$NDVI = (NIR-R)/(NIR+R) \qquad \text{(Eq. 1)}$$

where NIR is the reflectance in the near-infrared channel and R is the reflectance in the red channel. Vegetated areas in general yield high values for these indices due to their high near infrared reflectance and low visible reflectance. Reflectance for cloud, snow and water is larger in red than in near infrared. Hence, these features yield negative index values. Rock and bare soil have similar reflectances in red and near infrared channels and result in indices near zero.
The NDVI (and hence the VI) equation has a simple, open loop structure. This renders the NDVI susceptible to large sources of error and uncertainty over variable atmospheric and soil background conditions, imaging geometry, and with changes within the canopy itself (Sellers 1986; Jackson and Pinter 1986; Jackson and Huete 1991; and Myneni et. al. 1992). This is less than satisfactory in meeting the need for accurate detection of vegetation types and other features. Hence, several studies to improve the stability of the NDVI by correcting for soil and atmospheric sources of variance have been done. In our study we used several vegetation indices for detection of archeological features, etc.

4.c. Results

4.c.1. Automatic classification procedure

The IKONOS and Quicbird images were classified using the "hyper-clustering" classification procedure presented in 4.a. The images were clustered in 255 classes and the results are presented in the figs. 33 and 34. The use of over-lay techniques with the locations of the registered cultural heritage sites in the area did not reveal any significant relationship between the cluster-classes and the cultural remains unless for a couple of classes which consists of "islands of semi-natural vegetation" (not ploughed and treated) in the farmland. Here the relationship was significant and robust.

The Quickbird-image was influenced by clouds and was from the peak vegetation season. The IKONOS was from a better time of the season (September), but it would be relevant to try out images from the early growing season (spring) and with a higher sun elevation.

4.c.2 Vegetation indices

The figs. 35 and 36 present the normalised difference vegetation indices. No significant relationship was observed between the vegetation indices and the registered cultural heritage sites, unless for the "islands of semi-natural vegetation" (areas that are not ploughed due to exposed bed-rock or mounds that are difficult to remove). But also here could the time of the season play a major role. In the future other indices should be tested as the iron-oxide index which is the red band (band 3) divided with the blue band (band 1) which revealed some relationships between this index image and cultural remains (fig.47).

Even though there was no significant correlation between the results of the methods employed and the list of registered cultural heritage sites this analysis has resulted in the recognition of a number of anomalies that have not been distinguished in the visual inspection and may represent unregistered cultural heritage sites. It is planned to conduct fieldwork to confirm or reject their status as such.

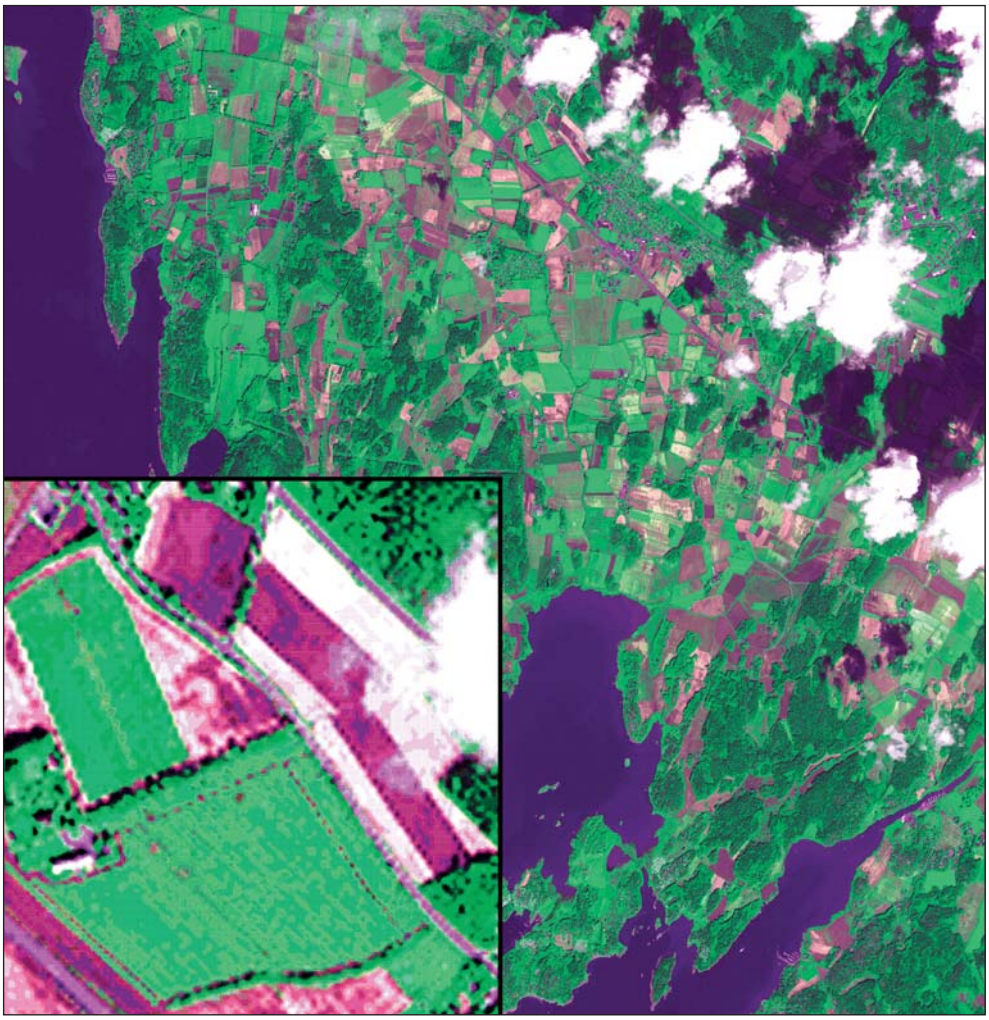

Fig. 33 The result of the automatic classification on the basis of the IKONOS image. Detail from Gipsund Farm in lower left corner (copyright: Space Imaging and the Satellite Data Archive of the Norwegian Mapping Authority).

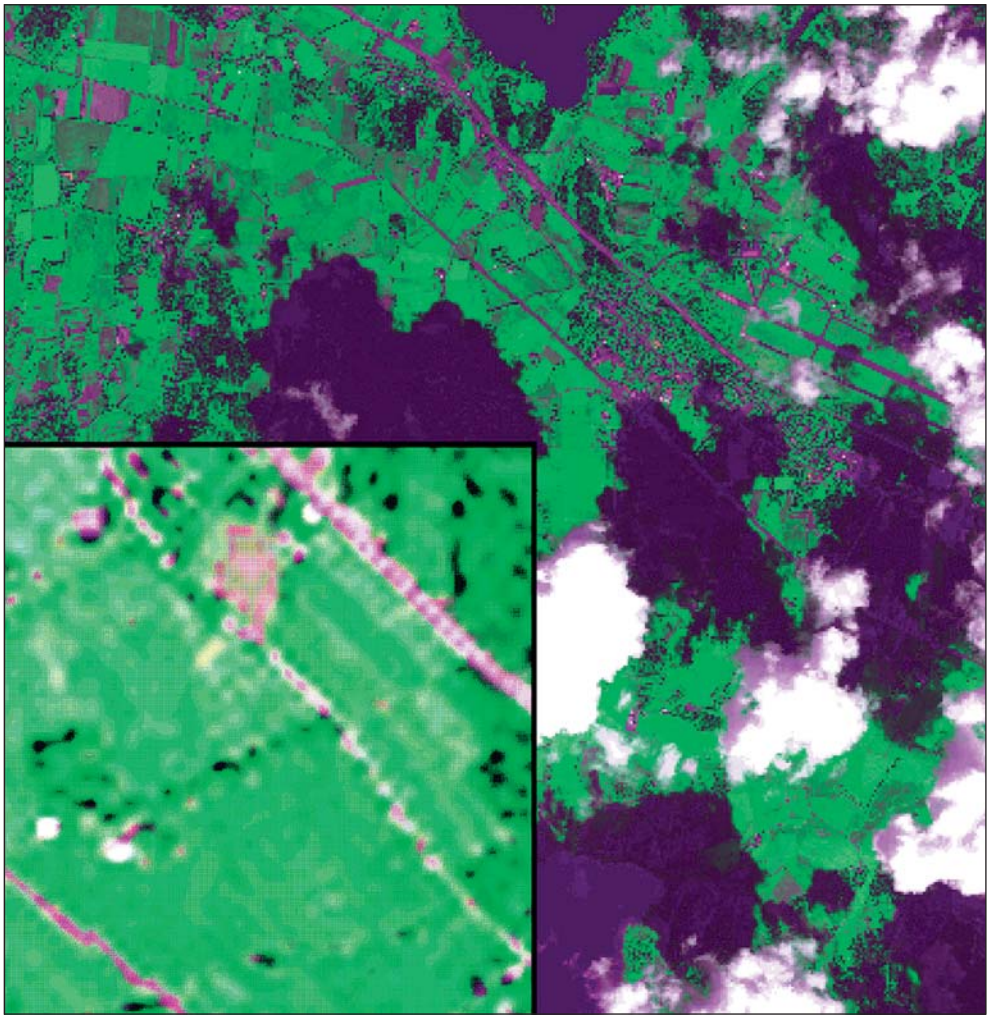

Fig.34 The result of the automatic classification on the basis of the Quickbird image. Detail from Gipsund Farm in lower left corner (copyright: Digital Globe and the Satellite Data Archive of the Norwegian Mapping Authority).

Fig.35 The vegetation index based on the IKONOS image (copyright: Space Imaging and the Satellite Data Archive of the Norwegian Mapping Authority).

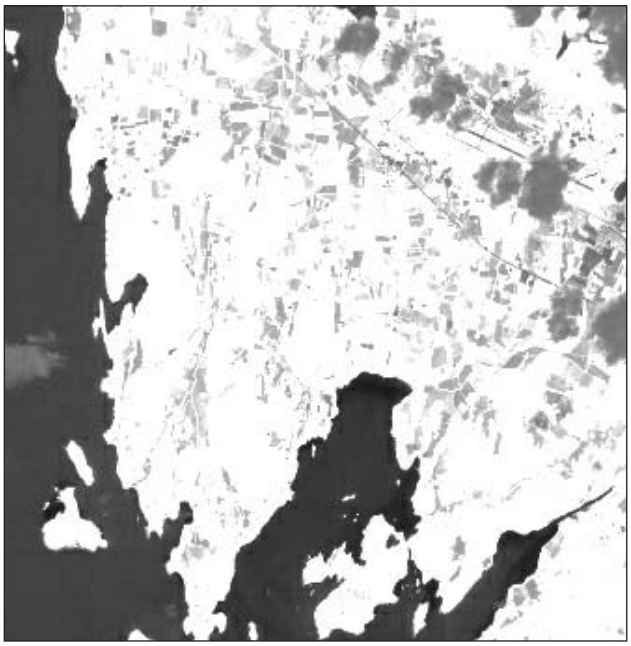

Fig.36 The vegetation index based on the Quickbird image (copyright: Digital Globe and the Satellite Data Archive of the Norwegian Mapping Authority).

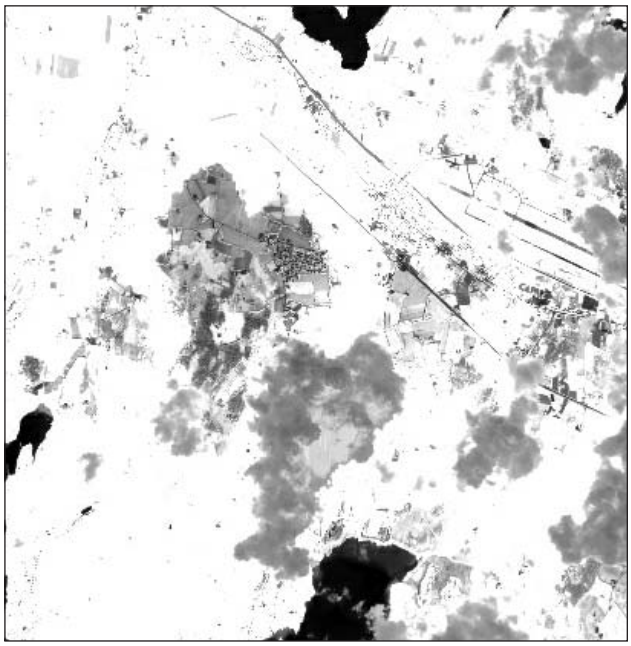

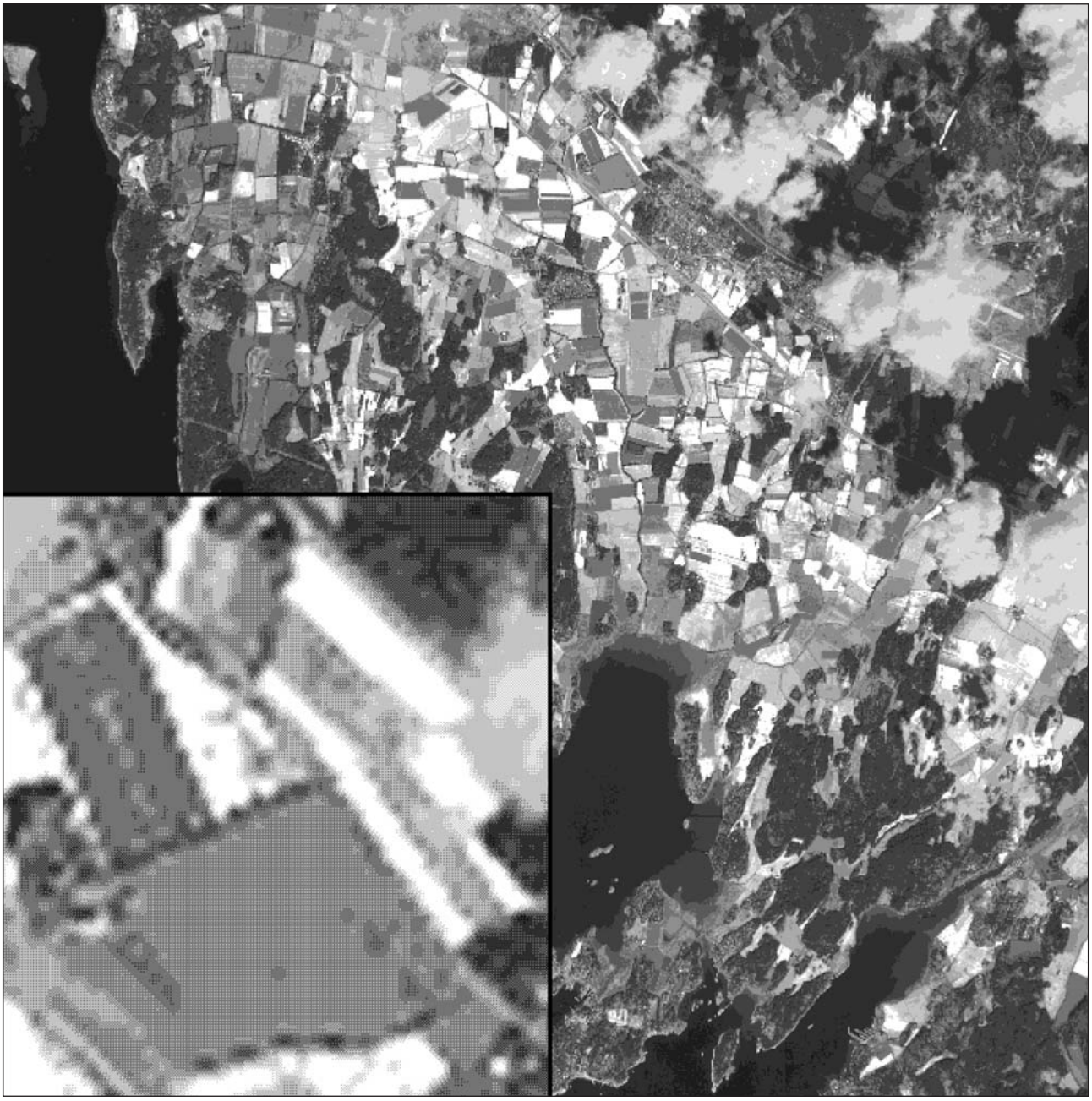

Fig.37 The iron-oxide index is based on the IKONOS image. It reflects the content of iron-oxide and can thus give important information about cultural heritage sites. Detail from Gipsund Farm in lower left corner (copyright: Space Imaging and the Satellite Data Archive of the Norwegian Mapping Authority).

5. Pattern recognition of cultural heritage sites in satellite images

As a part of the project, Lars Aurdal, The Norwegian Computing Centre (NR), has carried out initial experiments with pattern recognition related to locating cultural heritage sites. There seems to be a potential for the development of a partly automated method for distinction of anomalies that represent cultural heritage sites in multispectral satellite images.

5.a. Data coverage

Three multispectral satellite images form the basis for the project at present. An IKONOS image from the study area (August 2001) comprising a panchromatic image with a 1 m resolution and a multispectral (four channels, near infrared, red, green and blue) data set with a 4 m resolution was made available by the Satellite Data Archive of the Norwegian Mapping Authority.

A Quickbird image (July 2003) covering a central part of the same study area was purchased by the project in 2003 (fig. 38) . Although the resolution of this image is high (2.4 m for the multispectral part and 0.6 m for the panchromatic), comparison with the IKONOS image shows that the latter contains more information of relevance for cultural heritage monitoring than the former. The difference seems to be due to the fact that multispectral recordings with a highly dynamic vegetation reflect cultural heritage sites to a lesser degree than recordings from periods with a minimum of vegetation. A Landsat ETM+ image (June 2001) covering the study area has proved to be useless for this study, due to its low resolution (30 m for the multispectral part and 15 m for the panchromatic), which is too coarse to catch up most cultural heritage sites (Shennan and Donoghue 1991).

5.b. Basis for the analysis

The multispectral IKONOS data were analysed with ENVI (Research Systems, Inc.) using the Maximum Noise Fraction transform to check whether a data dimensionality reduction should be performed. This analysis indicated that the information in the four bands was so de-correlated that no dimensionality reduction should be performed. The result of this analysis (fig. 38) is not surprising, considering the low number of bands and the high spectral separation between them (for more details concerning the Maximum Noise Fraction transform see Green et al. 1988 or the ENVI (Research Systems, Inc.) documentation). Analysis was therefore based on the panchromatic and full multispectral data. To allow for easy comparison of the panchromatic and multispectral data, the multispectral data were interpolated to a 1 m grid using nearest neighbour interpolation. This report is exclusively based on these interpolated IKONOS data.

The size of the study area is more than 100 square kilometres and the IKONOS data comprise more than 100 million pixels (at a resolution of 1_1 m). For this report we have chosen to concentrate on small parts of the project's study area, in particular the area around Gipsund Farm known to be rich in cultural heritage sites. To demonstrate the potential of automatic image processing applied to the satellite data, we therefore chose to extract sub-images of this farm and use these sub-images for the image processing.

With the current technology for satellite-borne imaging sensors it will not be possible to obtain useful results from forest areas. The focus is therefore on the agricultural fields. The limits of these could possibly be determined automatically, but a much better alternative for a general approach is to use the digital land-use maps provided by the Norwegian Institute of Land Inventory (www.nijos.no). Such maps were not available for this study, and masks for the fields were therefore made by hand. This does not detract from the relevance of this study, since it is expected that such masks could easily be made using the digital land-use maps.

5.c. Gipsund Farm

Gipsund Farm is situated in the northeastern corner of the study area, and its fields are known to comprise many interesting cultural heritage sites. We therefore extracted a sub-image from the IKONOS image (fig. 38). This sub-image (fig. 39) comprises the central farm area along with the neighbouring fields. Fig. 40 shows the same sub-image with the limits of the three fields of interest overlaid. This figure also indicates possible cultural heritage sites visible in the sub-image.

5.d. Methods and results

5.d.1. Ideal result

The ideal result of the application of an algorithm for automatic detection of cultural heritage sites to satellite

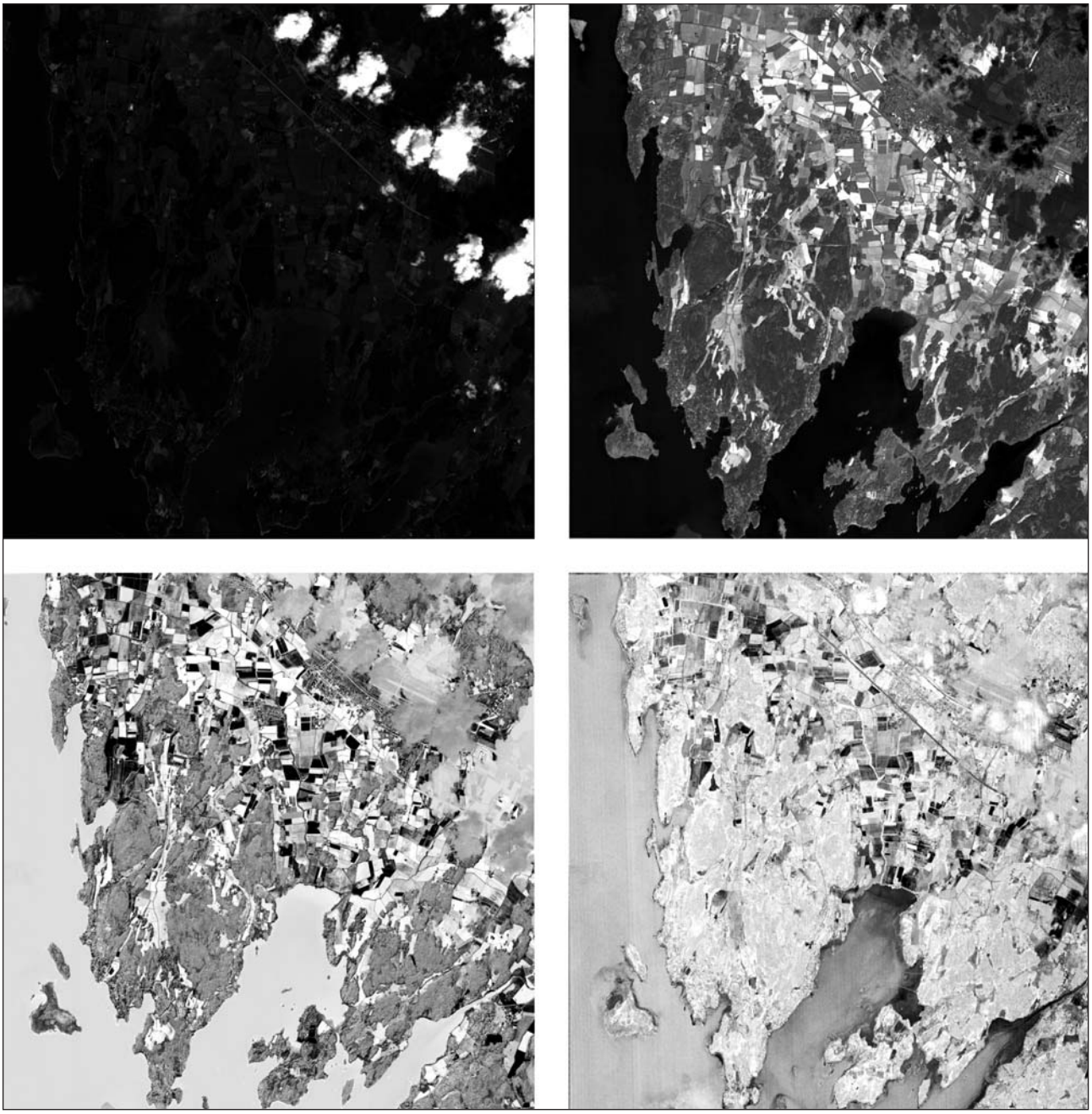

Fig. 38 The result of the Maximum Noise Fraction analysis of the multispectral data. The images are ordered lexicographically in order of falling corresponding eigenvalue. It is clear that the spatial correlation in all images is sufficiently high to exclude the use of dimensionality reduction methods (IKONOS - copyright: Space Imaging and the Satellite Data Archive of the Norwegian Mapping Authority).

data might be something like the result shown in fig. 41. In this figure we show the sub-image of the Gipsund Farm area from fig. 39 with the sites of possible interest labeled.

Obtaining a result like the one shown in fig. 41 is not trivial, and based on the current project it is obviously impossible to indicate the exact methods and algorithms to be used. However, based on experience, it is clear that the process leading from the raw input data to the kind of labelling shown in fig. 41 would comprise a pre-processing step, a segmentation (clustering) step (1), and a classification step. In the following sections we will detail methods that we believe are relevant for the different steps of the overall algorithm.

5.d.2. Preprocessing

As already stated, the current sensor technology restricts the application of the method to cultural heritage sites in the agricultural fields. It is probably possible to distinguish these from the raw images by statistical texture-classification methods, but a much better alternative is to use the digital land-use maps to create a proper masking (fig. 40) as a first pre-processing step.

Fig. 39 (over) Gipsund Farm and the surrounding fields, panchromatic IKONOS data (1 m resolution). The scene comprises 741 rows of 917 pixels for a total of 679,497 pixels. The delimiting UTM co-ordinates are given in the corners of the image (IKONOS - copyright: Space Imaging and the Satellite Data Archive of the Norwegian Mapping Authority).

Fig. 40 Gipsund Farm and the surrounding fields, panchromatic IKONOS data (1 m resolution). The coloured lines indicate masks for the three fields of interest. The figure also indicates possible cultural heritage sites. (IKONOS - copyright: Space Imaging and the Satellite Data Archive of the Norwegian Mapping Authority).

Fig. 41 Gipsund Farm and the surrounding fields, panchromatic IKONOS data (1 m resolution). This image shows the conceptual output of an ideal algorithm for the processing of such data (IKONOS - copyright: Space Imaging and the Satellite Data Archive of the Norwegian Mapping Authority).

The next pre-processing step addresses noise and artifact removal from the masked images. The noise present in the images is so low that no counter-measures are required. The primary disturbance affecting the processing of the images is plough furrows in the fields. It is suggested that these be removed with standard Fourier analysis techniques (2). In a Fourier analysis, the images analysed are projected onto a set of complex exponential functions. These projections basically measure to what degree the images analysed resemble the different members of the set of complex exponentials. The set of complex exponentials is designed so that it contains slowly a well as rapidly oscillating members. If the image comprises slow oscillations, then the projection onto the part of the set of complex exponentials that themselves vary slowly will be important. Likewise, images with rapid variation will have an important projection onto the rapidly varying complex exponentials. Thus the Fourier analysis will provide a measure of the ***frequency content*** of the image being analysed.

Plough furrows represent a fairly high frequency-component in the image, as a Fourier transformation reveals in the so-called ***spectrum*** of the image of field 2 (fig. 42). Once the part of the spectrum corresponding to the unwanted plough furrows has been detected, this part of the spectrum can be masked and the original image reconstructed without the disturbing features (fig. 43). The masking of these furrows facilitates the remaining processing.

The principal and non-trivial problem with this method is to determine the exact parts of the frequency spectrum to mask. In order to do this, it is essential to detect the plough furrows in such a way that their orientation and spacing can be determined. Here, morphological methods (3) prove useful. They comprise a set of image-processing tools that address the local shape of the image when viewed as a surface. The image to be analysed is actually analysed using a small image, typically referred to as a structuring element that captures some local feature of the overall image. In our case, we choose the structuring element to consist of a small linear image that we can rotate to search for local fits with the image. Since the plough-furrows are linear structures, the structuring element will give a good local match when oriented along the plough furrows. This can be used to make an overall map of the plough-furrow orientation.

Formally, the images to be analysed, represented by their sub-graphs, are successively eroded by small linear structuring elements and the volume of the resulting sub-graph is calculated. The erosion resulting in the largest sub-graph volume is assumed to correspond with an erosion in which the structuring elements are aligned with the plough furrows. This method seems very robust

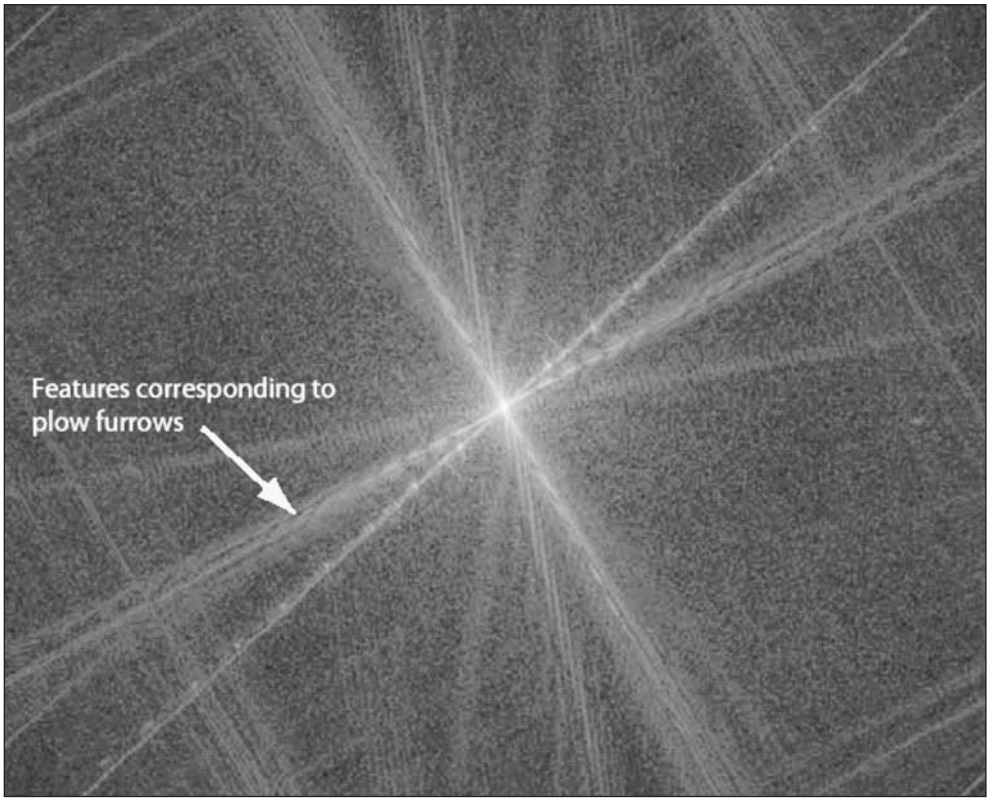

Fig. 42 The Fourier spectrum of an image of the field labelled as field 2 in fig. 40. The indicated line corresponds to the unwanted plough furrows.

Fig.43 Sub-image of field 2 before and after masking of the plough furrows (IKONOS - copyright: Space Imaging and the Satellite Data Archive of the Norwegian Mapping Authority).

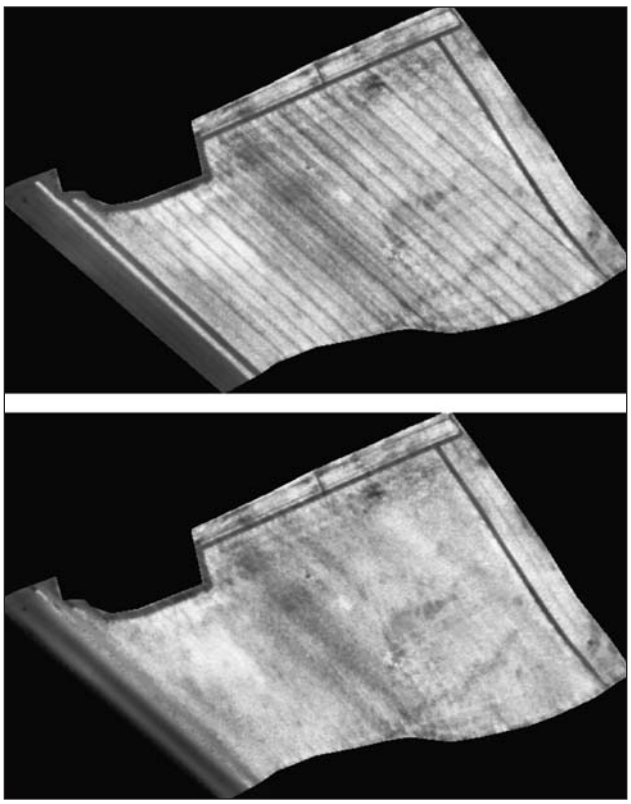

and could be made even more so by exchanging the erosion with a parametric erosion. In fig. 44 we show the sub-image of field 2 along with a polar plot of the eroded sub-graph volumes. We use a polar plot in order to illustrate the dependence on the structuring element's orientation. Notice the clear peak occurring at roughly 135 degrees, indicating the orientation of the plough furrows.

5.d.3. Segmentation (clustering) methods

Once the images are pre-processed, every field should have a mask and have periodic artifacts such as plough furrows heavily suppressed. Our aim at this stage is to group the pixels in the fields into clusters sharing certain spectral properties. There are many ways of doing this, but first it must be decided whether the fields should be treated all together or one at a time.

The different segmentation (or clustering) algorithms can roughly be divided into two types: supervised and non-supervised segmentation algorithms. In supervised segmentation, the user ***trains*** the algorithm by indicating what pixels should be grouped together. Thus the user chooses some groups of pixels representative of cultural heritage sites to train the system to distinguish and mark other groups with similar characteristics.

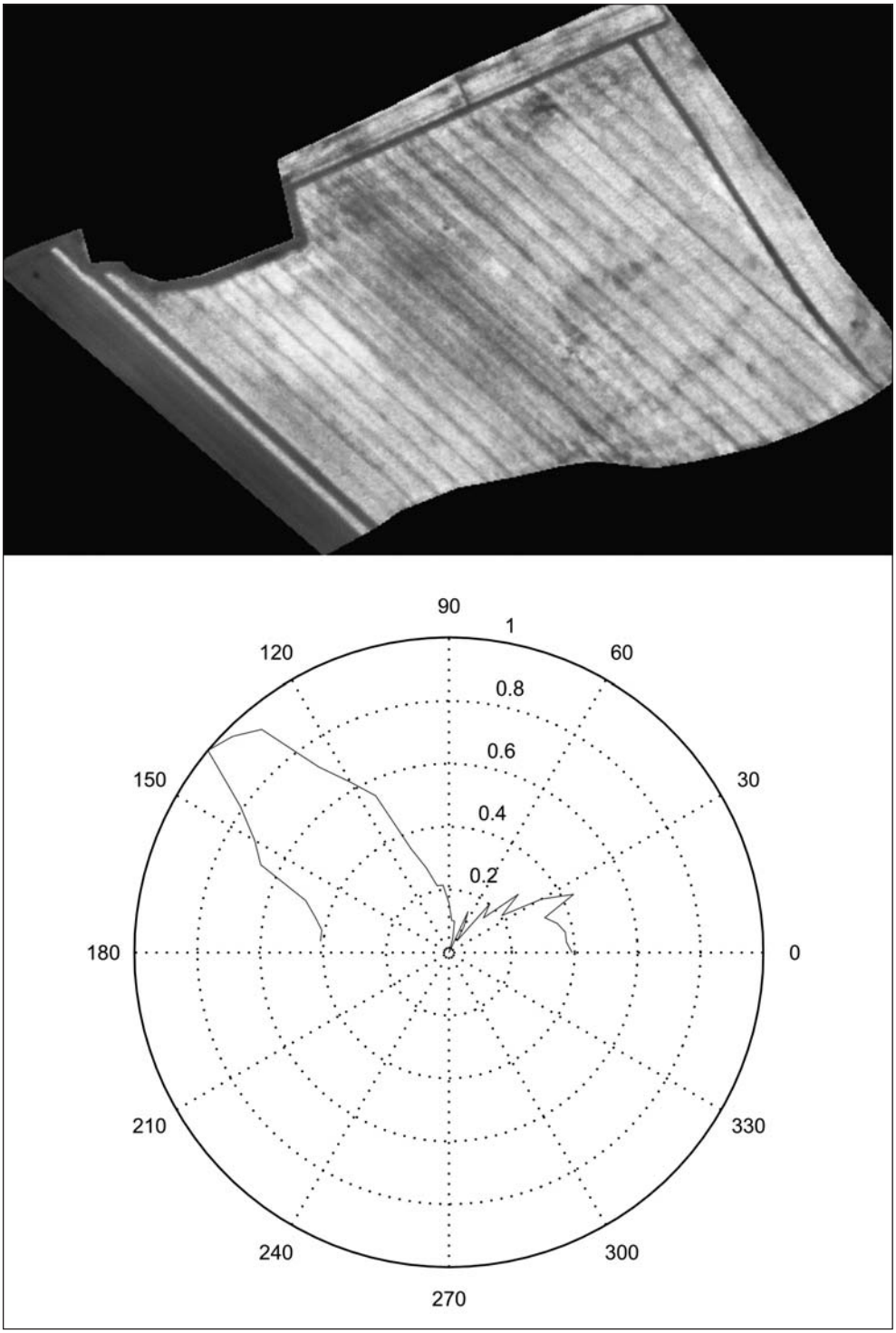

Fig. 44 Sub-image of field 2 and polar plot of normalised eroded sub-graph volume. Notice the distinct peak at roughly 135 degrees, indicating the predominant direction of plough furrows (IKONOS - copyright: Space Imaging and the Satellite Data Archive of the Norwegian Mapping Authority).

In unsupervised segmentation, the pixels are grouped autonomously by the algorithms on the basis of a user-defined criterion. These algorithms locate and mark pixels with sufficiently similar spectral characteristics without user interaction. In general, these methods will be outperformed by the supervised segmentation methods, for the simple reason that the latter employ extensive operator input to guide their operation. For the problem at hand, however, good training data are not available, because pixels that belong and pixels that do not belong to interesting sites may still share spectral properties to a point where it is impossible to distinguish between them solely on the basis of their spectral properties. As a consequence, training of the algorithm in one field or in a small number of fields will in no way allow for overall segmentation of pixels into interesting/uninteresting groups. In the sections 5.d.4. and 5.d.5. this will be dealt with in further detail.

5.d.4. Supervised segmentation (clustering) methods

The attractiveness of this approach is twofold. First, the algorithm can be trained according to the user's desires.

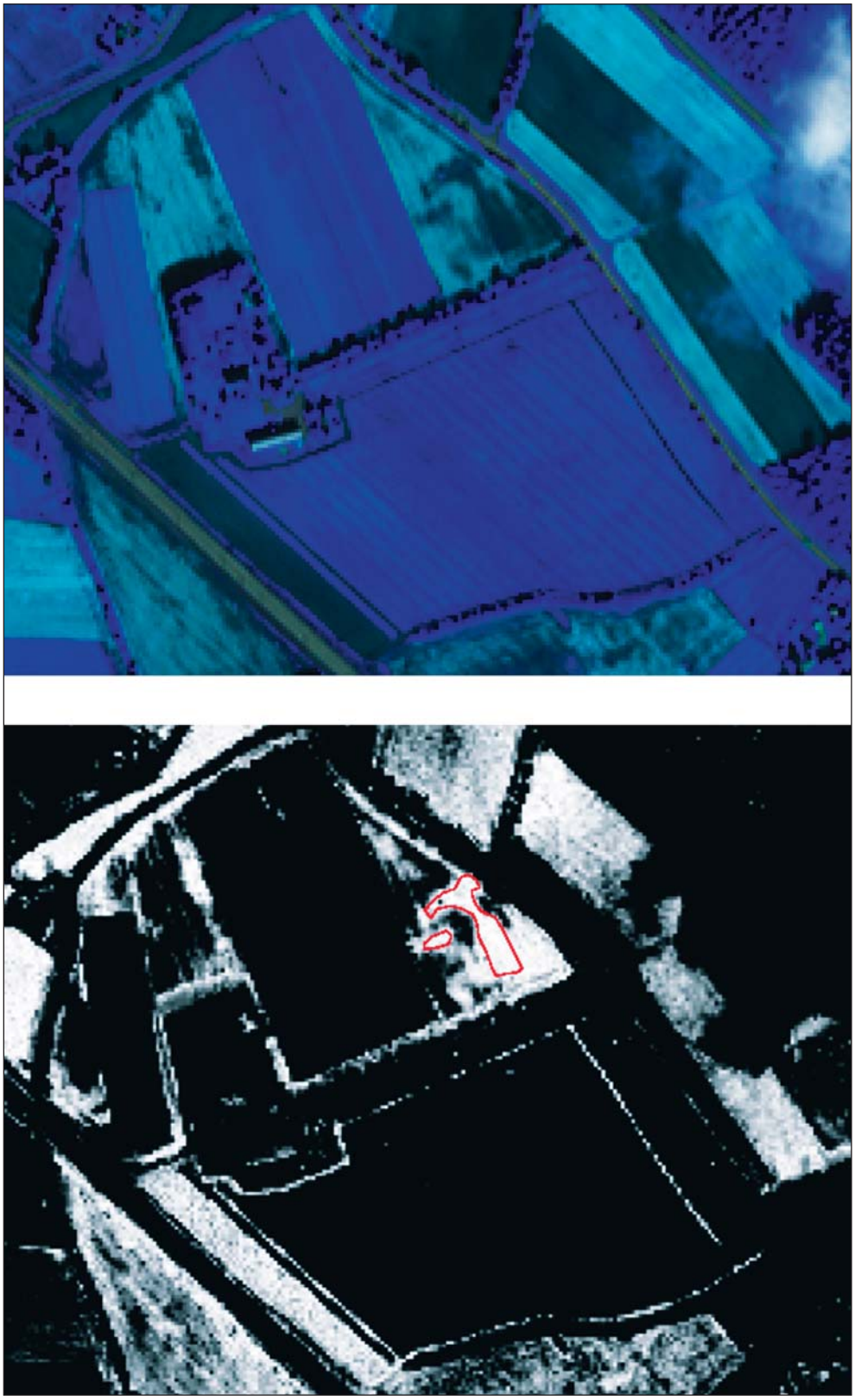

Fig. 45 The region used as a training region and the resulting rule image. Probabilities are mapped to gray levels. Dark colours indicate a low probability, light a high probability. Notice the high degree of confusion, with very many pixels outside the training region sharing the spectral properties of the training region. Among the pixels sharing the spectral properties of the training region are those that clearly do not represent interesting sites (IKONOS - copyright: Space Imaging and the Satellite Data Archive of the Norwegian Mapping Authority).

By including, or excluding, certain regions in the images, the user can partly control the performance of these algorithms. Secondly, these algorithms are designed, once trained, to process all the fields in one large operation. This is unfortunately also a weak point. The aim is obviously to keep the training set as small as possible and still obtain the desired segmentation (clustering). But small training sets typically represent only a few very local characteristics of the cultural heritage sites. In fields far from the training site, the truth represented by the training data might no longer be valid. The alternative to supervised segmentation (clustering), unsupervised segmentation, is the subject of section 4.d.5.

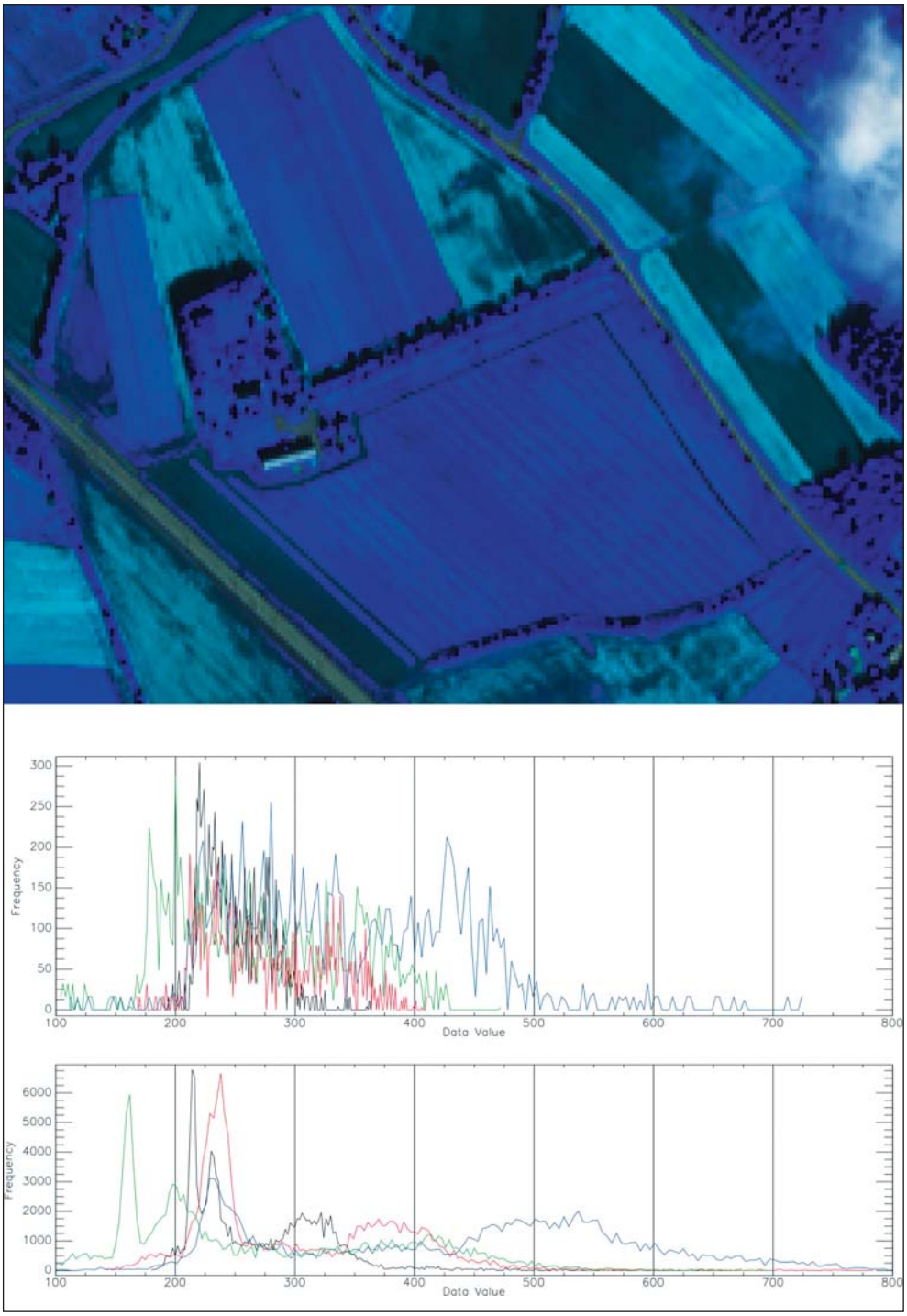

Fig. 46 The upper image shows the two different regions used to compare regional histograms. The histogram of the red region appears in the middle plot, that of the orange region in the bottom plot. The four different lines in each plot correspond to the four different spectral ranges in the multispectral data. Notice the large degree of overlap. This explains the difficulties we have in separating these regions based purely on spectral values (IKONOS - copyright: Space Imaging and the Satellite Data Archive of the Norwegian Mapping Authority).

The segmentation (clustering) problem is basically that of assigning labels or ***classes*** to all pixels in the image. In the case of segmentation (clustering) based on spectral properties, pixels sharing the same label or class will have similar spectral properties. The supervised segmentation (clustering) scheme that we evaluated in this project is the so-called ***maximum likelihood*** segmentation (clustering). Here we will give only a very brief introduction to this algorithm, and the reader is referred to the bibliography for details. Omitting the next sections will not detract from the overall understanding of this document.

In maximum likelihood segmentation (clustering) we seek to assign a class ω_i, $i = 1, \ldots, M$ to each pixel, there are thus M classes. When trying to determine what class to assign to a given pixel, only the conditional probability is considered:

$$p(\omega_i|\mathbf{x}),\ i = 1, \ldots, M$$

Here, the vector **x** is a column vector of spectral values for the pixel being considered. $p(\omega_i|\mathbf{x})$ is the ***likelihood*** that the correct class for the pixel considered is ω_i given

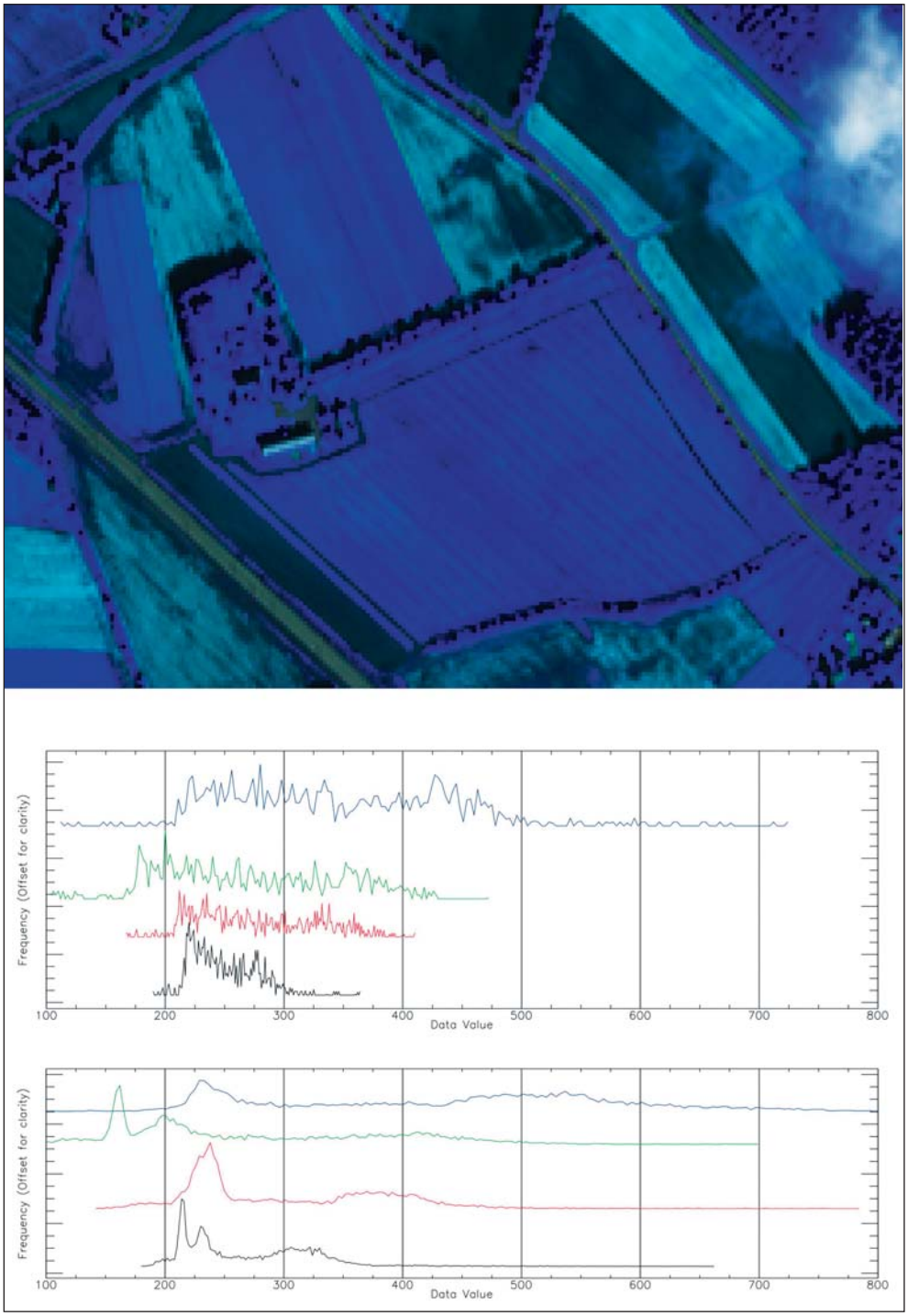

Fig. 47 The upper image shows the two different regions used to compare regional histograms. The histogram of the red region appears in the middle plot, that of the orange region in the bottom plot. The four different lines in each plot correspond to the four different spectral ranges in the multispectral data. In this figure the histograms have been normalised and offset for clarity. Notice the large degree of overlap. This explains the difficulties we have in separating these regions based purely on spectral values (IKONOS - copyright: Space Imaging and the Satellite Data Archive of the Norwegian Mapping Authority).

that the pixel has spectral values **x.** The classification is based on the following simple rule:

$$x \in v_i \quad \text{if} \quad p(v_i|x) > p(v_j|x) \text{ for all } j \neq i$$

That is, the pixel with spectral values **x** belongs to class v_i if $p(v_i|x)$ is the largest.

The problem with this seemingly simple decision rule is that the probabilities $p(v_i|x)$ are unknown. But if training data are available, that is, if we had marked regions of pixels to which the user had ***assigned*** a class we could use this to estimate the probability $p(x|v_i)$ – that is the probability of certain spectral signatures ***given its class membership.*** For each class we would then know what the probability is that a given spectral signature should belong to the class. The beauty of this approach is that the two types of probabilities are related by the following simple formula (Bayes formula):

$$p(v_i|x) = p(x|v_i)p(v_i)/p(x),$$

where $p(v_i)$ is the probability that the class v_i occurs in the image, and $p(x)$ is simply the probability of a given

spectral signature. Based on this formula, we can now make the following decision rule:

$$x \in v_i \quad \text{if} \quad p(x|v_i)p(v_i) > p(x|v_j)p(v_j) \text{ for all } j \neq i$$

where the $p(x)$ has been removed as a common factor. This simple decision rule is at the basis of the so-called ***maximum likelihood classification***. An introduction to the vast subject of supervised clustering can be found in Richards and Jia 1999. An excellent in-depth treatment is provided in Duda et al. 2000.

A simple test of this algorithm on our images reveals its weaknesses in the present situation. Starting by defining a training area for a single class, we mark a region

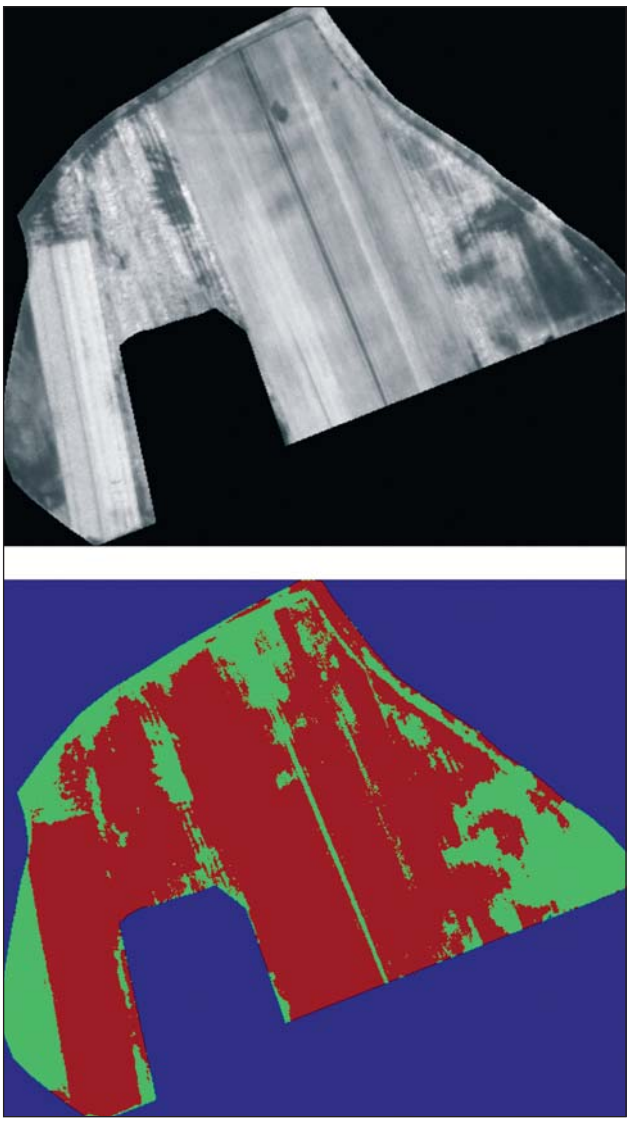

Fig.48 A Gipsund field masked from the remaining image using manually made masks. The bottom part of the figure shows a k-means clustering of this image into three (k = 3) clusters. One cluster is intentionally used to capture the background, the other two are used to cluster actual field data (IKONOS - copyright: Space Imaging and the Satellite Data Archive of the Norwegian Mapping Authority).

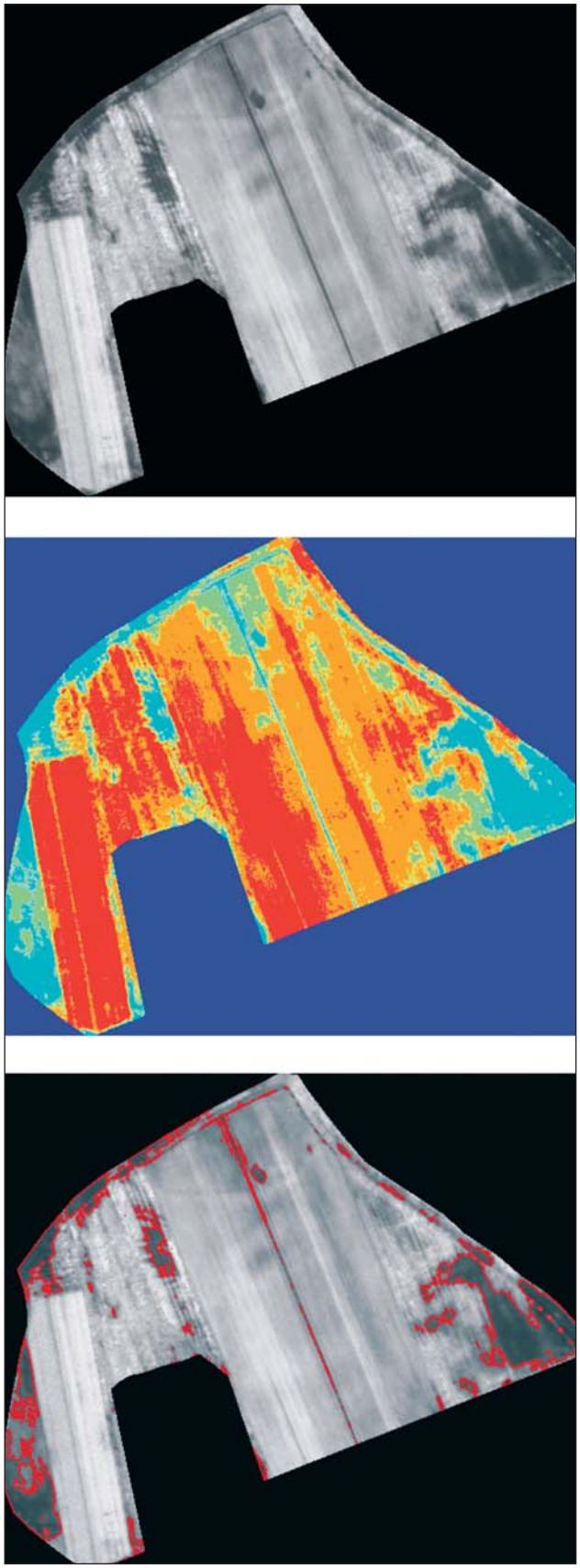

Fig. 49 k-means clustering using 5 classes on a Gipsund field. The upper left image shows the initial field, the upper right image shows the clustering result and the lower image shows the contour of the interesting class overlaid on the original image (IKONOS - copyright: Space Imaging and the Satellite Data Archive of the Norwegian Mapping Authority).

on the Gipsund fields as belonging to the class of cultural heritage sites (the particular site marked is identified by the collaborating archaeologist as 'an interesting site'). Given this training region, we use ENVI to calculate the corresponding ***rule image***. This is simply a new image in which every pixel is labelled with its probability (its likelihood) of belonging to the class defined by the training class. The image showing the region used as a training region, as well as the resulting rule image, is shown in fig. 45. Notice in fig. 45 the high degree of confusion, where many pixels ***outside*** the training region share the spectral properties of the pixels inside it.

From this simple test it is possible to draw very important conclusions. In particular, we can conclude that it will **not** be possible to distinguish between interesting sites and features of no interest using this simple scheme. As is clearly seen from this example, interesting and noninteresting sites share spectral properties to a degree that excludes automatic distinction between them in an automatic manner. This is aggravated by the fact that the training region and the application region are close to each other, since the whole test is applied to only a few of the Gipsund fields. If the training and application regions were more distant from each other, the results would most likely become even worse.

Another simple way of observing this is by plotting the histograms of different regions around Gipsund. We show this in figs. 46 and 47. The upper part of these figures shows (in red and orange) the two different regions represented by the histograms we compare. Fig. 46 shows the raw histograms, while fig. 47 shows the same histograms, but normalised and offset for clarity. Notice the large degree of overlap between the histograms of the two regions. This explains why it is hard to distinguish between the regions based on purely spectral data.

Based on these observations, it is reasonable to assume that supervised segmentation (clustering) will play a very limited role in this project. As we have seen, interesting and uninteresting sites share spectral properties to a large

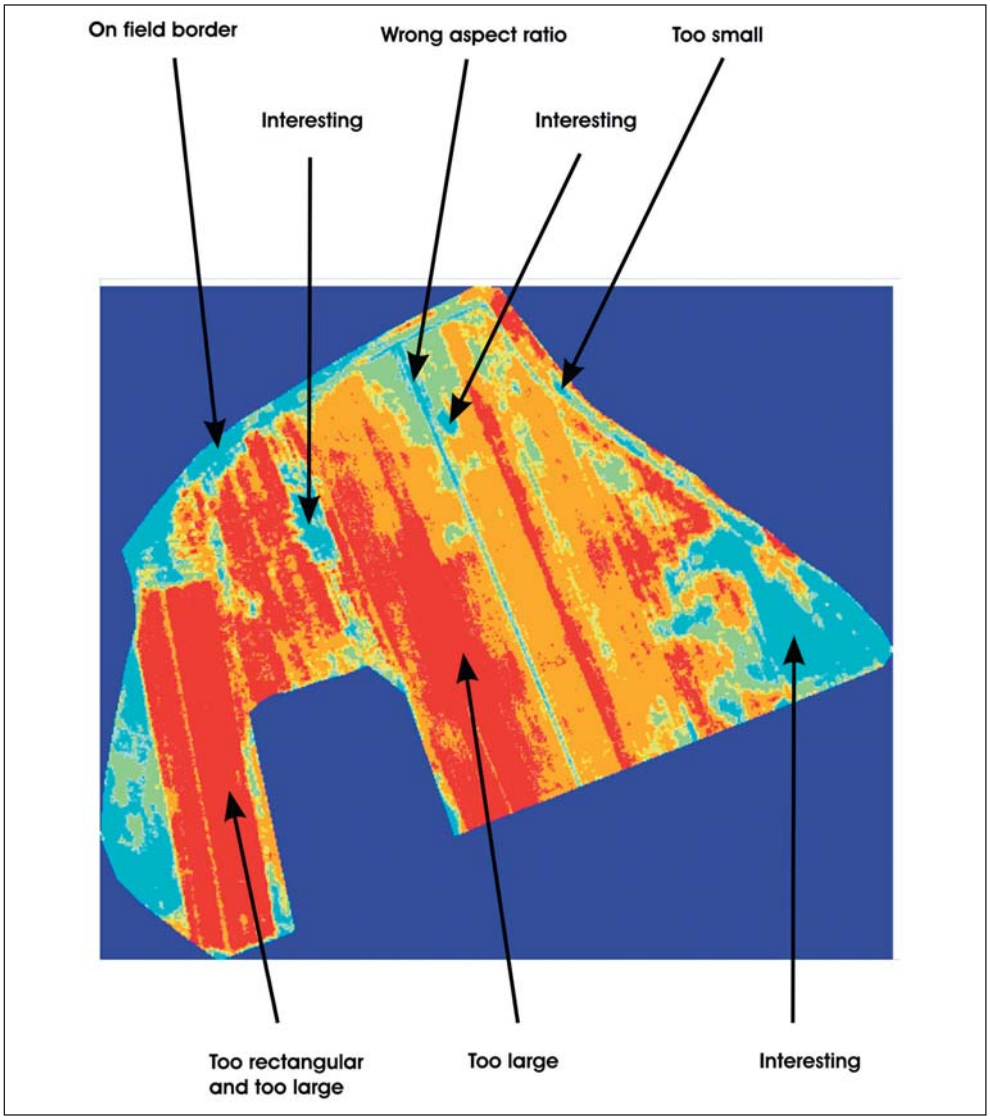

Fig. 50 Different properties of the clusters from fig. 49.

degree. Secondly, the fairly low resolution of the images relative to the features of interest also makes it difficult to obtain good statistical information to distinguish between interesting and uninteresting sites. As we shall see in section 4.d.6., supervised segmentation (clustering) will play a role in processing ***shape and size features*** of the spectral clusters. For this application, it will be more appropriate to refer to this method as a classification method.

5.d.5. Unsupervised clustering methods

For a segmentation problem like the one in hand, we have seen that the operator input is of little value. What we would actually like to have is an algorithm that could treat every field separately (or possibly in conjunction with its neighbours) and make ***local*** decisions as to whether the fields observed contain regions with desirable spectral parameters.

One much used method for unsupervised segmentation (clustering) is the so-called *k*-means algorithm. The name of this conceptually very simple algorithm reflects its basic operation. It tries, in an automatic fashion, to assign the pixels to one of *k* classes by assigning the pixel to the class whose mean spectral value is the closest. This algorithm therefore tends to assign pixels to classes in such a manner that the mean squared distances from pixels to class centra are minimized. Here we will only give a very brief introduction to this algorithm, and the reader is referred to the bibliography for details. Omitting the next sections will not detract from the overall understanding of this document. The algorithm works as follows:

1. Initialize the procedure by selecting *k* points in multispectral space to serve as candidate cluster centres. Let these be:

   $$1. \quad \hat{m}_i, \quad i = 1, \ldots, k$$

   The cluster centres can be chosen arbitrarily, but no two should be the same. A much used approach is simply to space the class centra uniformly in spectral space.

2. The location of each pixel in spectral space is examined, and the pixels are assigned to the centre of the nearest cluster. ‘Closeness’ would typically be measured using a Euclidean distance measure.

3. Based on the new grouping, recalculate cluster centres. Let these be:

   $$m_i, \quad i = 1, \ldots, k$$

4. If $m_i = \hat{m}_i$ for all *i* the procedure is terminated. Otherwise, $\hat{m}_i$ is redefined as the current value of $\mathbf{m_i}$ and the procedure is reiterated from step 2.

This very simple algorithm, once initialized, is capable of assigning pixels to classes in an autonomous fashion. The ***number*** of classes must be given by the user, as we shall see shortly, this is not necessarily a major problem. Our intended use of this algorithm is to apply it ***within each field***. As previously stated, the fields can be delimited using land-use masks, so the field-wise application should be no problem. Another problem that must be dealt with in the future is that of cultural heritage sites straddling several fields. This could be solved by treating small groups of neighbouring fields instead of each field on its own.

An initial attempt at using the algorithm in the Gipsund fields is illustrated in fig. 48. We use three clusters ($k = 3$) in this example. One is intentionally introduced to capture the background, the two others are used to cluster actual field data. This initial attempt is clearly seen to result in an under-clustering of the data. Increasing the total number of classes to five ($k = 5$), we get the result shown in fig. 49.

5.d.6. Classification methods

An important question to be answered is obviously what clusters among those resulting from the above procedures correspond to interesting sites. Notice that *k*-means will cluster the pixels only according to a distance measure applied in spectral space. The ***meaning*** of these clusters is not considered during the clustering, so ***any one of the clusters*** could represent an interesting cluster.

Although supervised segmentation (clustering) was found to perform poorly in grouping pixels according to ***spectral properties***, we expect these methods to perform better when trying to ***distinguish between clusters based on their shapes, etc***. The reason for this is simple: as we have seen, candidate sites may have a number of spectral signatures, not in any way distinct from those of non-candidate regions. This is why we suggest a ***field-wise*** treatment of the data, processing each field with a locally adaptive algorithm.

We expect the clusters corresponding to interesting regions to share shape (and other characteristics) to a much larger degree than was the case for spectral properties. This is so ***simply because remains of central prehistoric human activity areas (cultural heritage sites)***

must have certain shape and size restrictions. In particular, very large clusters can be ruled out based on the simple fact that man-made structures from the periods in question were of limited size. Furthermore, it is reasonable to assume that interesting regions will have certain compactness and shape properties that can be used to distinguish them from non-interesting regions.

We have not gone far in the investigation of this problem, but believe that the following properties might be appropriate for separating interesting from uninteresting clusters (see also examples in fig. 50).

1. **Upper limit on size:** The extent of remains of prehistoric human activity must have an upper limit.
2. **Lower limit on size:** Considering clusters that are too small will make the algorithms much too sensitive to noise.
3. **Rectangularity and polygonality:** Very rectangular or polygonal regions are probably results of present-day activity.
4. **Compactness:** Interesting clusters are probably fairly compact. Thus clusters surrounding others are probably not interesting.
5. **Aspect ratio:** This measure, closely related to the previous ones measures the ratio between the minimal and maximal length of lines inscribable in the considered cluster. If this is too small, the object will be a very elongated structure.
6. **Grouping:** Human activity is often concentrated in small areas, so the presence of one interesting cluster should increase the probability of nearby clusters being considered interesting.
7. **Others:** A very large number of shape properties have been devised. Testing all these for their discriminatory power will be necessary

5.d.7. Conclusion

Our principal conclusion based on this initial study is that computerised processing of satellite data in search of cultural heritage sites is feasible. Furthermore, the processing will most probably be a three-step process consisting of the following steps:

1. Pre-processing: We are convinced that a field-by-field treatment is necessary. In preparation for further processing, the field masks derived from land-use maps must be applied, so that each field can be treated apart. Furthermore, every field should be pre-processed in order to suppress artifacts that could interfere with the clustering. In particular, plough furrows must be removed. Fourier analysis in combination with mathematical morphology will probably be a good candidate.

2. Spectral segmentation (clustering): Again, this must be performed on a field-by-field basis. Due to the large variability in the data, an unsupervised clustering (***k***-means) must be applied, possibly in a multi-stage process, to each field. This will cluster the pixels in the field according to their spectral properties.

3. Object-parameter clustering (classification): Having clustered the pixels according to spectral properties, a final processing step is to process the different clusters (objects), looking for clusters with shape and size characteristics that make them candidates for being cultural heritage sites. It is our belief that this step will be fairly simple, since little can be said in general of the shape of a cultural heritage site. Most probably, the discrimination will be made on some very simple size and shape criteria.

We have had access to satellite images from three different satellites during this project. In order of increasing resolution these are: LANDSAT7 ETM+ , IKONOS and QuickBird. From this initial study it would seem that a resolution equal to or better than that of the IKONOS data is necessary, which means that the panchromatic data should have a resolution of roughly 1 m or better and the multispectral data a resolution of roughly 4 m or better. The multispectral part of the data can then be interpolated to the same scale as the panchromatic data, providing a reasonable resolution in the final images. The choice of a minimum of 1 m resolution also seems reasonable based on a consideration of the structures that are to be resolved on the ground. Data from the IKONOS or QuickBird satellites will probably be well suited for a project like this. Another issue concerning the satellite data is obviously the time of acquisition. It is very surprising to see how ground details visible in one set of data might be more or less invisible in others. We strongly suggest that a future project addresses this issue.

Furthermore, based on this initial study, we are convinced that a fully automated system is nearly impossible. This is due to the simple fact that even human specialists frequently reach different conclusions interpreting the images. The decision as to whether a site is or is not interesting depends on many details. The spectral signature and shape of the site is only one of several factors that must be taken into account. Knowledge in archaeology and local history coupled with ge-

ography and, obviously, knowledge from field surveys will often be of primary importance in the final interpretation. We believe that if the development of software for processing satellite images looking for cultural heritage sites is undertaken, the aim should be to provide the human specialists with a tool for detecting ***potentially interesting sites***, leaving the final interpretation to the human specialists. Such a tool would greatly reduce the burden on the human specialist, since it would be able to guide the specialist from site to site in the images. The specialist would then concentrate on the actual interpretation of the different sites that are detected. Furthermore, such a tool could learn from input from different users, thus paving the way for more objective decisions.

6. General conclusion and future activities

The general aim of the 2003-project has been through a feed-back process involving several interrelated themes to create the outlines of a system for interpretation of satellite data from agricultural fields and for ground-based verification/rejection of the anomalies distinguished, which can facilitate representative and cost-efficient mapping of cultural heritage sites.

It has been demonstrated that the density of registered cultural heritage sites in agricultural fields is probably only a few percent of what it should have been, because a large fraction of these sites have been damaged systematically through time (Grøn and Loska 2002). It has furthermore been shown likely that 1) geo-chemistry has quite a potential as a basis for the development of a ground-method for verification/rejection of anomalies distinguished as potential cultural heritage sites and that 2) the results in a reasonable number of the test cases support the assumed character of anomalies as reflections of the remains of cultural heritage sites. The results of the Norwegian Computing Center's evaluation of the satellite data suggest that the development of a partly automated procedure for the mapping of potential cultural heritage sites on the basis of multispectral satellite images is realistic and should be integrated into the project, underpinned by other analytic approaches to the images.

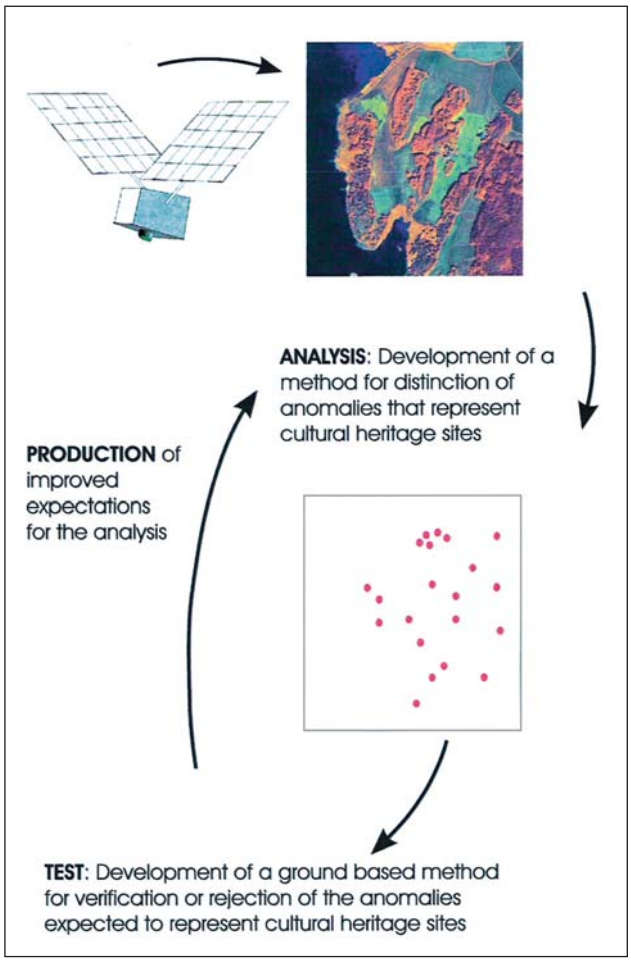

Fig. 51 The feed-back development process in the project.

On the basis of the results obtained so far, it seems realistic to engage in a larger-scale development of a methodology for a support system for an up-to-date cultural heritage administration. At the moment, a continuation of the activities as a national program is being negotiated, running over a period of several years.

Geographically, it seems optimal to maintain work in the already defined study area so that it can serve as a future reference area for method tests and further developments. It seems sensible to start work in one or two other study areas such as Vestfold and/or Røros during a larger-scale development project. Decisions about such developments of the project should be made on the basis of the methodological development in general.

Experiments should be carried out with other data than LANDSAT7 ETM+, IKONOS and QuickBird images. It is possible that hyperspectral recordings (airborne scanner) can serve as a basis for a precise testing of the optimal and the necessary resolutions for distinction of cultural heritage sites. It seems that a panchromatic resolution of 1m corresponding to a multispectral resolution of a few metres is required (Shennan and Donoghue 1991). Meanwhile more precise information about the resolutions required can be used to minimise the prices for satellite data in concrete cases.

Because of the significant lack of registered and known cultural heritage sites in the agricultural fields observed in the study area (Grøn and Loska 2002), geo-chemistry can contribute considerably to an improved ground truth that will be important for the development of the pattern recognition. It is promising that the results suggest that significant and structurally similar chemical anomalies are related to suggested cultural heritage sites. An important project element will therefore be the study of the chemical signatures of different types of cultural heritage sites. Such a study can lead to the distinction of the sizes and shapes of characteristic features related to the cultural heritage sites.

The surprising difference between the cultural heritage-relevant information that can be extracted from the IKONOS image from August 21, 2000, and the QuickBird image from July 3, 2003 shows that it is important to find the optimal time as well as the optimal climatic conditions for recording. These may vary for different types of images, as can the post-processing and classification procedures necessary for the application of pattern recognition based on different image types.

Analysis of the satellite images for all kinds of small-scale anomalies that relate to cultural heritage sites should be continued to improve the analytic understanding of the character of cultural heritage sites and thus underpin the development of a useful pattern recognition procedure.

Extensive testing of methods for pattern recognition will require a close connection to the system managing the satellite data. Because the development of such a system from scratch will be extremely work-intensive, adaptation of an already existing system to the problem at hand seems the only realistic approach. The locally adaptive method for clustering regions within each field should be further developed, and the application of masks for agricultural land (available from NIJOS) should be tested in relation to the development of a pattern-recognition procedure.

A realistic goal for a four-year project period could be the testing of a pilot version of a support system for cultural-heritage administration based on the results obtained. This should be to test out the system's basic functionality, whereas the development of user features lies outside the scope of this project.

A basic element in the project's strategic thinking is that it is seen as important to approach the cultural heritage problem in hand at the small-scale level. Not before the methodology is mastered at this level will it be possible to apply it to larger-scale settings and modelling.

With the rapid development one can observe today of remote-sensing based tools in other sectors, it is most likely that one can expect 1) a continuous development of the methodology supporting the cultural heritage administration driven by the demands of a modern administration and 2) an increasing integration of the methodologies employed in the different administrative sectors, due to their use of the same types of basis-data.

Notes

(1) There is much overlap in terminology concerning algorithms for grouping pixels according to their spectral properties. Some authors will use the term segmentation for this process, others will refer to this as clustering. We will continue to use both terms throughout this report.
(2) Fourier analysis is a standard technique in image processing, a very good reference being Jain 1989.
(3) This is a standard image-processing technique. A clear and detailed reference is Soille 2003.

References

Booth, D.J., and Oldfield, R.B. 1989: A comparison of classification algorithms in terms of speed and accuracy after application of a post-classification modal filter. ***Int. J. Remote Sensing***, Vol. 10, No. 7, pp. 1271-1276.

Duda, R., Stork, D. and Hart, P. 2000: ***Pattern Classification***. John Wiley & Sons Inc., 2nd edition, 2000.

Green, A., Berman, M., Switzer, P. and Craig, M. 1988: A Transformation for Ordering Multispectral Data in Terms of Image Quality with Implications for Noise Removal***. IEEE Transactions on Geoscience and Remote Sensing***, 26(1):65–74, Jan 1988.

Grøn, O., and Loska, A. 2002**: *Development of methods for satellite monitoring of cultural heritage sites*.** Technical report, The Norwegian Directorate for Cultural Heritage, The Norwegian Spacecentre, NIKU. Oslo.

Jackson, R.D., and Huete, A.R. 1991: Interpreting vegetation indices. ***Prev. Vet. Med***., vol. 11, pp. 185-200.

Jackson, R.D., and Pinter jr., P.J. 1986: Spectral response of architecturally different wheat canopies. ***Remote Sens. Environ***., vol. 20, pp. 43-56.

Jain, A. 1989: ***Fundamentals of Image Processing***. Prentice Hall Inc., 1st edition, 1989.

Justice, C.O., Townshend, J.R.G., Holben B.N., and Tucker, C.J. 1985: Analysis of the phenology of global vegetation using meteorological satellite data. ***Int. Jou. Remote Sens***., vol. 6, pp. 1271-1318.

Myneni, R.B., Asrar G., Tanre, D., and Choudhury, B.J. 1992. Remote sensing of solar radiation absorbed and reflected by vegetated land surfaces. ***IEEE trans. Geosci. Remote Sens***., vol. 30, pp. 302-314.

Myers, W. 1999: Remote sensing and quantitative geogrids in PHASES [Pixel Hyperclusters As Segmented Environmental Signals]. ***Release 3.4. Tech. Report ER9901***, Environmental Resources Research Institute, Penn State Univ., Univ. Park, PA 16802.

Myers, W., Patil, G.P., and Taillie, C. 1999: Cluster coordinated composites of diverse datasets on several spatial scales for designing extensive environmental sample surveys: prospectus on promising protocols. Chapter 5, pages 119-133 in Subir Ghosh (ed). ***Multivariate Analysis, Design of Experiments, and Survey Sampling***. Marcel Dekker Incorporation. New York.
Myers, W. and Shelton, R. 1998: ***Survey methods for ecosystem management***. Wiley-Interscience, New York. p. 403.

Prince, S.D. 1991: Satellite remote sensing of primary production: comparison of results for Sahelian grassland 1981-1988. ***International Journal of Remote Sensing***. Vol 12.
1991. pp. 1301-1311.

Rees, W.G. 1990: ***Physical Principles of Remote Sensing***. Cambridge: Cambridge University Press.

Richards, J. and Jia, X. 1999: ***Remote Sensing Digital Image Analysis: An Introduction***. Springer Verlag, 2nd edition.

Sellers, P.J. 1986: Canopy reflectance, photosynthesis and transpiration. ***International Journal of Remote Sensing***. Vol.6. 1986. pp. 1335-1372.

Shennan, I., and Donoghue, D. 1991: Remote Sensing in Archaeological Research***. Proceedings of the British Academy.*** Vol.77. 223-232

Soille, P. 2003: ***Morphological Image Analysis, Principles and Applications***. Springer Verlag, 2nd edition.

Tucker, C.J., and Sellers, P.J. 1986: Satellite remote sensing of primary production. International ***Journal of Remote Sensing***. Vol.7. pp. 1395-1416.

Tømmervik, H., Johansen, M.E., Pedersen, J.P., and Guneriussen, T. 1998: Integration of remote sensed and in-situ data in an analysis of the air pollution effects on terrestrial ecosystems in border areas between Norway and Russia (Russia). ***Environmental Monitoring and Assessment*** Vol. 49: 51-85. Kluwer Academic Publishers.

Appendix

SITE A

id	x-UTM	y-UTM	Niveau	[P]/ppm	[Fe]/‰	[Zn]/ppm	[Cu]/ppm	[Mn]/ppm	Niveau	[P]/ppm	[Fe]/‰	[Zn]/ppm	[Cu]/ppm	[Mn]/ppm
A:1	598993.3	6584517.7	T	527.54	1.49	7.32	6.67	105.06	B	371.01	2.05	9.36	0.00	18.31
A:2	598993.7	6584519.6	T	459.42	2.21	8.51	8.00	93.98	B	378.26	3.95	5.45	0.00	19.28
A:3	598994.3	6584521.6	T	473.91	2.26	8.68	10.67	95.90	B	463.77	8.00	5.96	0.00	41.45
A:4	598994.8	6584523.5	T	427.54	1.90	9.36	6.67	92.53	B	452.17	4.67	8.51	4.00	34.70
A:5	598995.3	6584525.4	T	360.87	1.13	6.98	5.33	76.63	B	223.19	4.26	5.45	0.00	34.70
A:6	598995.8	6584527.3	T	601.45	1.74	9.36	8.00	105.06	B	450.72	1.95	3.91	0.00	36.14
A:7	598996.4	6584529.2	T	665.22	1.54	8.85	4.00	101.69	B	478.26	1.69	2.89	0.00	59.76
A:8	598996.8	6584531.2	T	666.67	1.49	7.83	9.33	107.95	B	813.04	3.79	4.77	4.00	46.75
A:9	598997.4	6584533.1	T	671.01	1.38	8.34	4.00	86.75	B	831.88	4.05	6.47	5.33	203.86
A:10	598997.9	6584535.1	T	653.62	1.49	7.66	8.00	86.75	B	814.49	6.36	5.62	9.33	7.52
A:11	598998.3	6584537.0	T	678.26	1.23	7.32	8.00	90.12	B	434.78	1.64	4.43	0.00	33.25
A:12	598998.9	6584538.9	T	723.19	1.44	8.85	4.00	84.34	B	243.48	1.85	5.11	0.00	24.10
A:13	598999.4	6584540.8	T	736.23	1.69	7.49	8.00	70.36	B	700.00	1.59	5.79	0.00	38.07
A:14	598999.9	6584543.8	T	672.46	1.69	6.98	4.00	75.18	B	779.71	1.74	6.47	0.00	24.58
A:15	599000.4	6584544.7	T	633.33	1.49	5.62	13.33	67.47	B	489.86	0.67	3.57	0.00	31.33
A:16	599000.9	6584546.7	T	685.51	1.74	7.49	6.67	67.95	B	766.67	0.82	4.09	0.00	8.19
A:17	598991.3	6584518.2	T	520.29	1.49	7.83	6.67	93.49	B	521.74	2.31	4.09	0.00	71.81
A.18	598991.8	6584520.1	T	508.70	1.69	8.34	10.67	98.80	B	446.38	2.46	4.77	0.00	46.75
A:19	598992.3	6584522.1	T	508.70	1.54	7.83	8.00	98.31	B	408.70	2.92	5.62	0.00	29.88
A:20	598992.8	6584524.0	T	552.17	1.59	8.34	8.00	105.06	B	471.01	2.67	4.94	0.00	33.73
A:21	598993.4	6584525.9	T	581.16	1.85	8.17	5.33	100.72	B	513.04	1.54	6.30	0.00	65.06
A:22	598993.9	6584527.8	T	585.51	1.79	8.17	9.33	96.87	B	833.33	2.36	5.79	0.00	81.93
A.23	598994.4	6584529.7	T	640.58	1.49	8.34	10.67	86.27	B	814.49	1.79	5.45	0.00	113.25
A:24	598994.9	6584531.7	T	669.57	1.59	8.17	8.00	91.57	B	578.26	2.72	4.43	0.00	69.40
A:25	598995.4	6584533.6	T	602.90	1.38	8.00	6.67	74.22	B	676.81	3.74	5.45	4.00	38.07
A.26	598995.9	6584535.5	T	586.96	1.23	8.00	4.00	78.55	B	853.62	3.33	5.62	6.67	58.31
A:27	598996.4	6584537.5	T	657.97	1.59	8.00	4.00	76.14	B	566.67	4.36	4.26	0.00	41.45
A:28	598997.0	6584539.4	T	636.23	0.97	7.49	6.67	65.06	B	785.51	4.77	4.43	0.00	68.43
A:29	598997.5	6584541.4	T	656.52	1.79	7.83	4.00	76.14	B	620.29	0.97	5.28	0.00	18.80
A:30	598998.0	6584543.3	T	647.83	1.44	6.64	5.33	68.43	B	771.01	1.85	6.64	0.00	40.00
A:31	598998.5	6584545.2	T	689.86	2.21	8.85	6.67	81.93	B	618.84	0.92	4.60	0.00	21.69
A:32	598999.0	6584547.1	T	617.39	1.95	7.32	4.00	67.95	B	552.17	0.87	4.94	0.00	54.46
A:33	598989.4	6584518.7	T	601.45	1.64	8.85	12.00	108.92	B	331.88	1.38	4.94	0.00	34.70
A:34	598989.9	6584520.6	T	547.83	2.67	8.51	10.67	105.06	B	320.29	1.69	4.94	0.00	73.25
A:35	598990.4	6584522.6	T	646.38	1.49	8.51	13.33	91.57	B	360.87	3.59	3.91	0.00	41.45
A:36	598990.9	6584524.5	T	591.30	1.44	7.83	6.67	107.95	B	356.52	1.69	6.13	0.00	101.20
A.37	598991.5	6584526.4	T	582.61	1.85	8.00	8.00	87.71	B	539.13	2.72	5.62	0.00	47.71
A:38	598992.0	6584528.3	T	618.84	2.15	9.70	9.33	107.95	B	443.48	2.36	5.96	0.00	72.77
A:39	598992.5	6584530.3	T	639.13	1.33	8.00	0.00	93.01	B	869.57	2.97	5.62	5.33	95.90
A:40	598993.0	6584532.2	T	717.39	1.59	8.51	5.33	110.84	B	566.67	1.28	4.77	0.00	53.49
A:41	598993.5	6584534.1	T	686.96	1.33	8.34	5.33	91.57	B	705.80	3.44	3.91	6.67	117.59
A:42	598994.0	6584536.1	T	721.74	1.79	8.17	8.00	99.28	B	607.25	2.41	5.28	0.00	100.24
A:43	598994.5	6584538.0	T	610.14	1.44	7.66	5.33	67.47	B	605.80	1.95	6.13	4.00	69.40
A:44	598995.0	6584540.0	T	591.30	1.33	7.15	6.67	62.17	B	679.71	2.10	4.77	4.00	37.11
A:45	598995.5	6584541.9	T	497.10	1.23	8.00	8.00	74.22	B	692.75	1.64	5.45	0.00	26.99

SITE A

id	x-UTM	y-UTM	Niveau	[P]/ppm	[Fe]/‰	[Zn]/ppm	[Cu]/ppm	[Mn]/ppm	Niveau	[P]/ppm	[Fe]/‰	[Zn]/ppm	[Cu]/ppm	[Mn]/ppm
A:46	598996.0	6584543.8	T	601.45	1.64	6.13	5.33	64.58	B	591.30	2.67	5.45	0.00	44.82
A.47	598996.5	6584545.8	T	757.97	2.05	8.00	6.67	89.16	B	669.57	1.18	4.77	0.00	28.43
A:48	598997.0	6584547.7	T	613.04	1.85	6.98	6.67	68.92	B	624.64	1.28	8.00	0.00	19.76
A:49	598987.5	6584519.2	T	692.75	1.69	9.02	13.33	116.63	B	489.86	3.23	6.13	0.00	78.55
A:50	598988.0	6584521.1	T	549.28	1.44	7.66	9.33	91.57	B	450.72	4.15	4.26	0.00	53.98
A:51	598988.5	6584523.0	T	533.33	1.13	7.32	8.00	96.87	B	142.03	0.62	3.91	0.00	21.69
A.52	598990.0	6584523.0	T	631.88	1.33	8.34	8.00	102.65	B	160.87	0.97	4.94	0.00	26.99
A.53	598989.5	6584526.9	T	586.96	1.49	8.34	5.33	92.53	B	114.49	0.87	3.57	0.00	55.42
A.54	598990.0	6584528.8	T	685.51	1.64	9.36	8.00	102.17	B	339.13	3.13	3.40	0.00	18.31
A.55	598990.5	6584530.8	T	524.64	1.08	5.62	5.33	78.55	B	253.62	2.10	5.96	0.00	70.36
A.56	598991.1	6584532.7	T	688.41	1.18	7.32	8.00	98.31	B	633.33	2.51	5.62	0.00	90.12
A:57	598991.6	6584534.7	T	630.40	1.35	9.70	9.55	9.59	B	694.40	2.03	9.31	4.78	95.86
A:58	598992.1	6584536.7	T	648.00	1.55	12.28	9.55	99.31	B	478.40	1.64	6.73	0.00	110.34
A:59	598992.6	6584538.6	T	744.00	1.53	9.90	13.13	95.86	B	736.00	2.86	6.73	5.97	46.21
A:60	598993.1	6584540.5	T	673.60	1.64	9.11	8.36	97.24	B	731.20	1.36	6.73	3.58	18.62
A:61	598993.6	6584542.5	T	657.60	2.04	9.31	9.55	96.55	B	627.20	1.92	6.93	4.78	22.76
A:62	598995.1	6584542.4	T	606.40	1.82	9.11	10.75	92.41	B	660.80	1.92	8.12	0.00	37.24
A:63	598994.6	6584546.3	T	618.84	1.85	6.81	4.00	60.72	B	627.20	2.55	7.52	7.16	35.17
A:64	598995.1	6584548.3	T	633.60	1.75	7.52	9.55	82.76	B	563.20	2.16	8.51	5.97	45.52
A:65	598985.6	6584519.8	T	608.00	1.45	9.90	16.72	117.24	B	297.60	1.53	5.94	0.00	34.48
A:66	598986.1	6584521.7	T	542.40	1.57	9.50	13.13	111.72	B	510.40	1.83	5.94	0.00	68.97
A:67	598986.6	6584523.7	T	526.40	1.47	10.10	13.13	100.69	B	297.60	1.92	7.13	0.00	48.97
A:68	598987.1	6584525.6	T	491.20	1.59	9.11	10.75	109.66	B	521.60	1.23	7.33	0.00	42.07
A:69	598987.6	6584527.6	T	540.80	1.55	9.70	9.55	102.76	B	376.00	2.20	7.72	5.97	132.41
A:70	598988.1	6584529.5	T	507.20	1.38	9.70	9.55	8.90	B	390.40	1.30	6.14	0.00	35.86
A:71	598988.6	6584531.4	T	683.20	1.70	11.29	11.94	114.48	B	392.00	1.15	6.73	0.00	46.90
A:72	598989.1	6584533.3	T	531.20	1.43	9.50	10.75	82.76	B	430.40	1.83	8.71	0.00	49.66
A:73	598989.6	6584535.3	T	593.60	1.35	10.50	8.36	93.10	B	372.80	1.62	7.33	3.58	51.72
A:74	598990.1	6584537.2	T	571.20	1.48	9.50	9.55	95.17	B	586.96	2.26	3.40	0.00	39.04
A:75	598990.6	6584539.2	T	616.00	1.65	9.31	7.16	102.76	B	321.60	1.78	6.34	0.00	22.76
A:76	598991.1	6584541.1	T	582.40	1.55	8.51	8.36	92.41	B	440.00	1.79	6.34	0.00	73.79
A:77	598991.6	6584543.0	T	625.60	1.59	8.32	0.00	86.21	B	672.00	2.60	5.74	4.78	20.69
A:78	598992.1	6584544.9	T	569.60	1.54	8.71	8.36	82.76	B	532.80	2.16	6.73	5.97	15.17
A:79	598992.6	6584546.8	T	699.20	1.82	8.71	0.00	91.03	B	344.00	2.14	10.10	0.00	46.21
A:80	598993.2	6584548.7	T	611.20	1.62	7.52	7.16	73.79	B	636.80	2.66	5.54	9.55	182.76
A:81	598983.6	6584520.3	T	494.40	1.22	9.50	13.13	92.41	B	366.40	1.07	5.35	0.00	43.45
A:82	598984.1	6584522.2	T	667.20	1.75	12.48	17.91	160.00	B	379.20	1.62	7.52	0.00	71.03
A:83	598984.6	6584524.1	T	596.80	1.71	10.50	14.33	135.86	B	366.40	1.64	7.52	0.00	53.10
A:84	598985.1	6584526.1	T	584.00	1.68	11.49	13.13	131.72	B	428.80	0.98	6.93	0.00	42.76
A:85	598985.6	6584528.0	T	523.20	1.67	10.89	9.55	122.07	B	409.60	1.56	6.73	0.00	65.52
A:86	598986.1	6584530.0	T	548.80	1.70	10.30	10.75	120.00	B	419.20	1.35	6.53	0.00	64.83
A:87	598986.6	6584531.9	T	471.01	1.13	6.30	5.33	63.13	B	356.52	0.72	3.57	0.00	54.46
A:88	598987.1	6584533.8	T	440.00	1.42	8.91	7.16	74.48	B	398.40	1.91	10.69	5.97	117.24
A:89	598987.6	6584535.7	T	556.80	1.55	9.50	8.36	101.38	B	339.20	2.71	6.53	0.00	91.03
A:90	598988.1	6584537.7	T	553.62	1.28	7.32	4.00	67.47	B	371.01	1.90	3.74	0.00	36.63

SITE A

id	x-UTM	y-UTM	Niveau	[P]/ppm	[Fe]/‰	[Zn]/ppm	[Cu]/ppm	[Mn]/ppm	Niveau	[P]/ppm	[Fe]/‰	[Zn]/ppm	[Cu]/ppm	[Mn]/ppm
A:91	598988.6	6584539.6	T	692.80	1.72	10.10	10.75	111.03	B	995.20	3.10	6.93	9.55	36.55
A:92	598989.1	6584541.6	T	564.80	1.70	10.30	10.75	100.00	B	457.60	2.47	6.93	0.00	51.72
A:93	598989.6	6584543.5	T	553.62	1.49	6.30	4.00	65.06	B	558.40	1.43	6.93	4.78	34.48
A:94	598990.1	6584545.4	T	511.59	1.49	6.30	4.00	62.65	B	485.51	2.62	3.74	0.00	23.13
A:95	598990.6	6584547.4	T	592.00	1.63	8.71	8.36	79.31	B	1003.20	2.99	5.54	8.36	31.72
A:96	598991.2	6584549.3	T	688.00	1.61	8.91	10.75	83.45	B	900.80	2.84	6.93	5.97	81.38
A:97	598981.7	6584520.8	T	547.20	1.70	12.08	16.72	136.55	B	417.60	1.68	7.92	3.58	73.79
A:98	598982.2	6584522.7	T	531.88	1.03	6.81	9.33	73.25	B	393.60	1.13	6.34	0.00	50.34
A:99	598982.7	6584524.7	T	542.40	1.58	10.10	14.33	114.48	B	441.60	1.48	7.52	0.00	75.86
A:100	598983.2	6584526.6	T	534.40	1.39	9.70	9.55	104.14	B	427.20	1.75	9.11	0.00	104.83
A:101	598983.7	6584528.5	T	659.20	1.61	12.48	15.52	131.03	B	407.25	0.87	3.74	0.00	28.92
A:102	598984.2	6584530.5	T	500.80	1.61	10.30	9.55	115.86	B	361.60	1.45	7.72	3.58	83.45
A:103	598984.7	6584532.4	T	494.40	1.47	9.50	9.55	106.90	B	360.87	1.64	3.74	0.00	63.13
A:104	598985.2	6584534.4	T	544.93	1.38	6.47	5.33	67.95	B	317.39	1.23	3.06	0.00	48.67
A.105	598985.7	6584536.3	T	544.00	1.36	9.11	7.16	90.34	B	379.20	1.55	8.12	0.00	63.45
A.106	598986.2	6584538.2	T	553.60	1.66	10.69	9.55	113.79	B	179.71	1.28	4.43	0.00	37.11
A.107	598986.7	6584540.1	T	565.22	1.18	10.69	5.33	70.84	B	508.70	1.59	3.40	0.00	28.43
A.108	598987.2	6584542.1	T	593.60	1.45	10.69	8.36	97.93	B	353.62	1.23	4.60	0.00	36.63
A.109	598987.7	6584544.0	T	556.52	1.33	5.45	4.00	63.61	B	542.40	2.87	6.93	4.78	20.69
A.110	598988.2	6584546.0	T	586.96	1.59	5.96	5.33	69.88	B	604.35	1.38	3.74	0.00	34.70
A:111	598988.7	6584547.9	T	668.80	1.44	7.92	8.36	85.52	B	675.20	1.73	7.92	4.78	37.93
A.112	598989.3	6584549.8	T	593.60	1.64	9.50	9.55	82.07	B	904.00	2.59	6.73	5.97	170.34
A:113	598979.7	6584521.3	T	485.51	0.92	7.15	8.00	70.36	B	363.20	1.51	6.53	4.78	69.66
A.114	598980.2	6584523.2	T	520.29	1.28	7.32	9.33	74.22	B	328.00	2.01	6.14	4.78	66.21
A:115	598980.7	6584525.2	T	616.00	1.65	11.29	20.30	142.76	B	369.60	1.00	6.14	3.58	55.17
A:116	598981.2	6584527.1	T	643.20	1.26	10.10	11.94	102.76	B	372.80	1.24	7.92	3.58	55.86
A.117	598981.7	6584529.0	T	625.60	1.46	10.89	10.75	106.90	B	376.00	1.31	7.52	4.78	41.38
A:118	598982.2	6584531.0	T	510.40	1.35	9.11	7.16	91.03	B	257.60	0.94	7.72	3.58	35.17
A:119	598982.7	6584532.8	T	424.64	0.92	9.53	4.00	65.06	B	356.52	1.13	3.74	0.00	37.59
A:120	598983.2	6584534.7	T	444.93	1.08	5.96	0.00	61.20	B	314.49	1.08	4.09	0.00	45.78
A:121	598983.7	6584536.3	T	547.20	1.40	10.69	9.55	106.90	B	278.26	1.28	4.09	0.00	53.49
A:122	598984.2	6584538.7	T	410.14	0.92	5.62	0.00	54.46	B	347.20	2.05	7.92	4.78	93.10
A:123	598984.7	6584540.6	T	534.78	1.44	6.30	4.00	69.88	B	389.86	1.08	3.57	0.00	23.61
A:124	598985.2	6584542.6	T	579.71	1.49	6.30	0.00	68.43	B	449.28	1.95	3.23	0.00	21.20
A:125	598985.7	6584544.5	T	545.60	1.38	9.31	4.78	87.59	B	627.54	2.36	4.43	0.00	56.39
A:126	598986.2	6584546.5	T	520.29	1.28	5.45	4.00	57.83	B	586.96	3.13	4.09	0.00	33.25
A:127	598986.7	6584548.4	T	559.42	1.13	6.30	4.00	65.06	B	481.60	2.37	6.73	0.00	30.34
A:128	598987.3	6584550.4	T	571.20	1.59	10.10	9.55	87.59	B	860.80	2.78	7.72	5.97	63.45

SITE B

id	x-UTM	y-UTM	Niveau	[P]/ppm	[Fe]/‰	[Zn]/ppm	[Cu]/ppm	[Mn]/ppm	Niveau	[P]/ppm	[Fe]/‰	[Zn]/ppm	[Cu]/ppm	[Mn]/ppm
B:1	596746.0	6583967.5	T	1019.05	3.51	53.05	32.00	166.46	B	1455.56	4.24	25.89	14.55	95.90
B:2	596746.9	6583966.9	T	1068.25	4.65	45.89	33.45	183.85	B	1169.84	3.35	25.68	21.82	96.89
B:3	596747.8	6583966.3	T	1036.51	3.51	42.32	33.45	147.58	B	1211.11	2.86	19.58	18.91	125.22
B:4	596748.8	6583965.6	T	1058.73	3.43	39.58	30.55	167.95	B	1192.06	4.82	23.79	23.27	108.32
B:5	596749.7	6583965.0	T	1046.03	4.65	51.58	33.45	186.34	B	1122.22	4.08	37.26	24.73	103.85
B:6	596750.6	6583964.4	T	1058.73	3.84	48.63	32.00	179.88	B	1004.76	4.16	43.16	24.73	98.88
B:7	596751.5	6583963.8	T	1355.56	4.82	66.53	39.27	138.63	B	1419.05	4.33	36.84	24.73	95.40
B:8	596752.4	6583963.1	T	1042.86	3.51	62.11	34.91	144.10	B	1211.11	4.08	38.74	23.27	100.87
B:9	596753.3	6583962.5	T	1052.38	3.76	49.05	34.91	191.30	B	1396.83	4.00	42.95	24.73	98.88
B:10	596754.3	6583961.9	T	1101.59	3.43	63.16	39.27	165.96	B	1823.81	4.00	44.84	32.00	97.39
B:11	596755.2	6583961.3	T	1830.00	5.06	69.00	44.00	146.00	B	1728.57	4.16	52.42	34.91	124.72
B:12	596756.1	6583960.6	T	1053.97	3.35	45.89	34.91	170.93	B	1622.22	3.84	49.05	29.09	112.80
B:13	596757.0	6583960.0	T	1060.32	3.92	67.79	34.91	195.78	B	1069.84	4.08	55.58	39.27	165.96
B.14	596757.8	6583959.5	T	1146.03	5.88	65.05	40.73	148.57	B	1322.22	4.49	62.74	26.18	111.80
B:15	596758.5	6583959.0	T	1026.98	1.91	64.00	18.91	170.43	B	1134.92	2.01	42.53	160.00	139.63
B:16	596759.3	6583958.5	T	1050.79	3.18	52.00	34.91	214.66	B	901.59	4.08	46.53	30.55	118.76
B:17	596760.0	6583958.0	T	923.81	1.95	56.63	16.00	193.79	B	900.00	2.00	41.05	17.45	169.44
B:18	596760.8	6583957.5	T	847.62	1.82	52.21	13.09	167.95	B	838.10	2.00	45.26	14.55	145.09
B:19	596761.6	6583957.0	T	1055.56	5.14	57.26	40.73	188.32	B	809.52	1.78	34.32	11.64	121.24
B:20	596762.3	6583956.5	T	822.22	1.84	56.21	20.36	155.03	B	938.10	4.65	43.79	32.00	154.53
B:21	596763.1	6583956.0	T	766.67	1.96	54.53	189.09	182.86	B	758.73	1.62	38.53	13.09	85.47
B:22	596763.8	6583955.5	T	761.90	1.85	54.11	1.45	182.36	B	980.95	3.76	44.84	34.91	172.42
B:23	596764.6	6583955.0	T	812.70	1.89	53.05	17.45	172.92	B	857.14	2.00	36.84	14.55	148.07
B:24	596765.4	6583954.5	T	836.51	1.85	51.58	17.45	138.14	B	792.06	1.86	34.32	11.64	90.43
B:25	596766.1	6583954.0	T	820.63	1.75	57.47	18.91	133.17	B	668.25	1.89	40.00	11.64	130.19
B:26	596766.8	6583953.5	T	928.57	3.59	57.68	37.82	179.88	B	630.16	1.71	41.26	13.09	94.91
B:27	596767.6	6583953.0	T	957.14	3.51	58.11	39.27	168.45	B	688.89	1.88	29.47	13.09	119.75
B:28	596768.4	6583952.5	T	898.41	3.59	62.11	39.27	168.94	B	768.25	3.27	36.63	29.09	133.17
B:29	596769.2	6583952.0	T	830.16	1.71	69.26	18.91	161.49	B	647.62	4.08	33.68	26.18	129.19
B:30	596769.9	6583951.5	T	990.48	4.41	72.42	37.82	209.69	B	611.11	1.58	22.74	13.09	73.04
B:31	596770.7	6583951.0	T	938.10	4.24	70.95	33.45	205.71	B	817.46	4.24	48.42	36.36	165.96
B:32	596771.4	6583950.5	T	839.68	1.86	70.11	20.36	167.95	B	615.87	1.87	47.37	13.09	139.13
B:33	596772.2	6583950.0	T	909.52	3.76	70.53	34.91	190.31	B	720.63	1.98	38.74	29.09	151.06
B:34	596773.0	6583949.5	T	968.25	3.84	69.47	37.82	197.27	B	734.92	1.96	50.95	13.09	163.98
B:35	596773.7	6583949.0	T	968.25	5.22	65.47	34.91	206.71	B	826.98	1.80	60.84	13.09	167.45
B:36	596774.5	6583948.5	T	850.79	1.83	50.95	13.09	162.98	B	1039.68	1.95	89.26	16.00	206.21
B:37	596775.2	6583948.0	T	731.75	1.88	43.37	11.64	128.20	B	1038.10	3.59	79.58	39.27	227.08
B:38	596776.0	6583947.5	T	901.59	3.59	48.00	33.45	182.36	B	801.59	1.95	97.05	16.00	205.22
B:39	596776.5	6583946.6	T	742.86	0.37	44.00	11.64	151.55	B	922.22	1.90	53.26	14.55	170.43
B:40	596777.0	6583945.6	T	679.37	1.66	33.05	0.00	129.69	B	669.84	1.88	38.95	0.00	176.89
B:41	596777.4	6583944.7	T	658.73	1.71	32.63	13.09	124.72	B	704.76	1.73	49.26	11.64	201.74
B:42	596777.9	6583943.8	T	590.48	1.76	27.37	0.00	118.76	B	696.83	4.57	50.32	23.27	240.00
B:43	596778.4	6583942.8	T	692.06	3.43	30.32	27.64	144.60	B	530.16	1.96	17.26	0.00	110.31
B:44	596778.9	6583941.9	T	723.81	4.57	30.11	24.73	149.57	B	569.84	5.06	25.05	20.36	187.33

SITE B

id	x-UTM	y-UTM	Niveau	[P]/ppm	[Fe]/‰	[Zn]/ppm	[Cu]/ppm	[Mn]/ppm	Niveau	[P]/ppm	[Fe]/‰	[Zn]/ppm	[Cu]/ppm	[Mn]/ppm
B:45	596779.3	6583941.0	T	577.78	1.70	26.74	16.00	119.75	B	603.17	4.90	30.32	26.18	166.46
B:46	596779.8	6583940.0	T	617.46	1.79	28.63	0.00	128.20	B	563.49	6.69	26.11	27.64	188.82
B:47	596780.3	6583939.1	T	677.78	1.82	29.05	0.00	146.09	B	676.19	4.90	30.95	36.36	169.94
B:48	596780.8	6583938.2	T	682.54	1.65	23.79	0.00	122.24	B	531.75	1.79	18.32	0.00	88.94
B:49	596781.3	6583937.2	T	690.48	1.76	26.95	0.00	120.25	B	414.29	1.78	21.05	0.00	82.98
B:50	596781.7	6583936.3	T	639.68	1.68	23.37	0.00	103.35	B	304.76	5.96	24.42	20.36	95.90
B:51	596782.2	6583935.3	T	671.43	1.73	25.89	0.00	127.70	B	438.10	1.98	19.79	0.00	75.03
B:52	596782.7	6583934.4	T	622.22	1.77	29.89	0.00	136.65	B	471.43	1.88	17.68	0.00	64.60
B:53	596783.2	6583933.5	T	703.17	1.73	26.11	0.00	131.18	B	561.90	1.76	22.95	0.00	101.37
B:54	596783.7	6583932.5	T	822.22	3.59	36.00	29.09	166.96	B	477.78	5.31	24.42	26.18	74.53
B:55	596784.1	6583931.6	T	814.29	4.73	28.42	26.18	176.40	B	633.33	3.27	22.95	26.18	123.23
B:56	596784.6	6583930.7	T	868.25	3.27	30.95	29.09	199.25	B	1115.87	6.61	63.58	59.64	207.21
B:57	596785.1	6583929.7	T	869.84	3.02	25.89	26.18	161.49	B	958.73	4.33	36.63	37.82	174.41
B:58	596785.5	6583928.8	T	866.67	4.16	38.95	32.00	187.33	B	874.60	5.14	36.00	37.82	191.80
B:59	596786.0	6583927.9	T	893.65	3.18	25.68	26.18	177.89	B	896.83	4.33	36.00	34.91	184.84
B:60	596786.5	6583926.9	T	933.33	5.47	36.84	30.55	199.75	B	898.41	4.00	33.68	45.09	178.88
B:61	59678.07	6583926.0	T	906.35	3.51	32.00	36.36	162.98	B	719.05	4.98	30.53	34.91	130.19
B:62	596787.5	6583925.1	T	903.17	4.57	37.47	33.45	182.36	B	723.81	3.02	46.95	24.73	108.82
B:63	596788.1	6583924.3	T	838.10	2.53	33.47	24.73	138.63	B	694.00	3.35	38.00	23.00	103.00
B:64	596788.6	6583923.4	T	798.41	3.02	33.26	24.73	143.60	B	663.49	3.67	28.21	20.36	96.40
B:65	596789.1	6583922.6	T	850.79	3.92	30.53	34.91	160.00	B	611.11	4.65	25.47	27.64	97.39
B:66	596789.6	6583921.7	T	828.57	4.00	35.16	33.45	166.96	B	642.86	5.06	32.42	32.00	114.29
B:67	596790.1	6583920.8	T	817.46	3.51	34.32	27.64	161.99	B	598.41	4.73	26.95	26.18	110.31
B:68	596790.7	6583920.0	T	760.32	3.18	32.84	29.09	140.62	B	555.56	3.76	25.89	27.64	99.38
B:69	596791.1	6583919.1	T	773.02	2.61	34.11	29.09	147.58	B	714.29	4.41	32.63	30.55	140.12
B:70	596791.7	6583918.2	T	795.24	4.16	33.89	27.64	163.48	B	747.62	4.82	35.16	32.00	155.03
B:71	596792.2	6583917.4	T	820.63	3.59	26.32	23.27	174.41	B	604.76	4.41	27.37	30.55	88.45
B:72	596792.7	6583916.5	T	792.06	3.10	32.21	24.73	137.64	B					
B:73	596793.2	6583915.7	T	833.33	3.10	33.05	23.27	123.23	B					
B:74	596793.7	6583914.8	T	736.51	3.84	30.11	27.64	125.22	B					
B:75	596794.2	6583913.9	T	753.97	6.12	33.26	27.64	149.07	B		Data mangler			
B:76	596794.8	6583913.1	T	747.62	4.24	29.26	30.55	123.23	B					
B:77	596795.3	6583912.2	T	749.21	3.10	29.47	21.82	112.80	B					
B:78	596795.8	6583911.3	T	777.78	5.31	24.21	21.82	137.64	B					
B:79	596796.3	6583910.5	T	790.48	2.53	26.95	24.73	106.34	B	584.13	3.59	27.58	24.73	79.01
B:80	596796.8	6583909.6	T	761.90	2.37	22.95	21.82	115.78	B	576.19	3.51	32.00	21.82	88.94
B:81	596797.3	6583908.8	T	725.40	2.94	27.79	21.82	109.81	B	665.08	4.08	30.32	21.82	85.96
B:82	596797.9	6583907.9	T	734.92	1.96	20.63	23.27	108.32	B	682.54	4.24	23.37	24.73	105.34
B:83	596798.4	6583907.0	T	766.67	3.43	31.16	21.82	128.70	B	692.06	3.92	25.26	21.82	121.74
B:84	596798.9	6583906.2	T	744.44	2.86	28.63	21.82	97.89	B	625.40	4.08	24.42	20.36	101.86
B:85	596799.4	6583905.3	T	733.33	2.78	28.21	20.36	101.86	B	617.46	5.55	23.58	23.27	83.48
B:86	596799.9	6583904.4	T	750.79	2.61	29.68	21.82	108.32	B	644.44	3.84	29.05	18.91	125.71
B:87	596800.4	6583903.6	T	722.22	2.69	29.26	21.82	99.88	B	619.05	2.94	21.05	23.27	100.87
B:88	596801.0	6583902.7	T	722.22	2.86	31.16	18.91	119.75	B	660.32	4.57	23.79	18.91	107.33
B:89	596801.5	6583901.9	T	768.25	2.53	30.74	20.36	105.84	B	658.73	3.10	29.05	18.91	104.84

SITE B

id	x-UTM	y-UTM	Niveau	[P]/ppm	[Fe]/‰	[Zn]/ppm	[Cu]/ppm	[Mn]/ppm	Niveau	[P]/ppm	[Fe]/‰	[Zn]/ppm	[Cu]/ppm	[Mn]/ppm
B:90	596802.0	6583901.0	T	820.63	2.94	31.37	20.36	109.32	B	685.71	5.14	22.53	18.91	112.80
B:91	596802.5	6583900.1	T	779.37	2.53	29.89	18.91	113.79	B	723.81	3.84	31.79	18.91	102.86
B:92	596803.0	6583899.2	T	793.65	3.59	28.21	17.45	133.17	B	607.94	4.33	23.58	20.36	120.25
B:93	596803.5	6583898.3	T	761.90	2.29	22.53	20.36	131.68	B	679.37	3.18	23.58	23.27	151.06
B:94	596804.0	6583897.4	T	753.97	2.78	34.53	20.36	100.87	B	622.22	3.10	20.42	21.82	113.79
B:95	596804.5	6583896.5	T	753.97	2.78	37.89	17.45	120.25	B	546.03	2.69	23.79	17.45	78.01
B:96	596805.0	6583895.6	T	773.02	2.61	27.16	18.91	122.73	B	493.65	3.35	26.74	16.00	98.88
B:97	596805.5	6583894.7	T	773.02	3.02	42.53	23.27	128.20	B	536.51	3.76	20.84	14.55	118.26
B:98	596806.0	6583893.8	T	811.11	3.51	36.21	20.36	158.01	B	547.62	2.94	21.89	18.91	122.73
B:99	596806.5	6583892.9	T	768.25	2.29	52.84	20.36	125.22	B	588.89	2.69	31.58	16.00	86.46
B:100	596807.0	6583892.0	T	768.25	2.29	52.84	20.36	125.22	B	626.98	4.82	30.95	23.27	134.16
B1:1	596793.0	6583896.0	T	787.30	3.18	33.26	20.36	119.75	B	712.70	3.59	32.00	21.82	122.73
B1:2	596794.8	6583897.0	T	726.98	2.29	32.63	18.91	116.27	B	588.89	3.59	28.42	20.36	122.73
B1:3	596796.6	6583898.0	T	777.78	2.94	36.21	20.36	119.75	B	638.10	4.00	33.05	20.36	129.69
B1:4	596798.4	6583899.0	T	703.17	2.94	34.95	20.36	142.11	B	628.57	3.43	31.58	21.82	123.23
B1:5	596800.2	6583900.0	T	796.83	2.69	31.37	20.36	121.24	B	653.97	3.35	32.84	21.82	138.63
B1:6	596803.8	6583902.0	T	738.10	2.69	32.42	20.36	115.78	B	661.90	3.51	32.21	37.82	136.65
B1:7	596805.6	6583903.0	T	700.00	2.94	27.79	20.36	118.26	B	665.08	4.16	29.05	21.82	131.68
B1:8	596807.4	6583904.0	T	709.52	3.02	26.11	18.91	111.80	B	569.84	4.90	30.95	23.27	142.11
B1:9	596809.2	6583905.0	T	652.38	3.10	30.11	18.91	127.21	B	414.29	3.27	30.11	17.45	83.98
B1:10	596811.0	6583906.0	T	684.13	2.94	28.42	20.36	126.21	B	371.43	4.57	27.79	20.36	87.45
B2:1	596778.0	6583921.0	T	977.78	2.78	50.11	40.73	177.89	B	722.22	3.67	29.05	27.64	110.81
B2:2	596779.8	6583922.0	T	952.00	2.98	53.00	37.00	178.00	B	653.97	3.51	25.26	20.36	76.02
B2:3	596781.6	6583923.0	T	925.40	3.18	55.16	32.00	178.39	B	639.68	3.27	32.00	23.27	96.89
B2:4	596783.4	6583924.0	T	971.43	3.27	43.16	33.45	181.86	B	765.08	4.08	36.63	27.64	108.82
B2:5	596785.2	6583925.0	T	952.38	3.27	43.16	33.45	155.03	B	796.83	3.67	41.89	33.45	167.95
B2:6	596788.8	6583927.0	T	858.73	2.53	36.21	24.73	150.06	B	814.29	3.67	42.95	29.09	156.52
B2:7	596790.6	6583928.0	T	936.51	3.27	36.63	24.73	154.53	B	750.79	3.84	38.11	24.73	133.66
B2:8	596792.4	6583929.0	T	758.73	2.94	30.32	21.82	138.63	B	609.52	2.86	28.63	20.36	125.22
B2:9	596794.2	6583930.0	T	700.00	2.61	28.00	17.45	137.14	B	485.71	3.43	26.11	14.55	79.01
B2:10	596796.0	6583931.0	T	696.83	2.61	27.16	14.55	127.21	B	495.24	3.51	21.89	13.09	78.51
B3:1	596769.0	6583940.5	T	822.86	3.50	114.36	40.00	363.64	B	558.57	3.30	37.82	16.00	278.79
B3:2	596770.4	6583941.9	T	781.43	3.05	82.55	34.67	334.55	B	810.00	3.70	73.64	32.00	364.85
B3:3	596771.8	6583943.3	T	761.43	2.85	62.36	30.67	338.18	B	1075.71	3.25	80.18	33.33	431.52
B3:4	596773.2	6583944.7	T	732.86	2.95	55.27	28.00	320.00	B	871.43	2.62	66.73	36.00	396.36
B3:5	596774.6	6583946.1	T	711.43	3.35	49.64	29.33	361.21	B	815.71	3.85	60.73	29.33	367.27
B3:6	596777.4	6583948.9	T	775.71	3.05	38.36	24.00	338.18	B	882.86	2.86	64.73	25.33	456.97
B3:7	596778.8	6583950.3	T	797.14	3.18	66.73	24.00	495.76	B	825.71	4.10	38.73	30.67	360.00
B3:8	596780.2	6583951.7	T	745.71	3.18	32.91	21.33	380.61	B	637.14	3.60	29.82	28.00	260.61
B3:9	596781.6	6583953.1	T	734.29	3.35	35.09	22.67	412.12	B	754.29	3.10	34.18	22.67	427.88
B3:10	596783.0	6583954.5	T	744.29	3.15	31.09	26.67	333.33	B	777.14	3.60	32.91	30.67	333.33
B4:1	596751.0	6583952.0	T	1808.82	3.75	14.00	38.67	144.39	B	1879.41	3.75	13.08	44.00	140.98
B4:2	596752.2	6583953.6	T	1202.94	3.25	13.84	34.67	144.88	B	1755.88	3.05	11.35	40.00	115.12
B4:3	596753.4	6583955.2	T	1375.00	3.05	14.16	42.67	148.78	B	1875.00	3.35	11.83	40.00	137.07
B4:4	596754.6	6583956.8	T	1177.94	2.80	13.84	38.67	159.02	B	1863.23	3.25	10.46	34.67	114.15

SITE B

id	x-UTM	y-UTM	Niveau	[P]/ppm	[Fe]/‰	[Zn]/ppm	[Cu]/ppm	[Mn]/ppm	Niveau	[P]/ppm	[Fe]/‰	[Zn]/ppm	[Cu]/ppm	[Mn]/ppm
B4:5	596755.8	6583958.4	T	1070.59	3.35	12.80	36.00	137.56	B	1683.82	3.65	9.50	30.67	103.41
B4:6	596758.2	6583961.6	T	839.71	2.65	11.91	36.00	129.27	B	1122.06	3.15	10.62	33.33	119.51
B4:7	596759.4	6583963.2	T	1163.23	3.25	12.15	30.67	139.51	B	1486.77	3.40	10.22	32.00	120.98
B4:8	596760.6	6583964.8	T	1230.88	2.90	13.36	38.67	139.51	B	914.71	3.15	8.73	30.67	104.39
B4:9	596761.8	6583966.4	T	976.47	2.85	10.91	32.00	133.66	B	1004.41	3.35	9.54	30.67	120.00
B4:10	596763.0	6583968.0	T	1001.47	2.50	10.14	30.67	133.17	B	1029.41	3.30	9.42	25.33	121.95

SITE C

id	x-UTM	y-UTM	Niveau	[P]/ppm	[Fe]/‰	[Zn]/ppm	[Cu]/ppm	[Mn]/ppm	Niveau	[P]/ppm	[Fe]/‰	[Zn]/ppm	[Cu]/ppm	[Mn]/ppm
C:0	597436.2	6583691.3	T	938.84	3.04	48.17	20.77	906.19	B	980.17	3.04	41.91	24.62	815.93
C:5	597437.3	6583696.2	T	961.98	3.32	41.57	20.77	674.34	B	894.21	3.32	44.00	18.46	706.19
C:10	597438.4	6583701.1	T	1036.36	3.43	46.43	23.08	691.15	B	869.42	3.43	31.13	16.15	353.10
C:11	597438.6	6583702.1	T	996.69	3.40	42.78	21.54	812.39	B	851.24	3.40	33.04	18.46	492.04
C:12	597438.8	6583703.1	T	973.55	3.45	46.96	20.77	733.63	B	851.24	3.45	35.13	17.69	543.36
C:13	597439.0	6583704.1	T	909.09	3.41	49.39	20.77	900.88	B	826.45	3.41	34.26	17.69	512.39
C.14	597439.3	6583705.1	T	1008.26	3.41	48.35	23.85	636.28	B	826.45	3.41	33.22	18.46	387.61
C:15	597439.5	6583706.1	T	1018.18	3.41	41.22	21.54	639.82	B	831.40	3.41	34.43	53.08	452.21
C:16	597439.7	6583707.0	T	991.74	3.41	51.48	20.77	761.95	B	947.11	3.41	31.13	18.46	528.32
C:17	597439.9	6583708.0	T	1018.18	3.80	34.26	23.08	847.79	B	938.84	3.80	26.61	15.38	405.31
C:18	597440.1	6583709.0	T	966.94	3.35	42.61	54.62	645.13	B	925.62	3.35	24.87	14.62	372.57
C:19	597440.4	6583710.0	T	1028.10	3.62	46.26	23.85	711.50	B	869.42	3.62	26.96	9.23	307.96
C:20	597440.6	6583711.0	T	1014.88	3.45	38.78	23.08	637.17	B	980.17	3.45	28.87	13.85	450.44
C:21	597440.8	6583712.0	T	1038.02	3.73	40.17	23.85	723.01	B	983.47	3.73	38.09	17.69	600.88
C:22	597441.0	6583713.0	T	955.37	3.34	41.22	22.31	766.37	B	1023.14	3.34	30.61	17.69	495.58
C:23	597441.3	6583713.9	T	998.35	3.43	42.26	23.08	846.90	B	1009.92	3.43	37.74	18.46	646.90
C:24	597441.5	6583714.9	T	973.55	3.38	48.52	23.08	805.31	B	877.69	3.38	26.26	13.85	507.96
C:25	597441.7	6583715.9	T	1009.92	3.49	43.13	24.62	753.98	B	914.05	3.49	32.35	12.31	462.83
C:26	597441.9	6583716.9	T	942.15	3.11	36.35	23.85	815.93	B	1023.14	3.11	32.70	13.85	476.11
C:27	597442.1	6583717.9	T	1019.84	3.74	40.70	24.62	800.00	B	842.98	3.74	26.78	10.77	436.28
C:28	597442.4	6583718.8	T	1064.46	3.41	38.43	24.62	750.44	B	836.36	3.41	26.78	16.15	527.43
C:29	597442.6	6583719.8	T	1036.36	3.61	38.43	25.38	820.35	B	842.98	3.61	25.57	13.08	413.27
C:30	597442.8	6583720.8	T	938.84	3.73	42.26	26.92	807.08	B	993.39	3.73	34.26	20.77	617.70
C:31	597443.0	6583721.8	T	1033.06	3.72	42.96	27.69	819.47	B	915.70	3.72	36.35	22.31	693.81
C:32	597443.2	6583722.8	T	1014.88	3.77	45.04	27.69	852.21	B	1023.14	3.77	43.65	35.38	641.59
C:33	597443.5	6583723.8	T	1039.67	3.58	38.09	29.23	831.86	B	1026.45	3.58	46.09	30.77	663.72
C:34	597443.7	6583724.7	T	1064.46	3.99	38.78	27.69	821.24	B	1011.57	3.99	41.57	27.69	707.96
C:35	597443.9	6583725.7	T	1051.24	3.77	48.70	29.23	36.28	B	1052.89	3.77	30.61	19.23	587.61
C:36	597444.1	6583726.7	T	1066.12	4.15	44.87	30.00	903.54	B	1130.58	4.15	30.09	16.92	543.36
C:37	597444.3	6583727.7	T	1064.46	2.91	19.48	20.00	541.59	B	765.29	3.82	18.26	16.15	450.44
C:38	597444.6	6583728.7	T	1112.40	3.88	40.52	30.00	837.17	B	928.93	2.91	31.30	20.77	728.32
C:39	597444.8	6583729.7	T	1077.69	3.70	46.61	30.00	856.64	B	942.15	3.88	33.91	20.00	641.59
C:40	597445.0	6583730.6	T	1138.84	4.13	46.43	30.77	865.49	B	947.11	3.70	36.35	24.62	674.34
C:41	597445.2	6583731.6	T	1165.29	3.99	45.39	32.31	861.06	B	851.24	4.13	32.35	46.92	717.70
C:42	597445.4	6583732.6	T	1143.80	3.84	46.61	30.77	826.55	B	885.95	3.99	25.91	18.46	468.14
C:43	597445.7	6583733.6	T	1201.65	4.07	49.57	31.54	853.98	B	996.69	3.84	36.52	23.08	685.84
C:44	597445.9	6583734.6	T	1200.00	4.18	42.09	33.08	840.71	B	971.90	4.07	33.22	22.31	646.02
C:45	597446.1	6583735.6	T	1272.73	4.33	37.91	34.62	698.23	B	1112.40	4.18	14.78	20.77	300.88
C:46	597446.3	6583736.5	T	1165.29	4.31	2.33	34.62	738.05	B	1272.73	4.33	13.91	20.77	505.31
C:47	597446.5	6583737.5	T	1252.89	4.02	46.61	30.77	545.13	B	1380.17	4.31	23.30	22.31	425.66
C:48	597446.8	6583738.5	T	1280.99	4.33	36.17	37.69	761.06	B	1368.60	4.02	22.26	23.85	604.42
C:49	597447.0	6583739.5	T	1272.73	4.68	38.96	42.31	726.55	B	1361.98	4.33	25.22	26.15	562.83
C:50	597447.2	6583740.5	T	1256.20	4.30	51.48	43.08	794.69	B	1600.00	4.68	38.43	30.00	383.19
C:51	597447.4	6583741.5	T	1227.83	3.55	56.42	22.76	560.00	B	1441.74	4.30	61.68	24.83	312.26

SITE C

id	x-UTM	y-UTM	Niveau	[P]/ppm	[Fe]/‰	[Zn]/ppm	[Cu]/ppm	[Mn]/ppm	Niveau	[P]/ppm	[Fe]/‰	[Zn]/ppm	[Cu]/ppm	[Mn]/ppm
C:52	597447.6	6583742.4	T	1315.70	4.68	38.78	58.46	510.62	B	1266.12	3.55	33.39	76.92	366.37
C:53	597447.9	6583743.4	T	1256.20	4.13	32.35	40.77	552.21	B	1097.52	4.68	25.04	153.08	353.10
C:54	597448.1	6583744.4	T	1307.44	4.34	46.96	43.85	748.67	B	1170.25	4.13	38.43	33.85	470.80
C:55	597448.3	6583745.4	T	1315.70	4.15	39.83	41.54	819.47	B	1347.11	4.34	36.17	27.69	469.03
C:56	597448.5	6583746.4	T	1444.63	4.07	45.04	39.23	684.96	B	1094.21	4.15	25.04	20.77	435.40
C:57	597448.7	6583747.4	T	1507.44	3.75	44.52	35.38	709.73	B	1299.17	4.07	34.61	27.69	442.48
C:58	597448.9	6583748.3	T	1403.31	4.10	63.13	43.08	881.42	B	1385.12	3.75	34.43	23.08	491.15
C:59	597449.2	6583749.3	T	1400.00	4.42	58.43	41.54	784.96	B	1512.40	4.10	36.00	20.00	480.53
C:60	597449.4	6583750.3	T	1380.17	4.44	55.83	43.08	821.24	B	1479.34	4.42	41.57	20.00	569.03
C:61	597449.6	6583751.3	T	1629.75	3.11	50.43	39.23	665.49	B	1300.83	4.44	23.65	18.46	415.04
C:62	597449.9	6583752.3	T	1410.43	3.54	66.53	21.38	703.23	B	1495.65	3.11	59.16	17.24	525.16
C:63	597450.1	6583753.3	T	1555.37	4.01	47.48	36.15	687.61	B	1690.91	3.54	32.35	16.92	656.64
C:64	597450.3	6583754.2	T	1560.33	3.87	47.13	42.31	728.32	B	1416.53	4.01	33.74	25.38	425.66
C:65	597450.5	6583755.2	T	1590.08	3.82	44.70	40.77	746.90	B	1519.01	3.87	25.57	20.77	695.58
C:66	597450.7	6583756.2	T	1333.88	4.30	50.43	30.77	607.96	B	1462.81	3.82	41.74	25.38	546.02
C:67	597450.9	6583757.2	T	1449.59	4.20	42.61	40.00	903.54	B	1492.56	4.30	41.74	25.38	652.21
C:68	597451.2	6583758.2	T	1504.13	4.12	59.30	40.00	792.92	B	1961.98	4.20	41.74	26.15	769.91
C:69	597451.4	6583759.2	T	1469.42	4.07	69.74	40.00	755.75	B	1259.50	4.12	28.70	22.31	388.50
C:70	597451.6	6583760.1	T	1550.41	3.84	29.57	32.31	733.63	B	1067.77	4.07	20.70	19.23	432.74
C:71	597451.8	6583761.1	T	1601.65	3.86	39.48	32.31	579.65	B	1166.94	3.84	18.96	16.92	310.62
C:72	597452.1	6583762.1	T	1282.65	3.83	55.13	30.00	795.58	B	829.75	3.86	21.57	16.92	389.38
C:73	597452.3	6583763.1	T	1310.00		44.00	30.00	779.00	B	877.69	3.83	23.65	19.23	561.06
C:74	597452.5	6583764.1	T	1338.84	3.92	34.26	30.77	762.83	B	866.12	3.92	5.91	16.92	534.51
C:75	597452.7	6583765.1	T	1277.69	3.55	30.43	28.46	692.04	B	866.12	3.55	15.48	14.62	537.17
C:76	597452.9	6583766.0	T	1211.57	3.03	27.30	22.31	586.73	B	847.93	3.03	25.91	17.69	822.12
C:77	597453.2	6583767.0	T	1234.00		37.00	24.00	615.00	B	829.00	3.02	23.00	15.00	665.00
C:78	597453.4	6583768.0	T	1256.20	3.02	43.13	24.62	645.13	B	809.92	3.14	19.30	11.54	506.19
C:79	597453.6	6583769.0	T	1143.80	3.14	23.83	25.38	717.70	B	861.16	3.01	16.52	13.85	896.46
C:80	597453.8	6583770.0	T	1147.11	3.01	12.87	20.77	605.31	B	838.02	2.98	32.52	20.77	624.78
C:81	597454..0	6583771.0	T	1327.27	2.98	27.65	23.08	627.43	B	846.28	3.18	28.17	18.46	486.73
C:82	597454.3	6583771.9	T	1203.31	3.18	15.83	23.08	576.11	B	753.72	3.00	15.13	18.46	352.21
C:83	597454.5	6583772.9	T	1320.66	3.00	20.70	21.54	536.28	B	813.22	4.16	18.26	14.62	487.61
C:84	597454.7	6583773.9	T	1322.31	3.01	25.04	21.54	628.32	B	864.46	3.01	37.74	18.46	429.20
C:85	597454.9	6583774.9	T	1325.62	3.70	39.65	30.00	668.14	B	867.77	3.70	27.30	19.23	501.77
C:86	597455.1	6583775.9	T	1204.96	3.09	9.22	21.54	238.94	B	816.53	3.09	9.22	16.15	443.36
C:87	597455.4	6583776.9	T	1234.71	2.80	29.39	20.00	546.02	B	690.91	2.80	18.26	16.92	429.20
C:88	597455.6	6583777.8	T	1120.66	3.17	26.61	22.31	571.68	B	895.87	3.17	23.48	19.23	571.68
C:89	597455.8	6583778.8	T	1019.84	3.03	15.30	20.77	379.65	B	732.23	3.03	20.87	19.23	505.31
C:90	597456.0	6583779.8	T	958.68	2.92	4.87	17.69	540.71	B	666.12	2.92	8.70	16.15	551.33
C:91	597456.3	6583780.8	T	1024.79	3.08	8.00	19.23	550.44	B	727.27	3.08	17.39	20.00	444.25
C:92	597456.5	6583781.8	T	983.47	3.00	22.43	16.15	500.88	B	786.78	3.00	29.22	20.77	539.82
C:93	597456.7	6583782.8	T	993.39	3.12	10.26	17.69	533.63	B	775.21	3.12	12.70	19.23	523.01
C:94	597456.9	6583783.7	T	1044.63	3.04	8.17	18.46	575.22	B	771.90	3.04	12.87	21.54	500.00
C:95	597457.1	6583784.7	T	1042.97	3.37	24.17	20.00	586.73	B	714.05	3.37	16.52	17.69	440.71
C:96	597457.4	6583785.7	T	1102.48	3.00	20.52	19.23	545.13	B	900.83	3.00	25.74	18.46	478.76

SITE C

id	x-UTM	y-UTM	Niveau	[P]/ppm	[Fe]/‰	[Zn]/ppm	[Cu]/ppm	[Mn]/ppm	Niveau	[P]/ppm	[Fe]/‰	[Zn]/ppm	[Cu]/ppm	[Mn]/ppm
C:97	597457.6	6583786.7	T	1011.57	3.43	23.30	18.46	517.70	B	575.21	3.43	19.30	18.46	357.52
C:98	597457.8	6583787.7	T	953.72	3.36	21.22	17.69	517.70	B	714.05	3.36	21.91	18.46	415.93
C:99	597458.0	6583788.7	T	947.11	3.17	35.65	41.54	526.55	B	757.02	3.17	15.13	20.00	483.19
C:100	597458.2	6583789.6	T	957.02	3.67	20.35	20.77	746.90	B	720.66	3.67	15.30	19.23	381.42
C:101	597458.5	6583790.6	T	925.62	3.59	23.48	19.23	557.52	B	657.85	3.59	24.35	20.00	544.25
C:102	597458.7	6583791.6	T	938.84	3.28	28.52	19.23	553.98	B	608.26	3.28	19.83	19.23	498.23
C:103	597458.9	6583792.6	T	948.76	3.67	34.09	20.00	520.35	B	659.50	3.67	21.39	29.23	519.47
C:104	597459.1	6583793.6	T	1009.92	3.51	26.78	19.23	593.81	B	593.39	3.51	20.00	26.15	469.91
C:105	597459.3	6583794.6	T	955.37	3.78	26.09	17.69	576.99	B	677.69	3.78	26.09	21.54	669.03
C:106	597459.6	6583795.5	T	862.81	3.57	24.52	18.46	544.25	B	705.79	3.57	22.61	16.92	492.92
C:107	597459.8	6583796.5	T	899.17	3.51	26.09	16.92	548.67	B	644.63	3.51	17.22	16.92	349.56
C:108	597460.0	6583797.5	T	877.69	3.36	28.00	17.69	584.96	B	740.50	3.36	20.35	13.08	428.32
C:109	597461.0	6583797.7	T	910.74	3.52	25.04	18.46	536.28	B	603.31	3.52	27.30	16.15	417.70
C:110	597461.9	6583798.0	T	866.12	3.41	17.74	17.69	592.04	B	669.42	3.41	16.52	20.77	438.94
C:111	597462.9	6583798.2	T	877.69	3.30	25.74	17.69	569.91	B	633.06	3.30	18.78	162.31	474.34
C:112	597463.9	6583798.5	T	862.81	3.25	14.09	25.38	492.92	B	649.59	3.25	15.83	17.69	298.23
C:113	597464.9	6583798.7	T	819.83	3.25	21.57	18.46	558.41	B	555.37	3.25	20.17	16.15	290.27
C:114	597465.8	6583798.9	T	887.60	3.41	25.22	17.69	626.55	B	553.72	3.41	25.74	16.92	319.47
C:115	597466.8	6583799.2	T	776.86	3.17	22.61	17.69	561.95	B	571.90	3.17	25.39	30.00	437.17
C:116	597467.8	6583799.4	T	836.36	3.09	26.61	18.46	581.42	B	634.71	3.09	25.39	17.69	478.76
C:117	597468.7	6583799.7	T	814.88	3.16	29.39	16.92	583.19	B	614.88	3.16	22.61	19.23	373.45
C:118	597469.7	6583799.9	T	728.93	3.44	22.43	16.15	548.67	B	634.71	3.44	21.91	28.46	419.47
C:119	597470.7	6583800.1	T	813.22	3.32	21.04	16.15	509.73	B	766.94	3.32	21.22	16.15	396.46
C:120	597471.6	6583800.4	T	790.08	3.16	20.00	16.15	483.19	B	750.41	3.16	23.83	18.46	565.49
C:121	597472.6	6583800.6	T	755.37	3.20	25.04	16.92	565.49	B	528.93	3.20	18.96	16.92	291.15
C:122	597473.6	6583800.8	T	809.92	3.35	32.87	19.23	545.13	B	616.53	3.35	23.48	17.69	477.88
C:123	597474.6	6583801.1	T	738.84	3.26	36.52	18.46	568.14	B	533.88	3.26	20.35	16.15	307.08
C:124	597475.5	6583801.3	T	677.69	3.18	19.65	17.69	528.32	B	550.41	3.18	32.17	23.08	406.19
C:125	597476.5	6583801.6	T	682.64	3.03	25.74	16.92	575.22	B	543.80	3.03	23.48	19.23	438.05
C:126	597477.5	6583801.8	T	725.62	3.14	21.74	15.38	576.99	B	512.40	3.14	24.00	16.92	328.32
C:127	597478.4	6583802.0	T	821.49	3.26	22.26	16.15	544.25	B	761.98	3.26	20.35	16.92	594.69
C:128	597479.4	6583802.3	T	732.23	3.08	19.30	15.38	549.56	B	547.11	3.08	22.09	15.38	361.95
C:129	597480.4	6583802.5	T	705.79	3.03	19.83	14.62	517.70	B	649.59	3.03	22.96	16.15	423.01
C:130	597481.3	6583802.8	T	765.29	3.16	18.96	15.38	558.41	B	766.94	3.16	23.48	15.38	561.06
C:131	597482.3	6583803.0	T	806.61	3.10	29.39	15.38	650.44	B	747.11	3.10	22.96	15.38	597.35
C:132	597483.3	6583803.2	T	684.30	3.41	20.35	14.62	557.52	B	682.64	3.41	23.13	15.38	558.41
C:133	597484.3	6583803.5	T	707.44	3.01	20.17	13.85	505.31	B	679.34	3.01	19.83	15.38	572.57
C:134	597485.2	6583803.7	T	781.82	3.66	22.43	16.92	590.27	B	684.30	3.66	23.13	16.92	573.45
C:135	597486.2	6583804.0	T	758.68	3.22	22.43	23.85	600.00	B	672.73	3.22	12.17	15.38	556.64
C:136	597487.2	6583804.2	T	639.67	3.44	20.70	14.62	562.83	B	688.00	3.44	15.00	16.00	582.00
C:137	597488.1	6583804.4	T	657.85	3.39	22.26	17.69	600.88	B	709.09	3.39	18.61	16.92	603.54
C:138	597489.1	6583804.7	T	644.63	3.50	22.26	16.15	553.98	B	728.93	3.50	18.26	14.62	576.11
C:139	597490.1	6583804.9	T	642.98	3.32	22.09	15.38	550.44	B	694.21	3.32	21.22	14.62	577.88
C:140	597491.0	6583805.2	T	674.38	2.94	16.87	16.92	593.81	B	720.66	2.94	19.65	16.15	600.00
C:141	597492.0	6583805.4	T	618.18	2.72	10.61	13.08	570.80	B	727.27	2.72	23.65	12.31	557.52

SITE C

id	x-UTM	y-UTM	Niveau	[P]/ppm	[Fe]/‰	[Zn]/ppm	[Cu]/ppm	[Mn]/ppm	Niveau	[P]/ppm	[Fe]/‰	[Zn]/ppm	[Cu]/ppm	[Mn]/ppm
C:142	597493.0	6583805.6	T	619.13	2.04	27.16	6.90	504.52	B	646.96	2.04	29.26	6.90	464.52
C:143	597494.0	6583805.9	T	710.74	3.08	17.39	13.85	571.68	B	818.18	3.08	20.87	13.85	561.06
C:144	597494.9	6583806.1	T	677.69	3.25	22.96	12.31	573.45	B	715.70	3.25	18.26	13.85	560.18
C:145	597495.9	6583806.4	T	654.00		26.00	9.00	545.00	B	617.39	1.94	26.11	6.21	472.26
C:146	597496.9	6583806.6	T	629.57	1.94	29.68	6.21	518.71	B	629.57	3.08	30.74	6.90	507.10
C:147	597497.8	6583806.8	T	628.10	3.08	21.04	13.85	561.06	B	604.96	2.03	23.65	14.62	564.60
C:148	597498.8	6583807.1	T	615.65	2.03	27.37	5.52	483.87	B	617.39	1.98	31.37	7.59	547.10
C:149	597499.8	6583807.3	T	612.17	1.98	29.68	6.90	525.16	B	634.78	2.80	29.89	6.21	517.42
C:150	597500.8	6583807.5	T	623.14	2.80	16.87	1393.85	682.30	B	579.13	2.60	24.84	7.59	455.48
C:151	597501.7	6583807.8	T	621.49	2.60	9.04	10.77	529.20	B	600.00	1.81	20.84	6.90	349.68
C:152	597502.7	6583808.0	T	594.78	1.81	29.89	6.21	540.65	B	588.00	1.74	21.00	7.00	453.00
C:153	597503.7	6583808.3	T	565.22	1.74	20.63	6.90	562.58	B	575.65	2.62	21.47	6.90	556.13
C:154	597504.6	6583808.5	T	623.14	2.62	7.30	10.00	535.40	B	568.60	1.68	22.43	12.31	541.59
C:155	597505.6	6583808.7	T	542.61	1.68	29.89	14.48	464.52	B	532.17	1.98	22.11	6.90	370.32
C:156	597506.6	6583809.0	T	584.35	1.98	19.58	6.21	588.39	B	528.00	3.03	25.00	7.00	449.00
C:157	597507.5	6583809.2	T	580.17	3.03	19.13	13.08	523.89	B	525.22	2.03	28.42	6.90	522.58
C:158	597508.5	6583809.5	T	561.74	2.03	31.16	6.90	530.32	B	446.96	1.79	29.26	6.90	403.87
C:159	597509.5	6583809.7	T	518.26	1.79	87.16	7.59	562.58	B	502.61	2.08	30.11	6.90	517.42
C:160	597510.5	6583809.9	T	591.30	2.08	22.32	6.90	366.45	B	554.78	2.83	21.05	7.59	325.16
C:161	597511.4	6583810.2	T	542.15	2.83	19.39	12.31	490.27	B	502.48	1.95	17.39	13.08	454.87
C:162	597512.4	6583810.4	T	553.04	1.95	27.58	5.52	482.58	B	478.26	1.87	26.11	6.90	460.65
C:163	597513.4	6583810.7	T	523.48	1.87	29.05	6.21	495.48	B	535.65	1.84	30.74	5.52	503.23
C:164	597514.3	6583810.9	T	549.57	1.84	24.63	5.52	467.10	B	544.35	1.95	22.95	6.21	360.00
C:165	597515.3	6583811.1	T	530.43	1.95	29.68	6.21	490.32	B	506.09	1.91	26.53	5.52	500.65
C:166	597516.3	6583811.4	T	525.22	1.91	26.74	5.52	437.42	B	551.30	2.00	17.89	7.59	238.71
C:167	597517.2	6583811.6	T	518.26	2.00	28.21	7.59	483.87	B	446.96	1.95	20.42	9.66	221.94
C:168	597518.2	6583811.9	T	537.39	1.95	26.74	5.52	451.61	B	490.00	1.90	17.00	8.00	400.00
C:169	597519.2	6583812.1	T	558.26	1.90	18.74	6.21	336.77	B	532.17	1.95	15.16	5.52	561.29
C:170	597520.2	6583812.3	T	526.96	1.95	26.95	6.21	445.16	B	516.52	2.59	25.47	6.90	437.42
C:175	597525.0	6583813.5	T	588.43	2.59	10.43	11.54	325.66	B	537.19	2.90	11.30	10.00	294.69
C.180	597529.9	6583814.7	T	543.80	2.90	33.22	12.31	533.63	B	510.00	2.91	19.00	10.00	380.00
C:182	597531.8	6583815.2	T	614.88	2.91	38.61	11.54	492.92	B	492.56	3.74	29.39	10.00	461.95
C1:1	597460.2	6583798.5	T	902.61	3.29	27.30	7.52	517.33	B	864.35	3.29	24.60	6.84	456.00
C1:2	597460.4	6583799.5	T	857.39	3.05	23.02	5.47	446.67	B	841.74	3.05	30.63	8.21	504.00
C1:3	597460.6	6583800.4	T	902.61	3.32	22.70	6.84	422.67	B	633.04	3.32	22.22	6.15	212.00
C1:4	597460.8	6583801.4	T	836.52	2.61	25.71	6.15	434.67	B	617.39	2.61	23.17	5.47	185.33
C1:5	597461.0	6583802.4	T	838.26	3.07	21.27	5.47	389.33	B	676.52	3.07	25.08	5.47	188.00
C1:6	597461.2	6583803.4	T	885.22	3.25	22.70	6.15	470.67	B	699.13	3.25	23.49	4.10	205.33
C1:7	597461.4	6583804.4	T	834.78	2.92	24.44	6.84	418.67	B	620.87	2.92	26.98	6.84	229.33
C1:8	597461.6	6583805.3	T	824.35	2.75	23.65	6.84	508.00	B	622.61	2.75	23.81	6.15	226.67
C1:9	597461.8	6583806.3	T	845.22	3.22	26.67	7.52	498.67	B	657.39	3.22	22.06	6.15	298.67
C1:10	597462.0	6583807.3	T	806.96	2.95	26.03	7.52	484.00	B	593.04	2.95	21.90	6.15	202.67
C1:11	597462.2	6583808.3	T	831.30	2.82	26.03	4.79	554.67	B	645.22	2.82	26.19	5.47	278.67
C1:12	597462.4	6583809.3	T	906.09	6.75	26.19	6.84	485.33	B	660.87	6.75	21.90	4.79	194.67
C1:13	597462.6	6583810.2	T	853.91	3.04	28.10	6.84	534.67	B	640.00	3.04	26.98	6.15	277.33

SITE C

id	x-UTM	y-UTM	Niveau	[P]/ppm	[Fe]/‰	[Zn]/ppm	[Cu]/ppm	[Mn]/ppm	Niveau	[P]/ppm	[Fe]/‰	[Zn]/ppm	[Cu]/ppm	[Mn]/ppm
C1:14	597462.8	6583811.2	T	791.30	2.99	27.62	7.52	501.33	B	593.04	2.99	21.59	6.15	237.33
C1:15	597463.0	6583812.2	T	798.26	2.81	20.00	6.84	394.67	B	629.57	2.81	22.54	6.84	254.67
C1:16	597463.2	6583813.2	T	787.83	2.94	28.25	6.84	538.67	B	633.04	2.94	26.83	6.15	233.33
C1:17	597463.4	6583814.2	T	780.87	2.87	24.92	7.52	492.00	B	700.87	2.87	23.81	5.47	325.33
C1:18	597463.6	6583815.1	T	829.57	3.05	23.49	6.84	392.00	B	603.48	3.05	23.02	4.79	186.67
C1:19	597463.8	6583816.1	T	789.57	2.72	21.43	5.47	416.00	B	587.83	2.72	21.27	4.79	244.00
C1:20	597464.0	6583817.1	T	791.30	2.87	24.13	6.15	430.67	B	779.13	2.87	30.16	5.47	420.00
C1:21	597464.2	6583818.1	T	770.43	2.88	22.38	6.15	404.00	B	580.87	2.88	24.44	4.79	224.00
C1:22	597464.4	6583819.1	T	800.00	2.79	22.86	5.47	386.67	B	622.61	2.79	22.06	5.47	268.00
C1:23	597464.6	6583820.0	T	793.04	4.20	26.98	8.21	593.33	B	580.87	4.20	19.37	4.10	190.67
C1:24	597464.8	6583821.0	T	798.26	4.27	27.94	6.84	596.00	B	702.61	4.27	23.17	6.15	344.00
C1:25	597465.0	6583822.0	T	806.96	4.47	28.41	7.52	626.67	B	539.13	4.47	20.95	6.84	472.00
C1:26	597465.2	6583823.0	T	796.52	4.22	25.71	7.52	592.00	B	566.96	4.22	25.24	7.52	517.33
C1:27	597465.4	6583824.0	T	779.13	4.16	26.98	7.52	577.33	B	645.22	4.16	22.22	5.47	333.33
C1:28	597465.6	6583824.9	T	777.39	4.31	29.05	6.84	662.67	B	697.39	4.31	21.43	4.79	336.00
C1:29	597465.8	6583825.9	T	775.65	3.93	29.84	6.15	624.00	B	636.52	3.93	19.84	2.74	322.67
C1:30	597466.0	6583826.9	T	784.35	3.97	30.79	7.52	653.33	B	624.35	3.97	20.63	2.05	342.67
C1:31	597466.2	6583827.9	T	761.74	3.88	25.08	6.84	600.00	B	716.52	3.88	15.40	5.47	205.33
C1:32	597466.4	6583828.9	T	770.43	3.92	28.57	6.84	649.33	B	702.61	3.92	23.65	4.10	417.33
C1:33	597466.6	6583829.8	T	714.78	2.46	18.57	4.79	429.33	B	699.13	2.46	19.37	2.74	322.67
C1:34	597466.8	6583830.8	T	714.78	2.38	17.78	5.47	394.67	B	669.57	2.38	15.08	0.68	184.00
C1:35	597467.0	6583831.8	T	711.30	2.42	20.48	5.47	445.33	B	761.74	2.42	17.62	2.74	314.67
C1:36	597467.2	6583832.8	T	780.87	4.14	29.37	7.52	652.00	B	768.70	4.14	17.94	2.05	244.00
C1:37	597467.4	6583833.8	T	777.39	2.64	26.35	4.79	464.00	B	766.96	2.64	16.35	1.37	216.00
C1:38	597467.6	6583834.7	T	780.87	3.59	24.76	5.47	537.33	B	775.65	3.59	20.79	2.74	300.00
C1:39	597467.8	6583835.7	T	791.30	4.04	28.89	6.84	592.00	B	765.22	4.04	22.54	3.42	430.67
C1:40	597468.0	6583836.7	T	777.39	3.95	31.11	6.15	649.33	B	732.17	3.95	22.38	4.79	366.67
C1:41	597468.2	6583837.7	T	726.96	3.81	27.94	6.15	646.67	B	761.74	3.81	20.95	4.10	348.00
C1:42	597468.4	6583838.7	T	756.52	3.81	29.05	6.15	640.00	B	756.52	3.81	22.70	4.10	394.67
C1:43	597468.6	6583839.6	T	756.52	3.90	27.30	6.84	601.33	B	756.52	3.90	23.65	8.21	524.00
C1:44	597468.8	6583840.6	T	725.22	3.78	24.60	6.15	550.67	B	791.30	3.78	30.16	10.26	510.67
C1:45	597469.0	6583841.6	T	702.61	2.27	17.78	5.47	393.33	B	760.00	2.27	19.37	7.52	473.33
C1:46	597469.2	6583842.6	T	742.61	3.95	29.05	6.84	637.33	B	707.83	3.95	16.83	5.47	264.00
C1:47	597469.4	6583843.6	T	739.13	3.58	30.16	5.47	634.67	B	725.22	3.58	28.73	7.52	538.67
C1:48	597469.6	6583844.5	T	766.96	4.06	27.46	6.84	633.33	B	714.78	4.06	24.92	4.79	473.33
C1:49	597469.8	6583845.5	T	726.96	4.20	22.38	5.47	590.67	B	594.78	4.20	23.17	4.79	365.33
C1:50	597470.0	6583846.5	T	747.83	3.74	27.62	6.15	546.67	B	568.70	3.74	21.90	4.10	405.33
CP1	597444.0	6583772.5	T	1429.75	3.74	56.35	40.00	912.39	B	988.43	3.74	32.35	12.31	511.50

S I T ES D & G

id	x-UTM	y-UTM	Niveau	[P]/ppm	[Fe]/‰	[Zn]/ppm	[Cu]/ppm	[Mn]/ppm	Niveau	[P]/ppm	[Fe]/‰	[Zn]/ppm	[Cu]/ppm	[Mn]/ppm
D:1	598906.0	6584588.5	T	793.65	1.56	14.79	27.59	150.34	B	509.52	1.55	4.36	4.14	27.83
D:2	598906.7	6584587.8	T	715.87	1.51	14.06	23.45	131.01	B	595.24	1.64	8.00	9.66	129.47
D:3	598907.5	6584587.1	T	1342.86	1.56	30.55	45.52	160.00	B	480.95	1.39	6.06	4.14	40.58
D:4	598908.2	6584586.5	T	661.90	1.36	13.58	19.31	111.30	B	603.17	1.69	6.79	5.52	84.25
D:5	598909.0	6584585.8	T	671.43	1.43	13.09	20.69	130.24	B	847.62	2.28	6.06	8.28	108.21
D:6	598909.7	6584585.1	T	811.11	1.47	9.45	23.45	138.36	B	892.06	2.12	8.48	4.14	65.31
D:7	598910.5	6584584.4	T	712.70	1.52	12.36	17.93	115.17	B	547.62	1.46	3.64	2.76	42.13
D:8	598911.2	6584583.7	T	819.05	1.41	14.55	19.31	116.33	B	533.33	1.17	4.12	4.14	49.86
D:9	598911.9	6584583.0	T	677.78	1.36	10.91	15.17	112.46	B	507.94	1.64	9.45	13.79	103.19
D:10	598912.7	6584582.4	T	626.98	1.42	14.06	16.55	91.59	B	555.56	1.68	7.76	13.79	119.42
D:11	598913.4	6584581.7	T	701.59	1.42	12.36	19.31	119.42	B	607.94	1.41	4.12	4.14	38.26
D:12	598914.2	6584581.0	T	530.16	1.27	10.18	15.17	96.23	B	696.83	1.65	3.88	2.76	34.01
D:13	598914.9	6584580.4	T	768.25	1.44	11.15	19.31	122.51	B	533.33	1.22	5.09	4.14	29.76
C.14	598915.7	6584579.7	T	657.14	1.42	11.15	13.79	99.32	B	523.81	1.19	4.12	0.00	36.33
D:15	598916.4	6584579.0	T	612.70	1.28	11.39	13.79	85.41	B	674.60	1.71	8.48	8.28	59.90
D:16	598917.1	6584578.4	T	779.37	1.54	9.70	17.93	120.97	B	425.40	1.44	6.06	5.52	95.85
D:17	598917.9	6584577.7	T	742.86	1.48	14.55	19.31	120.19	B	506.35	1.30	4.12	4.14	51.40
D:18	598918.6	6584577.0	T	603.17	1.26	12.12	16.55	84.25	B	768.25	1.70	8.48	8.28	52.95
D:19	598919.4	6584576.3	T	771.43	1.48	14.79	22.07	124.44	B	719.05	1.81	6.06	11.03	112.08
D:20	598920.1	6584575.6	T	717.46	1.34	12.85	15.17	93.91	B	595.24	1.34	5.82	6.90	74.59
D:21	598920.9	6584575.0	T	584.13	1.22	8.73	12.41	89.28	B	728.57	1.77	6.06	5.52	114.01
D:22	598921.6	6584574.3	T	606.35	1.23	6.55	16.55	98.55	B	534.92	1.37	5.82	4.14	43.67
D:23	598922.4	6584573.6	T	604.76	1.21	12.61	12.41	89.28	B	622.22	1.35	9.70	6.90	59.13
D:24	598923.1	6584572.9	T	915.87	1.46	16.97	22.07	134.11	B	495.24	1.14	6.79	0.00	36.71
D:25	598923.8	6584572.3	T	638.10	1.30	12.85	15.17	90.05	B	800.00	1.63	6.30	2.76	52.56
D:26	598924.6	6584571.6	T	698.41	1.32	11.15	16.55	102.80	B	733.33	1.81	9.70	6.90	87.34
D:27	598925.3	6584570.9	T	641.27	1.39	22.79	16.55	100.10	B	657.14	1.83	6.79	5.52	87.34
D:28	598926.1	6584570.2	T	742.86	1.24	12.36	16.55	112.85	B	334.92	2.36	4.12	4.14	32.85
D:29	598926.8	6584569.6	T	763.49	1.35	9.45	19.31	129.86	B	419.05	2.07	8.24	5.52	68.41
D:30	598927.6	6584568.9	T	642.86	1.35	8.00	15.17	96.23	B	947.62	2.30	6.30	8.28	88.12
D:31	598928.3	6584568.2	T	728.57	1.48	12.85	16.55	116.72	B	770.00	2.53	7.00	7.00	62.00
D:32	598913.4	6584570.0	T	650.79	1.46	14.79	20.69	106.28	B	607.94	2.76	7.52	5.52	36.71
D:33	598913.8	6584579.0	T	792.06	1.63	26.42	34.48	161.55	B	200.00	1.84	9.45	8.28	104.35
D:34	598914.2	6584571.8	T	693.65	1.47	11.39	19.31	121.35	B	1144.44	2.50	9.21	5.52	34.40
D:35	598914.6	6584572.8	T	806.35	1.62	10.91	28.97	134.11	B	1152.38	3.05	7.76	5.52	60.29
D:36	598915.0	6584573.7	T	490.48	1.28	9.70	11.03	84.64	B	1015.87	2.49	8.97	12.41	54.11
D:37	598915.4	6584574.6	T	728.57	1.57	15.03	27.59	112.85	B	933.33	2.41	3.64	8.28	106.67
D:38	598915.9	6584575.5	T	731.75	1.49	9.70	20.69	127.92	B	874.60	2.07	9.94	8.28	56.81
D:39	598916.3	6584576.4	T	787.30	1.68	14.06	23.45	129.47	B	506.35	1.64	4.12	0.00	35.56
D:40	598916.7	6584577.3	T	673.02	1.34	8.00	19.31	106.28	B	439.68	1.62	8.24	9.66	90.43
D:41	598917.5	6584579.2	T	650.79	1.32	8.73	15.17	91.98	B	479.37	1.46	8.48	5.52	39.42
D:42	598917.9	6584580.1	T	753.97	1.33	9.94	17.93	103.19	B	469.84	1.14	7.76	0.00	32.85
D:43	598918.3	6584581.0	T	593.65	1.34	10.42	16.55	85.41	B	876.19	2.11	8.97	13.79	79.23
D:44	598918.8	6584582.0	T	733.33	1.42	9.45	17.93	108.99	B	453.97	1.47	6.30	0.00	28.60
D:45	598919.2	6584582.8	T	719.05	1.50	10.18	19.31	118.26	B	442.86	1.39	4.36	2.76	54.11

S I T ES D & G

id	x-UTM	y-UTM	Niveau	[P]/ppm	[Fe]/‰	[Zn]/ppm	[Cu]/ppm	[Mn]/ppm	Niveau	[P]/ppm	[Fe]/‰	[Zn]/ppm	[Cu]/ppm	[Mn]/ppm
D:46	598919.6	6584583.8	T	736.51	1.51	11.39	17.93	113.62	B	333.33	1.36	8.00	5.52	36.71
D:47	598920.0	6584584.7	T	550.79	1.31	8.48	12.41	82.71	B	488.89	1.53	5.09	2.76	35.17
D:48	598920.4	6584585.6	T	636.51	1.37	8.97	16.55	97.00	B	390.48	1.91	8.73	6.90	43.29
D:49	598920.8	6584586.5	T	765.08	1.56	10.91	16.55	116.33	B	514.29	2.33	4.85	6.90	24.35
D:50	598921.3	6584587.4	T	600.00	1.52	13.09	17.93	103.96	B	292.06	2.17	7.76	0.00	47.54
D:51	598921.7	6584588.3	T	563.49	1.38	10.18	16.55	95.46	B	282.54	1.49	3.88	4.14	36.33
D:52	598922.0	6584589.3	T	647.62	1.42	7.03	16.55	105.51	B	304.76	1.53	9.45	5.52	36.33
D:53	598922.5	6584590.2	T	592.06	1.37	7.52	16.55	79.61	B	238.10	1.61	4.12	4.14	25.12
D:54	598922.8	6584591.1	T	673.02	1.56	12.85	19.31	104.73	B	355.56	1.46	4.61	0.00	42.13
D:55	598923.3	6584592.0	T	498.41	1.49	7.52	13.79	71.88	B	393.65	1.62	7.76	0.00	38.65
G:1	598897.8	6584570.1	T	938.00	1.75	16.00	54.00	140.00	B	541.00	1.79	7.00	7.00	58.00
G:2	598898.5	6584569.4	T	883.00	2.13	14.00	26.00	184.00	B	858.00	2.66	11.00	13.00	97.00
G:3	598899.2	6584568.8	T	739.00	1.94	14.00	19.00	156.00	B	512.00	1.89	6.00	6.00	49.00
G:4	598900.3	6584568.1	T	682.00	2.06	12.00	16.00	154.00	B	550.00	1.89	6.00	4.00	34.00
G:5	598900.8	6584567.4	T	824.00	2.08	15.00	23.00	183.00	B	571.00	2.09	9.00	0.00	50.00
G:6	598901.5	6584566.8	T	890.00	2.21	15.00	24.00	191.00	B	766.00	2.24	8.00	8.00	49.00
G:7	598902.3	6584566.0	T	765.00	1.82	13.00	24.00	154.00	B	541.00	2.53	7.00	0.00	50.00
G:8	598903.0	6584565.4	T	667.00	2.03	12.00	17.00	150.00	B	422.00	1.92	7.00	4.00	24.00
G:9	598903.7	6584564.7	T	637.00	1.63	9.00	26.00	104.00	B	906.00	2.31	11.00	0.00	63.00
G:10	598904.5	6584564.1	T	728.00	2.23	14.00	22.00	167.00	B	483.00	2.13	6.00	0.00	41.00
G:11	598905.2	6584563.4	T	653.00	2.20	12.00	13.00	156.00	B	526.00	2.36	6.00	0.00	61.00
G:12	598906.0	6584562.7	T	675.00	2.26	13.00	19.00	157.00	B	410.00	1.99	6.00	6.00	57.00
G:13	598906.7	6584562.1	T	746.00	2.07	14.00	23.00	153.00	B	403.00	2.32	8.00	0.00	108.00
C.14	598907.5	6584561.4	T	774.00	2.20	12.00	21.00	165.00	B	549.00	2.32	13.00	0.00	114.00
G:15	598907.8	6584560.7	T	597.00	1.65	9.00	21.00	99.00	B	453.00	1.77	6.00	4.00	41.00
G:16	598908.9	6584560.1	T	1034.00	2.31	19.00	38.00	201.00	B	474.00	1.60	7.00	4.00	38.00
G:17	598909.7	6584559.4	T	525.00	1.78	15.00	16.00	124.00	B	562.00	1.68	7.00	0.00	57.00
G:18	598910.4	6584558.7	T	606.00	2.09	10.00	9.00	147.00	B	405.00	2.08	6.00	0.00	73.00
G:19	598911.2	6584558.0	T	690.00	2.01	10.00	9.00	150.00	B	533.00	1.97	7.00	0.00	53.00
G:20	598911.9	6584557.4	T	648.00	1.74	8.00	25.00	124.00	B	544.00	1.53	7.00	0.00	52.00
G:21	598912.7	6584556.7	T	578.00	1.63	8.00	22.00	115.00	B	466.00	1.46	8.00	4.00	35.00
G:22	598913.4	6584556.0	T	787.00	2.13	11.00	20.00	186.00	B	587.00	1.96	6.00	0.00	74.00
G:23	598914.2	6584555.4	T	712.00	1.74	9.00	29.00	135.00	B	568.00	1.39	8.00	0.00	69.00
G:24	598914.9	6584554.7	T	661.00	1.70	12.00	22.00	149.00	B	547.00	1.57	7.00	0.00	58.00
G:25	598915.6	6584554.0	T	763.00	1.76	13.00	28.00	157.00	B	531.00	1.50	7.00	0.00	54.00
G:26	598916.4	6584553.4	T	720.00	1.85	8.00	26.00	145.00	B	634.00	1.80	6.00	11.00	87.00
G:27	598917.1	6584552.7	T	510.00	1.45	9.00	16.00	123.00	B	584.00	1.15	6.00	0.00	67.00
G:28	598917.9	6584552.0	T	694.00	1.79	9.00	25.00	149.00	B	574.00	1.63	5.00	3.00	53.00
G:29	598918.6	6584551.3	T	806.00	1.51	15.00	21.00	137.00	B	621.00	2.00	7.00	0.00	62.00
G:30	598919.4	6584550.7	T	736.00	2.16	14.00	22.00	191.00	B	437.00	2.92	8.00	0.00	52.00
G:31	598920.1	6584550.0	T	725.00	2.09	13.00	22.00	198.00	B	520.00	2.88	8.00	0.00	54.00
G:32	598902.8	6584546.3	T	846.00	1.47	13.00	28.00	121.00	B	440.00	1.30	6.00	0.00	39.00
G:33	598903.2	6584547.2	T	741.00	1.77	15.00	13.00	137.00	B	533.00	1.58	6.00	0.00	66.00
G:34	598903.6	6584548.1	T	704.00	1.55	13.00	19.00	130.00	B	496.00	1.51	7.00	0.00	41.00
G:35	598904.0	6584549.0	T	760.00	1.63	14.00	20.00	137.00	B	629.00	1.69	7.00	0.00	50.00

S I T ES D & G

id	x-UTM	y-UTM	Niveau	[P]/ppm	[Fe]/‰	[Zn]/ppm	[Cu]/ppm	[Mn]/ppm	Niveau	[P]/ppm	[Fe]/‰	[Zn]/ppm	[Cu]/ppm	[Mn]/ppm
G:36	598904.4	6584550.0	T	782.00	1.78	7.00	23.00	121.00	B	472.00	1.15	5.00	4.00	29.00
G:37	598904.9	6584550.9	T	688.00	1.82	13.00	20.00	162.00	B	546.00	1.56	8.00	0.00	57.00
G:38	598905.3	6584551.8	T	720.00	2.17	14.00	21.00	149.00	B	555.00	1.71	4.00	3.00	47.00
G:39	598905.7	6584552.7	T	587.00	2.18	13.00	15.00	161.00	B	517.00	1.94	7.00	0.00	77.00
G:40	598906.1	6584553.6	T	642.00	1.70	10.00	14.00	126.00	B	371.00	2.52	8.00	0.00	119.00
G:41	598906.5	6584554.5	T	578.00	1.67	10.00	15.00	121.00	B	315.00	2.91	6.00	0.00	31.00
G:42	598906.9	6584555.4	T	653.00	1.77	8.00	22.00	114.00	B	309.00	2.02	5.00	7.00	60.00
G:43	598907.3	6584556.3	T	749.00	2.15	12.00	16.00	177.00	B	483.00	1.89	6.00	0.00	61.00
G:44	598907.7	6584557.2	T	757.00	2.18	12.00	13.00	173.00	B	562.00	1.82	6.00	0.00	65.00
G:45	598908.2	6584558.2	T	736.00	1.56	12.00	22.00	117.00	B	558.00	1.86	8.00	6.00	112.00
G:46	598908.6	6584559.1	T	645.00	1.83	11.00	19.00	135.00	B	413.00	1.36	5.00	3.00	42.00
G:47	598909.4	6584560.9	T	637.00	2.13	13.00	20.00	167.00	B	571.00	2.22	8.00	0.00	53.00
G:48	598909.8	6584561.8	T	666.00	1.70	9.00	25.00	118.00	B	485.00	1.67	6.00	4.00	44.00
G:49	598910.2	6584562.7	T	581.00	1.67	8.00	25.00	107.00	B	622.00	2.49	5.00	0.00	114.00
G:50	598910.6	6584563.6	T	739.00	1.77	13.00	26.00	152.00	B	677.00	2.23	9.00	6.00	137.00
G:51	598911.0	6584564.5	T	666.00	2.09	12.00	17.00	161.00	B	670.00	2.30	7.00	0.00	103.00
G:52	598911.5	6584565.5	T	622.00	1.61	11.00	19.00	124.00	B	491.00	1.49	6.00	0.00	57.00
G:53	598911.9	6584566.4	T	725.00	1.80	14.00	32.00	143.00	B	637.00	1.59	6.00	0.00	33.00
G:54	598912.3	6584567.3	T	723.00	2.03	14.00	23.00	174.00	B	560.00	1.94	10.00	16.00	111.00
G:55	598912.7	6584568.2	T	598.00	1.78	10.00	15.00	135.00	B	528.00	1.98	8.00	7.00	105.00
G:56	598913.1	6584569.1	T	662.00	1.93	12.00	14.00	153.00	B	798.00	2.78	9.00	0.00	43.00

SITE E

id	x-UTM	y-UTM	Niveau	[P]/ppm	[Fe]/‰	[Zn]/ppm	[Cu]/ppm	[Mn]/ppm	Niveau	[P]/ppm	[Fe]/‰	[Zn]/ppm	[Cu]/ppm	[Mn]/ppm
E:1	598946.9	6584526.0	T	671.21	1.74	9.41	6.47	175.75	B	380.30	1.45	0.00	1.76	49.76
E:2	598947.7	6584525.3	T	569.70	1.67	6.39	5.88	154.33	B	318.18	1.40	0.00	1.18	83.15
E:3	598948.3	6584524.7	T	631.82	1.56	5.71	6.47	149.92	B	489.39	1.50	0.00	0.00	34.02
E:4	598949.1	6584524.0	T	592.42	1.81	7.06	5.29	175.12	B	490.91	1.77	1.01	1.18	57.95
E:5	598949.9	6584523.3	T	701.52	1.65	5.71	5.88	180.79	B	518.18	1.60	0.00	0.59	34.02
E:6	598950.6	6584522.7	T	721.21	1.59	4.71	6.47	168.82	B	580.30	1.69	0.00	0.00	32.76
E:7	598951.3	6584522.0	T	684.85	1.68	5.71	7.06	170.71	B	398.48	1.90	2.69	4.12	146.14
E:8	598952.1	6584521.3	T	572.73	1.53	4.37	5.88	131.02	B	445.45	2.34	0.00	1.18	110.24
E:9	598952.8	6584520.7	T	459.09	1.46	3.36	6.47	131.02	B	304.55	2.31	0.67	1.76	86.93
E:10	598953.6	6584520.0	T	522.73	1.52	3.36	4.71	154.33	B	163.64	1.66	0.00	2.35	81.89
E:11	598954.3	6584519.3	T	565.15	1.45	3.36	6.47	136.06	B	148.48	1.91	3.36	2.35	124.72
E:12	598955.1	6584518.7	T	554.55	1.73	4.71	6.47	177.64	B	253.03	1.67	0.00	0.59	71.18
E:13	598955.8	6584518.0	T	565.15	1.74	5.04	7.06	183.31	B	262.12	1.58	0.00	1.76	102.05
E:14	598956.6	6584517.3	T	671.21	1.60	4.71	5.29	160.00	B	234.85	1.67	0.00	0.59	87.56
E:15	598957.3	6584516.7	T	603.03	1.77	7.06	5.88	175.75	B	346.97	1.57	0.00	1.76	83.78
E:16	598958.0	6584516.0	T	609.09	1.62	3.70	5.29	161.89	B	481.82	1.61	0.00	1.76	127.87
E:17	598958.8	6584515.3	T	610.61	1.64	5.71	4.71	172.60	B	433.33	1.58	0.00	1.18	84.41
E:18	598959.5	6584514.7	T	503.03	1.44	1.34	3.53	140.47	B	498.48	1.62	0.34	3.53	152.44
E:19	598960.2	6584514.0	T	546.97	1.57	5.04	4.12	168.19	B	451.52	1.50	0.00	2.35	92.60
E:20	598961.0	6584513.3	T	556.06	1.70	5.71	4.71	165.67	B	298.48	1.85	1.34	0.00	146.77
E:21	598961.8	6584512.7	T	548.48	1.64	6.05	4.12	166.93	B	328.79	1.48	0.00	1.18	105.20
E:22	598962.5	6584512.0	T	659.09	1.58	4.71	4.71	160.63	B	386.36	1.50	0.00	1.76	115.91
E:23	598963.2	6584511.3	T	719.70	1.82	8.07	5.88	195.28	B	375.76	1.50	0.00	2.94	130.39
E:24	598964.0	6584510.7	T	750.00	1.68	8.74	5.88	196.54	B	357.58	1.53	0.00	0.59	73.07
E:25	598964.8	6584510.0	T	637.88	1.79	8.40	5.88	194.65	B	350.00	1.48	0.00	1.76	76.85
E:26	598965.4	6584509.3	T	500.00	1.67	4.37	4.12	166.93	B	384.85	1.24	0.00	0.00	44.72
E:27	598966.2	6584508.7	T	524.24	1.67	5.04	4.12	175.75	B	287.88	1.48	0.00	1.18	83.78
E:28	598966.9	6584508.0	T	566.67	1.67	6.72	7.65	165.67	B	340.91	1.72	0.34	1.18	153.70
E:29	598967.6	6584507.2	T	700.00	1.88	6.39	8.24	217.32	B	228.79	1.65	2.02	2.94	202.20
E:30	598968.4	6584506.6	T	642.42	1.80	7.06	4.71	194.65	B	419.70	2.04	5.38	3.53	180.79
E:31	598969.1	6584505.9	T	477.27	1.50	4.03	5.29	147.40	B	142.42	2.11	0.34	1.18	47.24
E:32	598948.0	6584504.8	T	495.45	1.61	3.36	5.29	129.13	B	384.85	1.82	0.00	1.76	112.76
E:33	598948.7	6584505.6	T	522.73	1.58	3.03	5.88	127.87	B	274.24	1.98	0.00	0.59	54.17
E:34	598949.3	6584506.3	T	695.45	1.72	3.03	8.24	149.29	B	369.70	2.32	0.00	1.76	64.88
E:35	598950.0	6584507.1	T	546.97	1.74	4.37	5.88	142.36	B	295.45	1.81	0.00	1.18	52.91
E:36	598950.7	6584507.8	T	603.03	1.58	3.70	6.47	132.28	B	301.52	2.08	0.00	2.94	66.77
E:37	598951.4	6584508.6	T	504.55	1.51	2.35	6.47	125.35	B	419.70	1.46	0.00	2.35	52.91
E:38	598952.0	6584509.3	T	771.21	1.77	6.72	8.24	173.23	B	386.36	1.59	0.00	1.18	68.66
E:39	598952.7	6584510.1	T	603.03	1.71	6.39	6.47	172.60	B	439.39	2.05	0.00	3.53	138.58
E:40	598953.4	6584510.8	T	607.58	1.75	5.38	7.06	178.90	B	433.33	1.51	0.00	0.59	57.95
E:41	598954.0	6584511.6	T	518.18	1.53	2.69	3.53	136.06	B	501.52	1.35	0.00	2.35	57.95
E:42	598954.7	6584512.2	T	534.85	1.46	0.34	5.29	139.21	B	471.21	1.86	0.67	4.71	125.35
E:43	598955.3	6584513.0	T	650.00	1.54	4.37	6.47	166.30	B	837.88	1.70	0.00	2.94	115.91
E:44	598956.0	6584513.8	T	478.79	1.45	1.34	5.29	140.47	B	395.45	1.72	0.00	2.35	132.28
E:45	598956.7	6584514.5	T	589.39	1.66	5.04	6.47	166.93	B	437.88	1.55	0.00	1.18	99.53

SITE E

id	x-UTM	y-UTM	Niveau	[P]/ppm	[Fe]/‰	[Zn]/ppm	[Cu]/ppm	[Mn]/ppm	Niveau	[P]/ppm	[Fe]/‰	[Zn]/ppm	[Cu]/ppm	[Mn]/ppm
E:46	598957.4	6584515.3	T	560.61	1.59	0.34	7.65	160.00	B	340.91	1.86	1.01	2.35	145.51
E:47	598958.7	6584516.8	T	598.48	1.61	2.69	8.24	149.29	B	466.67	1.86	0.00	0.59	119.06
E:48	598959.4	6584517.5	T	639.39	1.63	5.04	4.12	154.96	B	404.55	1.46	0.00	1.76	120.32
E:49	598960.1	6584518.2	T	731.82	1.64	6.72	7.65	170.71	B	422.73	1.92	2.35	2.94	149.92
E:50	598960.7	6584519.0	T	490.91	1.28	1.34	3.53	117.17	B	483.33	1.30	0.00	0.59	62.99
E:51	598961.4	6584519.7	T	763.64	1.74	7.73	5.88	190.87	B	327.27	1.88	0.00	1.18	129.13
E:52	598962.0	6584520.5	T	527.27	1.62	5.38	3.53	142.36	B	203.03	1.80	0.00	2.35	50.39
E:53	598962.7	6584521.2	T	569.70	1.62	6.05	3.53	154.33	B	216.67	2.13	0.00	0.00	66.77
E:54	598963.4	6584522.0	T	581.82	1.90	11.43	4.71	190.24	B	393.94	1.79	0.67	0.59	111.50
E:55	598964.0	6584522.7	T	504.55	1.52	3.36	6.47	136.06	B	304.55	2.29	1.34	1.76	114.02
E:56	598964.7	6584523.5	T	437.88	1.34	2.35	2.94	100.79	B	363.64	1.98	1.01	2.35	136.06
E:57	598965.4	6584524.2	T	721.21	1.82	7.39	4.12	167.56	B	383.33	1.59	0.00	1.18	114.65
E:58	598966.0	6584525.0	T	531.82	1.58	4.03	4.71	115.28	B	513.64	1.93	4.71	2.35	69.92
E:59	598966.7	6584525.7	T	543.94	1.56	5.04	4.71	113.39	B	559.09	1.86	1.34	1.76	66.14
E:60	598967.4	6584526.4	T	609.09	1.38	2.69	3.53	97.01	B	530.30	1.70	1.01	1.76	93.23
E:61	598968.0	6584527.2	T	715.15	1.60	3.36	4.12	147.40	B	386.36	1.44	0.00	1.18	53.54

SITE F

id	x-UTM	y-UTM	Niveau	[P]/ppm	[Fe]/‰	[Zn]/ppm	[Cu]/ppm	[Mn]/ppm	Niveau	[P]/ppm	[Fe]/‰	[Zn]/ppm	[Cu]/ppm	[Mn]/ppm
F:1	598947.5	6584598.0	T	586.09	1.04	30.40	0.00	132.00	B	337.39	0.08	27.40	0.00	4.00
F:2	598949.5	6584598.5	T	617.39	0.98	10.60	0.00	114.67	B	462.61	0.14	9.00	0.00	8.00
F:3	598951.4	6584599.0	T	640.00	0.91	11.00	0.00	104.00	B	394.78	0.19	7.00	0.00	13.33
F:4	598953.4	6584599.5	T	685.22	1.07	11.40	0.00	122.67	B	480.00	0.48	31.00	0.00	36.00
F:5	598955.3	6584600.0	T	850.43	1.06	14.20	0.00	124.00	B	617.39	0.41	9.80	0.00	40.00
F:6	598957.3	6584600.5	T	716.52	1.02	11.80	0.00	109.33	B	594.78	0.08	10.20	0.00	37.33
F:7	598959.2	6584601.0	T	713.04	1.02	12.60	0.00	102.67	B	480.00	0.69	11.40	0.00	61.33
F:8	598961.1	6584601.5	T	716.52	1.10	12.00	0.00	97.33	B	403.48	0.56	8.80	0.00	52.00
F:9	598963.0	6584602.0	T	659.13	0.98	12.20	0.00	104.00	B	486.96	0.10	9.20	0.00	17.33
F:10	598965.0	6584602.5	T	589.57	0.71	11.60	0.00	73.33	B	375.65	0.59	10.20	0.00	28.00
F:11	598966.9	6584603.0	T	620.87	1.08	10.80	0.00	85.33	B	405.22	0.52	9.80	0.00	22.67
F:12	598968.8	6584603.5	T	662.61	1.01	11.20	0.00	72.00	B	379.13	0.68	7.40	0.00	17.33
F:13	598970.7	6584604.0	T	507.83	0.97	10.40	0.00	48.00	B	488.70	0.39	6.60	0.00	12.00
E.14	598972.7	6584604.5	T	551.30	0.82	10.20	0.00	56.00	B	71.30	0.17	5.80	0.00	2.67
F:15	598974.6	6584605.0	T	549.57	0.81	10.00	0.00	56.00	B	375.65	0.52	9.60	0.00	26.67
F:16	598976.6	6584605.5	T	633.04	0.89	10.40	0.00	65.33	B	342.61	0.94	8.40	0.00	40.00
F:17	598978.5	6584606.0	T	570.43	0.71	11.40	0.00	52.00	B	466.09	0.18	7.00	0.00	9.33

SITE H

id	x-UTM	y-UTM	Niveau	[P]/ppm	[Fe]/‰	[Zn]/ppm	[Cu]/ppm	[Mn]/ppm	Niveau	[P]/ppm	[Fe]/‰	[Zn]/ppm	[Cu]/ppm	[Mn]/ppm
H:1	598993.4	6584506.6	T	688.00	2.26	2.00	6.00	137.00	U	514.29	2.42	9.83	2.35	56.16
H:2	598994.6	6584505.0	T	626.00	1.98	0.00	6.00	111.00	U	258.73	2.25	9.49	4.12	138.99
H:3	598995.7	6584503.4	T	706.00	1.93	15.00	11.00	127.00	U	452.38	2.39	9.83	4.12	46.06
H:4	598996.9	6584501.8	T	627.00	1.80	14.00	9.00	116.00	U	1850.79	2.40	10.17	5.29	44.44
H:5	598998.1	6584500.1	T	571.00	2.07	0.00	5.00	104.00	U	553.97	2.57	12.88	6.47	39.60
H:6	598999.2	6584498.6	T	639.00	2.03	0.00	7.00	113.00	U	433.33	2.03	11.86	4.12	16.97
H:7	599000.4	6584496.9	T	633.00	2.05	1.00	6.00	106.00	U	811.11	2.34	12.20	7.06	83.23
H:8	599001.6	6584495.2	T	594.00	1.79	13.00	9.00	106.00	U	520.63	1.86	8.81	3.53	137.37
H:9	599002.8	6584493.8	T	780.00	1.90	0.00	6.00	105.00	U	701.59	2.38	8.14	5.88	21.41
H:10	599004.0	6584492.1	T	941.00	2.10	4.00	9.00	141.00	U	869.84	2.51	11.19	7.65	267.88
H:11	599005.2	6584490.6	T	656.00	2.16	2.00	5.00	112.00	U	1134.92	2.75	11.53	9.41	408.89
H:12	599006.4	6584488.9	T	656.00	1.81	0.00	6.00	103.00	U	928.57	2.64	11.86	8.24	272.32
H:13	599007.6	6584487.2	T	650.00	1.93	1.00	7.00	116.00	U	926.98	1.94	9.15	5.29	71.52
H:14	599008.8	6584485.6	T	1065.00	1.92	1.00	5.00	103.00	U	677.78	1.78	8.47	4.71	63.84
H:15	599010.0	6584484.0	T	776.00	1.89	2.00	8.00	108.00	U	1888.89	2.36	9.49	11.76	223.84
H:16	599011.2	6584482.4	T	647.00	1.82	1.00	5.00	94.00	U	453.97	1.74	8.81	7.65	115.15
H:17	599012.3	6584480.8	T	712.00	1.93	2.00	4.00	100.00	U	806.35	2.39	10.17	6.47	63.84
H:18	599013.4	6584479.1	T	652.00	1.95	1.00	4.00	57.00	U	785.71	2.19	10.17	5.29	94.14
H:19	598991.8	6584505.3	T	547.00	1.77	0.00	4.00	92.00	U	523.81	1.95	7.80	6.47	52.12
H:20	598993.0	6584503.8	T	752.00	2.13	3.00	6.00	118.00	U	533.33	2.17	10.51	5.29	83.64
H:21	598994.1	6584502.2	T	676.00	2.11	4.00	6.00	126.00	U	577.78	2.11	10.85	5.88	122.42
H:22	598995.2	6584500.6	T	717.00	1.98	1.00	7.00	113.00	U	484.13	2.37	9.15	4.12	60.20
H:23	598996.4	6584499.0	T	655.00	1.89	1.00	6.00	104.00	U	363.49	1.88	10.17	2.35	42.83
H:24	598997.6	6584497.4	T	558.00	1.78	0.00	5.00	87.00	U	409.52	2.26	11.86	5.88	52.12
H:25	598998.8	6584495.8	T	627.00	1.88	0.00	5.00	99.00	U	623.81	2.27	5.76	5.29	31.11
H:26	599000.0	6584494.2	T	777.00	2.00	0.00	8.00	125.00	U	515.87	2.20	8.81	5.88	46.46
H:27	599001.1	6584492.6	T	603.00	1.92	0.00	6.00	104.00	U	1076.19	2.26	9.83	5.88	51.72
H:28	599002.3	6584490.9	T	821.00	2.07	1.00	7.00	132.00	U	684.13	2.40	9.15	4.71	127.27
H:29	599003.5	6584489.4	T	614.00	1.75	0.00	5.00	90.00	U	671.43	2.28	8.14	5.29	83.64
H:30	599004.7	6584487.7	T	652.00	1.69	0.00	6.00	89.00	U	550.79	2.15	10.17	4.12	145.45
H:31	599005.9	6584486.0	T	614.00	1.78	2.00	5.00	94.00	U	444.44	1.58	7.80	2.94	53.33
H:32	599007.1	6584484.6	T	562.00	1.98	2.00	5.00	104.00	U	642.86	1.82	10.85	7.06	184.65
H:33	599008.2	6584482.9	T	680.00	1.81	1.00	6.00	108.00	U	720.63	2.45	10.17	2.35	88.08
H:34	599009.5	6584481.1	T	750.00	2.00	2.00	6.00	117.00	U	709.52	1.97	8.81	5.88	99.80
H:35	599010.7	6584479.7	T	603.00	1.89	1.00	6.00	111.00	U	553.97	1.71	8.14	3.53	50.10
H:36	599011.8	6584478.0	T	874.00	1.85	2.00	9.00	119.00	U	600.00	1.96	6.78	4.71	80.00
H:37	599013.0	6584476.4	T	712.00	1.79	1.00	6.00	109.00	U	680.95	2.37	8.14	5.29	41.21
H:38	599010.3	6584496.8	T	535.00	2.16	0.00	6.00	106.00	U	536.51	2.61	8.14	6.47	22.22
H:39	599008.8	6584495.6	T	612.00	2.17	0.00	6.00	114.00	U	553.97	2.52	11.19	6.47	25.45
H:40	599007.1	6584494.3	T	694.00	1.95	13.00	11.00	120.00	U	682.54	2.64	10.17	5.88	32.32
H:41	599005.8	6584492.7	T	595.00	2.10	0.00	7.00	103.00	U	536.51	2.19	7.80	4.12	132.12
H:42	599000.8	6584489.9	T	673.00	1.86	0.00	7.00	109.00	U	220.63	2.31	8.81	5.29	131.31
H:43	598998.8	6584488.8	T	865.00	2.31	7.00	8.00	167.00	U	493.65	2.35	9.15	5.29	69.49
H:44	598997.6	6584487.6	T	729.00	1.95	5.00	8.00	141.00	U	977.78	2.27	8.81	3.53	80.40
H:45	598996.0	6584486.4	T	650.00	1.97	1.00	7.00	122.00	U	528.57	1.89	8.14	4.71	97.78

SITE H

id	x-UTM	y-UTM	Niveau	[P]/ppm	[Fe]/‰	[Zn]/ppm	[Cu]/ppm	[Mn]/ppm	Niveau	[P]/ppm	[Fe]/‰	[Zn]/ppm	[Cu]/ppm	[Mn]/ppm
H:46	599013.0	6584476.4	T	656.00	1.96	0.00	5.00	95.00	U	693.65	2.27	7.46	4.71	63.43

SITE I

id	x-UTM	y-UTM	Niveau	[P]/ppm	[Fe]/‰	[Zn]/ppm	[Cu]/ppm	[Mn]/ppm	Niveau	[P]/ppm	[Fe]/‰	[Zn]/ppm	[Cu]/ppm	[Mn]/ppm
I:1	598951.4	6584571.1	T	609.23	0.16	10.34	0.00	293.33	B	256.92	2.19	10.15	0.00	78.73
I:2	598953.1	6584570.0	T	532.31	1.45	10.54	0.00	242.54	B	192.31	2.10	9.17	0.00	176.51
I:3	598954.8	6584568.9	T	518.46	1.27	7.61	0.00	200.63	B	96.92	3.09	6.05	0.00	55.87
I:4	598956.4	6584567.8	T	541.54	1.64	8.98	0.00	233.65	B	358.46	3.43	8.20	0.00	126.98
I:5	598958.1	6584566.6	T	475.38	1.54	10.54	0.00	228.57	B	540.00	2.49	10.34	20.87	846.98
I:6	598959.7	6584565.5	T	570.77	1.43	8.98	0.00	210.79	B	570.77	2.17	7.22	0.00	290.79
I:7	598961.4	6584564.3	T	569.23	1.63	8.20	0.00	255.24	B	449.23	1.50	8.78	0.00	311.11
I:8	598963.0	6584563.2	T	544.62	1.57	8.39	0.00	236.19	B	795.38	2.45	15.80	0.00	2375.87
I:9	598964.7	6584562.1	T	677.88	1.35	12.49	0.00	281.90	B	700.88	1.47	11.71	0.00	937.14
I:10	598950.2	6584569.5	T	595.38	1.58	11.12	0.00	253.97	B	255.38	1.76	6.44	0.00	85.08
I:11	598951.9	6584568.3	T	560.00	1.33	8.78	0.00	232.38	B	86.15	1.13	6.83	0.00	64.76
I:12	598953.5	6584567.2	T	904.62	1.55	14.05	9.74	331.43	B	170.77	1.66	6.05	0.00	99.05
I:13	598955.2	6584566.1	T	795.38	1.69	11.90	5.57	293.33	B	116.92	2.05	8.20	0.00	58.41
I:14	598956.8	6584564.9	T	503.08	1.63	10.34	0.00	273.02	B	396.92	3.48	10.54	0.00	195.56
I:15	598958.5	6584563.8	T	516.92	1.39	7.22	0.00	195.56	B	261.54	1.73	5.66	0.00	111.75
I:16	598960.2	6584562.7	T	527.69	1.37	8.39	0.00	181.59	B	301.54	1.28	7.02	0.00	189.21
I:17	598961.8	6584561.6	T	706.19	1.26	11.90	0.00	266.67	B	643.08	1.65	10.73	0.00	784.76
I:18	598963.5	6584560.5	T	544.62	1.23	7.22	0.00	204.44	B	476.11	1.45	9.17	0.00	261.59
I:19	598949.1	6584567.9	T	584.62	1.27	8.39	0.00	215.87	B	310.77	2.00	8.59	0.00	121.90
I:20	598950.9	6584566.8	T	626.15	1.64	11.32	0.00	276.83	B	150.77	1.92	7.41	0.00	60.95
I:21	598952.5	6584565.6	T	556.92	1.63	10.73	0.00	270.48	B	173.85	1.83	6.24	0.00	62.22
I:22	598954.1	6584564.5	T	643.08	1.73	11.12	0.00	288.25	B	315.38	1.85	8.00	0.00	62.22
I:23	598955.9	6584563.4	T	624.62	1.68	12.49	0.00	261.59	B	330.77	1.39	7.02	0.00	140.95
I:24	598957.4	6584562.3	T	780.53	1.19	13.66	0.00	270.48	B	336.92	1.84	8.39	0.00	302.22
I:25	598959.1	6584561.1	T	653.85	1.33	11.51	0.00	203.17	B	333.85	1.60	8.39	0.00	168.89
I:26	598960.8	6584559.9	T	706.19	1.21	11.12	0.00	257.78	B	576.92	1.79	8.20	0.00	327.62
I:27	598962.4	6584558.8	T	590.77	1.34	8.59	0.00	180.32	B	363.08	1.46	8.20	0.00	80.00

SITE J

id	x-UTM	y-UTM	Niveau	[P]/ppm	[Fe]/‰	[Zn]/ppm	[Cu]/ppm	[Mn]/ppm	Niveau	[P]/ppm	[Fe]/‰	[Zn]/ppm	[Cu]/ppm	[Mn]/ppm
I:17	598981	6584376	T	615.87	1.45	28.63	11.61	103.80	B	423.81	1.38	19.37	0.00	78.99
I:19	598983	6584377	T	582.54	1.41	26.11	0.00	96.71	B	403.17	1.35	24.00	0.00	80.51
I:21	598985	6584378	T	541.27	1.42	26.11	0.00	100.76	B	441.27	1.49	26.11	0.00	102.78
I:23	598986	6584379	T	533.33	1.35	26.11	0.00	85.57	B	415.87	1.35	26.53	0.00	80.00
I:25	598988	6584380	T	598.41	1.36	34.95	0.00	104.30	B	434.92	1.33	26.11	0.00	90.63
I:27	598990	6584381	T	541.27	1.44	26.95	0.00	98.23	B	323.81	1.57	20.63	0.00	71.90
I:29	598992	6584381	T	580.95	1.45	24.00	0.00	93.16	B	431.75	1.42	25.26	0.00	77.97
I:31	598994	6584382	T	568.25	1.35	29.05	0.00	95.70	B	488.89	1.35	28.63	0.00	103.80
I:33	598995	6584383	T	593.65	1.39	26.53	0.00	91.65	B	423.81	1.50	25.68	0.00	93.16
I:35	598997	6584384	T	579.37	1.50	28.21	0.00	103.80	B	384.13	1.60	21.47	0.00	89.62
I:36	598998	6584385	T	604.76	1.49	26.11	0.00	115.44	B	426.98	1.46	25.26	0.00	107.34
I:37	598999	6584385	T	539.68	1.58	28.63	0.00	117.97	B	398.41	1.43	22.74	0.00	79.49
I:38	599000	6584385	T	569.84	1.27	26.11	0.00	96.20	B	358.73	1.56	24.00	0.00	99.75
I:39	599001	6584386	T	550.79	1.34	21.89	0.00	86.08	B	363.49	1.49	24.42	0.00	82.53
I:40	599002	6584386	T	587.30	1.51	29.89	0.00	120.00	B	358.73	1.42	22.32	0.00	94.18
I:41	599003	6584387	T	580.95	1.43	27.37	0.00	118.99	B	192.06	1.96	22.74	0.00	132.15
I:42	599004	6584387	T	568.25	1.44	26.11	0.00	90.63	B	458.73	1.31	19.79	0.00	88.61
I:43	599005	6584388	T	490.48	1.38	24.42	0.00	109.37	B	441.27	1.51	282.11	0.00	8.56
I:44	599005	6584388	T	568.25	1.50	27.37	0.00	118.99	B	185.71	1.80	19.37	0.00	101.27
I:45	599006	6584388	T	555.56	1.65	29.89	0.00	119.49	B	417.46	1.35	23.58	0.00	94.68
I:46	599007	6584389	T	558.73	1.52	24.00	0.00	116.46	B	480.95	1.63	25.26	0.00	117.47
I:47	599008	6584389	T	526.98	1.51	27.37	0.00	111.39	B	431.75	1.43	24.84	0.00	92.66
I:48	599009	6584390	T	568.25	1.52	36.63	12.90	114.94	B	509.52	1.60	24.00	0.00	101.77
I:49	599010	6584390	T	509.52	1.31	23.16	0.00	101.77	B	244.44	1.56	21.89	0.00	61.77
I:50	599011	6584391	T	560.32	1.51	26.53	0.00	115.44	B	566.67	1.48	28.63	0.00	107.85
I:52	599013	6584391	T	533.33	1.36	27.37	0.00	91.14	B	395.24	1.44	25.26	0.00	110.89
I:54	599014	6584392	T	566.67	1.59	28.21	0.00	135.70	B	353.97	1.50	21.47	0.00	121.52
I:56	599016	6584393	T	569.84	1.48	27.79	0.00	125.57	B	446.03	1.47	26.53	0.00	104.81
I:58	599018	6584394	T	612.70	1.33	25.68	0.00	108.35	B	390.48	1.20	24.00	0.00	79.49
I:60	599020	6584395	T	573.02	1.51	30.32	0.00	114.43	B	503.17	1.55	28.21	0.00	117.97

SITE K

id	x-UTM	y-UTM	Niveau	[P]/ppm	[Fe]/‰	[Zn]/ppm	[Cu]/ppm	[Mn]/ppm	Niveau	[P]/ppm	[Fe]/‰	[Zn]/ppm	[Cu]/ppm	[Mn]/ppm
K:1	596096.0	6581077.5	T	498.41	1.80	16.84	0.00	44.05	B	303.17	1.43	18.53	0.00	13.67
K:2	596087.0	6581074.5	T	598.41	1.49	23.16	0.00	62.28	B	385.71	1.50	18.95	0.00	14.68
K:3	596066.0	6581066.5	T	555.56	1.45	19.79	0.00	61.27	B	363.49	1.69	23.58	0.00	34.43
K:4	596056.0	6581075.0	T	549.21	1.21	19.37	0.00	60.76	B	517.46	1.21	22.32	0.00	52.15
K:5	596048.0	6581081.0	T	525.40	1.19	20.21	0.00	49.11	B	392.06	0.66	20.21	0.00	13.67
K:6	596042.0	6581087.0	T	482.54	0.66	17.26	0.00	42.53	B	195.24	0.22	20.63	0.00	10.63
K:7	595966.0	6581138.5	T	558.73	1.11	30.74	0.00	36.96	B	661.90	1.14	31.16	0.00	35.44
K:8	595973.0	6581120.0	T	465.08	1.00	20.21	0.00	36.96	B	338.10	0.74	18.53	0.00	10.13
K:9	595985.0	6581087.5	T	471.43	1.17	21.89	0.00	62.78	B	363.49	0.84	17.26	0.00	16.20
K:1									B+	387.30	1.68	33.68	0.00	91.14
K:2									B+	377.78	1.43	28.21	0.00	53.67
K:3									B+	392.06	1.74	27.37	0.00	84.05
K:4									B+	269.84	1.01	19.79	0.00	48.61
K:5									B+	466.67	0.68	19.79	0.00	24.30
K:6									B+	279.37	0.33	14.74	0.00	10.13